12-2014

DUAL ASSEMBLY NANOPARTICLES ACHIEVE SUSTAINED SILENCING OF ZNF304: A NOVEL TRANSCRIPTION FACTOR FOR B1 INTEGRIN

Burcu Aslan

DUAL ASSEMBLY NANOPARTICLES ACHIEVE SUSTAINED SILENCING OF ZNF304: A NOVEL TRANSCRIPTION FACTOR FOR B1 INTEGRIN

by

Burcu Aslan, M.S.

APPROVED:

Gabriel Lopez-Berestein, M.D.

Anil K. Sood, M.D.

George Calin, M.D., PhD.

Mien-Chie Hung, Ph.D.

Zahid Siddik, Ph.D.

APPROVED:

Dean, the University of Texas
Graduate School of Biomedical Sciences at Houston

DUAL ASSEMBLY NANOPARTICLES ACHIEVE SUSTAINED SILENCING OF ZNF304: A NOVEL TRANSCRIPTION FACTOR FOR β1 INTEGRIN

A

DISSERTATION

Presented to the faculty of
The University of Texas
Health Science Center at Houston
And
The University of Texas
M.D. Anderson Cancer Center
Graduate School of Biomedical Sciences

in Partial Fulfillment
of the Requirements
for the Degree of

DOCTOR OF PHILOSOPHY

BY
Burcu Aslan
Houston, TX
December, 2014

Acknowledgments

First of all, I would like to offer special thanks to my mentor, Dr. Gabriel Lopez-Berestein, for his patience, guidance, and support throughout my career. I am grateful for the opportunities that he provided since the first day we met. He has continuously encouraged me to pursue excellence and enormously influenced my professional development. Dr. Lopez has not only been a dedicated supervisor but also a wonderful father who made me feel at home despite being in a different continent.

I would also like to thank the members of my supervisory committee: Drs. Anil Sood, Mien-Chie Hung, George Calin, and Zahid Siddik who dedicated their time and lent their expertise. There would be no success without their support and guidance.

My deepest appreciation is extended to all my colleagues in Dr. Lopez and Dr. Ozpolat lab: including Vianey Gonzalez and Cristian Aguayo-Rodriguez, whom I worked with more than five years as a team and a family. I would also like to extend my sincere thanks to Paloma Monroig for being extremely helpful to move my project forward. Furthermore, my thankfulness reaches out to Roxana Redis, Katrien Van Roosbroeck, and Maitri Shah for encouraging me maintain healthy and their valuable friendship.

In addition, I owe Guillermo Armaiz Pena a lot for taking me under his wings and mentally preparing me for this training from the very beginning of my career.

I really do not know if there is a way to express my appreciation to my family for their continuous and unconditional love, support, and encouragement. My

parents and my sister have always found a special way of motivating me even with a simple phone call to keep me moving forward. Also, I am grateful that Mustafa Korhan Guner has still not terminated our relationship after experiencing hard times with a grumpy girlfriend. I have been fortunate to have him beside me encouraging and cheering me on throughout my training.

Last but not least, my dreams would not have come true without such an opportunity that was provided by The University of Texas and UT MD Anderson Cancer Center. I am blessed with all the circumstances that brought me to Houston to advance my career.

TARGETING ZINC FINGER 304 (ZNF304) BY DUAL ASSEMBLY NANOPARTICLES (DANP) IN OVARIAN CANCER

Burcu Aslan, M.S.

Supervisory Professor: Gabriel Lopez-Berestein, M.D.

Abstract

Ovarian cancer (OC) is a highly metastatic disease, but no effective strategies to this process currently are known. Here, an integrated computational analysis of The Cancer Genome Atlas ovarian cancer dataset coupled with experimental validation identified a novel zinc finger transcriptional factor 304 (ZNF304) as one of the key factors for ovarian cancer metastasis. High tumoral ZNF304 expression was associated with poor overall survival in ovarian cancer patients. Through reverse phase protein array analysis, we demonstrated that ZNF304 promotes multiple proto-oncogenic pathways important for cell survival, migration, and invasion. ZNF304 transcriptionally regulates β1 integrin, which subsequently regulates Src/focal adhesion kinase and paxillin and prevents anoikis. Targeting ZNF304 using small interfering RNA (siRNA) reduces cell survival, anoikis and migration *in vitro.* A novel dual assembly nanoparticle system (DANP) was designed for *in vivo* delivery and sustained gene silencing. DANP-ZNF304 siRNA led to sustained ZNF304 silencing for 14 days, increased anoikis, and reduced tumor growth in orthotopic murine models of ovarian cancer. Taken together, ZNF304 is a novel transcriptional regulator of β1 integrin, promotes cancer cell survival, and protects against anoikis in ovarian

cancer; DANP is a safe and efficient delivery system that provides prolonged gene silencing following systemic administration.

Table of Contents

Approval page i

Title Page ii

Acknowledgments iii

Abstract v

Table of Contents vii

List of Figures x

List of Abbreviations xiv

CHAPTER I: Introduction 1

Nanotechnology In Cancer 2

Nanoparticles 3

Active Targeting 4

Drug Delivery Systems 6

Liposomes 6

Polymeric micelles 7

Dendrimers 8

Polymeric nanoparticles 9

Characteristics of Nanoparticles 11

Size 11

Shape 12

Surface characteristics 13
Release characteristics 15
Ovarian Cancer 19
Metastasis 26
Anoikis 28
Hypothesis and Aims of The Study 30
CHAPTER II: Methods 32
CHAPTER III: Results 43
Discovery of ZNF304 and its role in human HGSOC 44
Downregulation of ZNF304 inhibits invasion, migration, and proliferation of OC cells 48
ZNF304 transcriptionally regulates β1 integrin 55
ZNF304 protects tumor cells from anoikis 61
Development and characterization of DANP 64
Size, charge and morphology 64
Biodistribution 64
Duration of in vivo gene silencing 67
Toxicity 68
Effects of ZNF304 gene silencing on antitumor activity in orthotopic models of OC 73
CHAPTER IV: Discussion 80

CHAPTER IV: Discussion 80

CHAPTER V: Future Directions 91

Appendix 94

Bibliography 99

Vita 110

List of Figures

Figure 1. Drug levels in plasma after systemic administration.....16

Figure 2. Origin and histotypes of ovarian cancer 21

Figure 3. Evolution of chemotherapy for ovarian cancer 23

Figure 4. Overcoming obstacles in RNAi delivery 25

Figure 5. Invasion-metastasis cascade 26

Figure 6. Anoikis and integrins 29

Figure 7. Increased ZNF304 expression is associated with poor survival in HGSOC patients.....45

Figure 8. *CNTFR*, *MAGED1*, and *NR2F2* expression levels are not correlated with patient survival in HGSOC patients 46

Figure 9. ZNF304 is expressed in ovarian cell lines 47

Figure 10. ZNF304 siRNA decreases the ZNF304 levels in HeyA8 cells.....48

Figure 11. Silencing ZNF304 inhibits invasion and migration.....49

Figure 12. RPPA analysis revealed the link between ZNF304 and integrin signaling 51

Figure 13. ZNF304 and β1 integrin mRNA levels highly correlates in HGSOC patients.....52

Figure 14. Silencing ZNF304 leads to reduction in focal adhesion complex members 53

Figure 15. Silencing ZNF304 reduces proliferation through cell cycle arrest 54

Figure 16. *ZNF304* gene is located at chromosome 19q13.43 and ZNF304 protein consists of 16 zinc fingers. 55

Figure 17. Silencing ZNF304 decreases β1 integrin mRNA levels 56

Figure 18. β1 integrin is expressed in all cell lines tested 56

Figure 19. ZNF304 binds to β1 integrin promoter 58

Figure 20. ZNF304 regulates β1 integrin 60

Figure 21. ZNF304 mediates inside-out signaling 62

Figure 21 (continued). ZNF304 mediates inside-out signaling 63

Figure 22. Size and and zeta potential characteristics of DANP 65

Figure 23. DANP exhibits spherical morphology 65

Figure 24. DANP accumulates in tumor 66

Figure 25. DANP-ZNF304 siRNA downregulates ZNF304 *in vivo* up to 14 days after a single IV injection 67

Figure 26. BUN, Creatinine, ALT and alkaline phosphatase levels remain in normal range in blood after DANP-ZNF304 siRNA administration 70

Figure 27. No sign of inflammatory response in plasma after DANP-ZNF304 siRNA administration 71

Figure 28. No sign of toxicity in liver, kidney, spleen and brain tissues after DANP-ZNF304 siRNA administration 72

Figure 29. Silencing ZNF304 leads to increased antitumor activity in HeyA8 orthotopic murine model of OC 74

Figure 30. Targeting ZNF304 leads to increased antitumor activity in SKOV3 orthotopic murine model of OC 76

Figure 31. DANP-siRNA treatment does not affect body weight indicating no toxicity 77

Figure 32. Silencing ZNF304 decreases proliferation and angiogenesis *in vivo* .78

Figure 33. Silencing ZNF304 culminate in enhanced anoikis in vivo.....79

List of Tables

Table 1. Summary data of hematology parameters after administration of Empty DANP, DANP-Control siRNA, DANP-ZNF304 siRNA 69

Table 2. siRNA sequences used in zinc finger protein 304 (ZNF304) transfection experiments 95

Table 3. Antibodies used in the Western blotting, chromatin immunoprecipitation, and immunohistochemical analyses 96

Table 4. Oligonucleotide sequences for quantitative reverse transcription polymerase chain reaction 97

Table 5. Oligonucleotide sequences for quantitative polymerase chain reaction analysis of chromatin immunoprecipitation assays 98

List of Abbreviations

AFM	Atomic Force Microscopy
ALT	Alanine Transaminase
BUN	Blood Urea Nitrogen
ChIP	Chromatin Immunoprecipitation
CNTFR	Ciliary Neurotrophic Factor Receptor
ECM	Extracellular Matrix
EPR	Enhanced Permeability And Retention
FAK	Focal Adhesion Kinase
FDA	Food And Drug Administration
HGSOC	High Grade Serous Ovarian Cancer
ITGB1	Integrin β1
MAGED1	Melanoma Antigen Family D, 1
MSP	Mesoporous Silicon Particles
MYH9	Myosin II
NRG1	Neuregulin 1
NR2F2	Nuclear Receptor Subfamily 2, Group F, Member 2
OC	Ovarian Cancer
PARP	Poly ADP Ribose Polymerase
PBS	Phosphate Buffer Saline
PEG	Polyethylene Glycol
PLA	Poly Lactic Acid

PLGA	Poly-Lactic-Co-Glycolic Acid
Poly-HEMA	Polyhydroxyethylmethacrylate
RES	Reticulo-Endothelial System
RPPA	Reverse Phase Protein Array
TCGA	The Cancer Genome Atlas
ZNF304	Zinc Finger Protein 304

CHAPTER I: Introduction

(Parts of this section were adapted with permission in part from Aslan, B et al., Nanotechnology in Cancer Therapy from Journal of Drug Targeting, 2013; and from Aslan, B et al., Chitosan Nanoparticles, Encyclopedia of Nanotechnology, 2012)

Nanotechnology In Cancer

Cancer is one of the leading causes of morbidity and mortality worldwide and it is expected to be the major cause of death in the coming decades (Bray et al., 2012). Despite the advances and extensive research on novel approaches, current treatments are still limited to surgery, radiotherapy, chemotherapy, and immunotherapy. Treatment failure is related to either drug resistance, pharmacological or toxicity issues in most instances. In contrary, utilization of nanocarriers leads to increased therapeutic index and tumor tissue concentrations of the drugs and can enhance the efficacy of currently used regimens by providing superior pharmacokinetic features, extended blood circulation time, and elevated cellular uptake that are major factors for an improved therapeutic window and subsequent clinical success. Advances in nanotechnology are also expected to provide foundation for development of novel therapeutics and wide applications of diagnostic methods in cancer.

Key factors in selecting biomaterials are biocompatibility, biodegradability, safety and ease of assembly in the structures with the desired characteristics. Taken together, biomaterials and nanotechnology offer a unique opportunity to improve survival in cancer patients. In this part of the chapter, I will focus on strategies of nanoparticle design and highlight the latest developments in cancer nanomedicine.

Nanoparticles

The history of nanoparticles starts in 1950s with a polymer-drug conjugate that was designed by Jatzkewitz (Jatzkewitz, 1954), followed by Bangham who discovered the liposomes in mid-1960s (Bangham and Horne, 1964), (Bangham et al., 1965). In 1972, Scheffel and colleagues first reported albumin based nanoparticles (Scheffel et al., 1972), which formed the basis of albumin-bound paclitaxel (Abraxane). Abraxane was approved in 2005 by US Food and Drug Administration (FDA) for the treatment of breast cancer (Gradishar et al., 2005) and recently approved for the treatment of lung cancer (Casaluce et al., 2012). Abelcet, amphotericin B lipid complex, was approved by FDA (Chonn and Cullis, 1995) for the treatment of invasive fungal infections and it is widely used to treat systemic fungal disease, which is a source of major morbidity in cancer patients (Herbrecht, 1996).

In the 1980s, Maeda and colleagues observed the enhanced accumulation of nanoparticles in the tumor site due to the altered structure of tumor vasculature (Matsumura and Maeda, 1986). Blood vessels in tumors are different compared to normal blood vessels due to abnormal and leaky architecture. Impaired regulation in blood vessels leads to ‘enhanced permeability and retention (EPR) effect’ (Maeda et al., 2006). The reduced lymphatic drainage, increased size of fenestrations and gaps between endothelial cells, varies from 200 to 1200 nm, in contrast to normal endothelium with pores with 10 to 50 nm contributes to EPR effect. This effect has become a hallmark of the solid tumor vasculature leading to increased nanoparticle

accumulation in the tumor site due to ‘passive targeting’. Hereby drug carriers exhibit enhanced therapeutic efficacy in tumors, in addition to reduced side effects and toxicity.

Despite the advantages of passive targeting approaches, several limitations exist that still needs to be eliminated in the future. Certain tumors are difficult to deliver due to lack of EPR effect, hence the permeability in blood vessels may not be identical throughout the same tumor (Yuan et al., 1995). To overcome these limitations, nanoparticles are designed to bind to specific targets (active targeting) through the ligands that recognize particular receptors in target cells.

Active Targeting

Various receptors on the tumor cell surface have been studied as potential sites to achieve selective delivery. Nanoparticle surface can be modified by a variety of conjugation chemistries to attach specific receptor ligands (Torchilin, 2005). Nanoparticles recognize and bind to their targets with subsequent uptake through receptor mediated endocytosis. Once internalized, the drug or payload is released in the cytoplasm or nucleus. Such receptor ligands may be peptides, vitamins, antibodies, carbohydrates and other chemical structures. For instance, the overexpression of transferrin and folate in certain tumors have been exploited to deliver nanoparticles conjugated with these receptor’s ligands (Yang et al., 2010), (Fernandes et al., 2008). Another example is the αvβ3 integrin, which is overexpressed in a wide range of tumors and angiogenic tumor-associated endothelium, and is largely absent in normal tissues. Han and colleagues have recently reported that the administration of chitosan nanoparticles conjugated with cyclic Arg-Gly-Asp (RGD) led to increased tumor delivery

and enhanced anti-tumor activity in ovarian cancer models (Han et al., 2010) (Fig.1). A variety of targeting agents such as monoclonal antibodies (mAbs) and nucleic acids (aptamers) are also used to enhance tumoral uptake of nanoparticles. Using mAbs for targeting in cancer therapy was first described by Milstein in 1981 (Warenius et al., 1981). Since then, antibody-based targeting has made a significant progression as a feasible strategy in cancer therapy. Clinically approved and widely used mAbs include rituximab (Rituxan) for the treatment of non-Hodgkin's lymphoma (James and Dubs, 1997), trastuzumab (Herceptin) for breast cancer treatment (Albanell and Baselga, 1999), bevacizumab as an angiogenesis inhibitor in colorectal cancer (Ferrara, 2005). Since 1997, 12 mAb-based therapy have been approved and a large number of antibody-based strategy is in progress for preclinical or clinical trials (Scott et al., 2012). Conjugation of an antibody directly to a therapeutic agent has been also explored. Mylotarg was the first approved formulation with this regard in clinic. Calicheamicin is a chemotherapeutic agent and it was conjugated with the CD33 antibody (Peer et al., 2007). Zevalin and Bexxar are radio-immunoconjugates formulated by using CD20 antibody and approved for the treatment of non-Hodgkin's lymphoma (Grillo-López, 2002), (Blagosklonny, 2004).

Recently, nucleic acid aptamers have gained immediate attention after the *in vitro* selection of functional nucleic acids (termed SELEX) that was discovered in 1990 (Ellington and Szostak, 1990, Tuerk and Gold, 1990). Aptamers are single stranded oligonucleotides that can modulate molecular targets with high specificity and affinity through their three-dimensional structures. Aptamers exhibit significant advantages

such as the technical possibility in selection and chemical modification, specificity to target any given molecule, its substantial bio-activity in vivo, the low production costs, the simplicity in synthesis and storage for the marketing (Scaggiante et al., 2013). There are currently several aptamers that are in clinical trials (Scott et al., 2012). For instance, Pegaptanib was approved by FDA and used as a VEGF-specific aptamer that binds to VEGF and blocks the interaction with its receptor (VEGFR) thereby inhibiting its activity (Gragoudas et al., 2004). Moreover, aptamers seem alluring to modify the surface of nanoparticles for the design of targeted drug delivery systems.

Drug Delivery Systems

Liposomes

Liposomes are self-assembling nanoparticles formed by dispersion of phospholipids with hydrophilic heads and hydrophobic anionic/cationic long chain tails, creating closed membrane structures. Hydrophilic agents such as drugs and siRNA or hydrophobic drugs can be incorporated into the inner compartments and, into the hydrophobic membranes respectively. Currently, several liposomal anticancer drugs are used successfully as carriers in the clinic or studied in advanced stages of clinical trials. For instance, doxorubicin loaded liposomes were modified with polyethylene glycol (PEG) that alters the plasma pharmacokinetics and tissue distribution of doxorubicin and this PEGylated liposomal doxorubicin (Doxil) carriers, were approved by FDA for the treatment of Kaposi's sarcoma (Patel, 1996). Along with Doxil, approved liposomal formulations include non-pegylated liposomal doxorubicin (Myocet by Elan), liposomal daunorubicin (DaunoXome by Gilead), liposomal amphotericin B (abelcet), liposomal

cytarabine (DepoCyte by SkyePharma/Enzon/Mundipharma) and liposomal cisplatin (Lipoplatin by Regulon) (Huwyler et al., 2008). On the other hand, antisense oligonucleotides are also attractive to be used in liposomal formulations for cancer therapy (Tari et al., 1995). Antisense oligonucleotides can selectively inhibit disease-causing genes and thereby inhibiting the production of disease associated-proteins. For instance, liposomal formulation of bcl-2 oligos was demonstrated to inhibit bcl-2 protein production thereby leading to a growth inhibition in follicular lymphoma cell lines (Tormo et al., 1998). Furthermore, liposomal bcl-2 antisense oligos were studied to evaluate the in vivo behavior in rodents. The liposomes were widely distributed and no significant toxicity was observed over 6-week treatment of intravenously administered liposomal Bcl-2 oligos (Gutiérrez-Puente et al., 1999). Another example is *raf* antisense oligonucleotide that inhibits c-raf that leads to enhanced sensitivity to radiation and chemotherapy. LErafAON is the liposomal formulation of raf oligonucleotide that showed success for advanced solid tumors in its Phase I study (McGinnis et al., 2012).

Polymeric micelles

Polymeric micelles are formed from self-assembly of amphiphilic-block copolymers ranging between 10-100 nm in size. They are composed of a hydrophobic core and a hydrophilic corona. Micelles can improve the bioavailability of hydrophobic drugs, confer protection and inactivation of the drugs under the effect of biological surroundings (Torchilin, 2001). Polymeric micelle formulations are used for both passive and active targeting in anticancer therapy. For example, Genexol-PM is currently under investigation as a paclitaxel loaded polymeric micelle formulation for the treatment of

breast, lung, and pancreatic cancer. Pluronic and NK911 are doxorubicin loaded micelle formulations that are also currently studied in Phase I (Sultana et al., 2013). NC-6004 is carboplatin loaded formulation that is also studied in early clinical trials for the treatment of solid tumors (Wilson et al., 2008). Furthermore, there are polymeric micelle formulations that are designed for active targeting and modified with different ligands such as folate (binds to folate receptor) and mAb C225 (binds to EGF receptor). In a nude mice xenograft model, doxorubicin loaded PLGA-b-PEG polymeric micelle formulation has been shown to increase tumoral uptake and significant tumor regression (Yoo and Park, 2004).

Dendrimers

Dendrimers are hyperbranched nanoparticles composed of a core, branching units and functionalized terminal groups. The major advantage of dendrimers is that multiple anticancer agents can be incorporated in the central core or conjugated to functional end groups (Lee et al., 2005). In addition, depolymerization of dendrimers can be controlled to modify release profiles of the payload (Wong et al., 2012). For example, polyamidoamine (PAMAM) dendrimers can be tailored to enhance their biocompatibility and release properties through PEGylation, acetylation, and modified with anionic, neutral ligand molecules (Cai et al., 2013). As an example, doxorubicin was conjugated to PEGylated PAMAM dendrimers by acid-sensitive linkages in order to trigger the release of doxorubicin in acidic conditions (Zhu et al., 2010). Evaluations of pH-dependent payload release, cytotoxicity, cellular uptake and intracellular localization were performed using SKOV-3 ovarian cancer cell line. In addition, dendrimers with highest PEGylation degree showed the maximum- accumulation in SKOV3 tumor

xenografts in mice. On the other hand, polylysine dendrimers conjugated with a ligand for α5β1 also known as fibronectin receptor was designed for tumor targeting. Activated α5β1 is highly expressed in breast cancer cells compared to non-transformed cells and it plays a vital role in invasion and metastasis pathways in cancer. PHSCN peptide is a ligand that interacts with a specific region of the α5 subunit of integrin thereby blocking its activity. Polylysine dendrimers can be modified with this ligand for tumor targeting and the treatment with this carrier led to a significant reduction in the number of invasive human breast cancer cells (Yao et al., 2011). Furthermore, when tumor bearing mice were treated with polylysine dendrimers modified with integrin ligand, lung colony formation was obviously inhibited. In conclusion, despite the fact that dendrimers are extensively used for the design and development of therapeutics, further research is needed to improve its immunogenicity to assure the safety of long-term administration in clinic.

Polymeric nanoparticles

Polymer based delivery systems show great promise for biomedical applications due to their high biocompatibility and flexibility in which their structures can be modified to engineer multifunctional nanoparticles with desired shape, size, internal and external morphology as well as surface modifications. During the preparation stage of nanoparticles, polymers can be utilized through isolation from their natural sources such as chitosan that is produced from chitin or they can be synthesized in the desired structure such as poly-lactic-co-glycolic acid (PLGA). PLGA, arginine, chitosan, human serum albumin, alginate, and hyaluronic acid have been widely used in preclinical studies for drug delivery. Polymer based nanoparticles shows great promise in

preclinical studies. For example, chitosan nanoparticles are one of the most popular polymeric delivery system that is widely used in particular gene delivery. Chitosan nanoparticles serve as an attractive candidate for small interfering RNA (siRNA) delivery due its positive charge. Electrostatic interactions between negatively charged siRNA and positively charged chitosan create a safe carrier for siRNA in the blood circulation. Kim and coworkers analyzed the therapeutic effects of *src* and *fgr* inhibition using siRNA incorporated chitosan nanoparticles in orthotopic models of ovarian cancer. Dual silencing of *src* and *fgr* with chitosan nanoparticles *in vivo,* led to a significant reduction in tumor growth (Kim et al., 2011).

For clinical studies, albumin bound paclitaxel (abraxane) is the first polymeric formulation that is approved by FDA for the treatment of metastatic breast cancer (Gradishar et al., 2005) and it is recently approved for the treatment of lung cancer. Abraxane exploited the ability of albumin to bind to 60-kDa glycoprotein (gp60) receptor (albondin) (Miele et al., 2009). After this receptor-ligand interaction, albumin-gp60 complex triggers caveolin-1 mediated uptake of protein bound plasma molecules. On the other hand, albumin also binds to osteonectin (secreted protein acid rich in cysteine [SPARC] due to a sequence homology with gp60. SPARC is highly expressed in particular neoplasms (breast, prostate, and lung cancer) and contributes to intratumor accumulation of all albumin-bound drugs (Hawkins et al., 2008). In addition, Livatag (Doxorubicin Transdug) is a poly (isohexyl cyanoacrylate) nanoparticle formulation loaded with doxorubicin and approved for the treatment of multidrug-resistant protein-overexpressing hepatocellular carcinoma (Sultana et al., 2013).

Characteristics of Nanoparticles

Physical and chemical characteristics of nanoparticles including size, charge, shape, and surface properties individually play major roles for *in vivo* biodistribution and cellular internalization of these drug carriers. In this section, we will focus on the major parameters that determine the lifetime and delivery of the nanoparticles.

Size

Particle size is one of the crucial primary factors in determining the circulation time of the nanoparticles. After systemic administration, nanoparticles accumulate in spleen due to mechanical filtration and removed by reticulo-endothelial system (RES). For example, as the main constituent of RES, Kupffer cells play a major role for the removal of the particles accumulated in the liver (Moghimi et al., 2001). Currently, 100-200 nm is accepted as optimal size for drug delivery systems since nanocarriers take the advantage of EPR effect in tumors and avoid filtration in the spleen whereas they are large enough to avoid the uptake in the liver (Petros and DeSimone, 2010). Particles with a smaller diameter than 5nm are rapidly cleared from blood circulation through renal clearance or extravasation (Wong et al., 2008), (Alexis et al., 2008), (Choi et al., 2007). However, particles with a size up to 15 μm; accumulate in liver, spleen and bone marrow (Petros and DeSimone, 2010).

In addition, particle size has a significant impact on cellular internalization through phagocytosis, macropinocytosis, caveolar-mediated endocytosis, clathrin-mediated endocytosis. As mentioned above, size range has high influence on biodistribution and

cellular internalization. In addition, recent studies show that the geometry of the particles is as important as size range in terms of cellular internalization and distribution (Geng et al., 2007), (Decuzzi et al., 2010). In addition, Gratton and coworkers studied the correlation between shape and size on the internalization frequency in HeLa cells and interestingly, the particles with different shapes but similar volumes were internalized at extremely assorted rates (Gratton et al., 2008). In a distinct study, Godin and coworkers demonstrated that the accumulation of discoidal particles in breast tumors were five times higher than spherical particles despite their similar diameters (Godin et al., 2012). As a result, accumulating evidence shows that although size is a major parameter in the design of nanocarriers for decades, the shape as well, has a high impact along with the size.

Shape

Degradation properties of nanoparticles and subsequent payload release have been shown to be dependent on particle shape (Bawa et al., 1985). The importance of surface area and diameter were also demonstrated to be critical for cellular uptake of the nanoparticles (Panyam et al., 2003), (Dunne et al., 2000). Hemi-spherical particles were generated as sustained release devices in order to achieve zero-order. Spherical particles, however, can provide different degradation profiles as their shapes are susceptible upon degradation (Champion et al., 2007). Additionally, deformability of spherical nanoparticles is also playing a key role to avoid spleen filtration since spleen exhibit asymmetric filtering units (Moghimi et al., 2001). Therefore, nanoparticles which are especially larger than 200 nm should be either deformable enough to bypass the

filtration in spleen or flexible as erythrocytes that can avoid filtration even with 10 μm diameter.

In an elegant study, Decuzzi and co-workers studied the effect of size and shape of nanoparticles on biodistribution and tumor accumulation after intravenous injection. Spherical silica particles were generated in different sizes ranging from 700 nm to 3μm also in different shapes such as quasi-hemispherical, discoidal, and cylindrical silicon based particles. After a single, intravenous particle injection to tumor bearing mice, tumors and the major organs including liver, spleen, heart, lungs, kidneys, and brain were analyzed for silicon content and histological evaluation. This study elucidated the importance of shape properties of nanoparticles in addition to size distribution, indicating that geometry of the nanoparticles contributes to opsonization, *in vivo* biodistribution, the strength of adhesion and internalization rate in the cells (Decuzzi et al., 2009).

Surface characteristics

Surface properties play a key role on the period of nanoparticles in blood circulation subsequent systemic administration. After administration, nanoparticles may be associated with proteins, which are known as ‘opsonins’, such as immunoglobulins, and complement proteins that contribute to recognition of nanoparticles by macrophages. Therefore, opsonization is the key factor that determines the fate of nanoparticles to an extent in blood circulation. Modifying the surface of nanoparticles can be used as a strategy to enhance or reduce their circulation time in blood and tissues. For instance, negatively charged nanoparticles result in rapid RES clearance from circulation (Zahr et al., 2006). Cationic surfaces may induce cell membrane permeability and enhance

cellular uptake (Chen et al., 2009) however, cationic nanoparticles prepared from polycationic polymers such as polyethyleneimine and diethylaminoethyl-dextran can induce disruption in the cell, through formation of holes, membrane thinning and membrane erosion in lipid bilayers (Leroueil et al., 2008). On the other hand, the use of neutrally charged particles as well as particles coated with polyethylene glycol (PEG) lead to a major reduction of particle uptake by the RES (Torchilin and Trubetskoy, 1995, Otsuka et al., 2003).

The surface modification of PEGylated liposomes with rat serum albumin (RAS), compared with non-modified PEGylated liposomes, showed prolonged blood circulation in rats. To further analyze, total serum protein amounts were determined quantitatively in the absence and presence of RAS coating. As a result, RAS-modified liposomes significantly reduced the total amount of serum proteins that can induce opsonization in serum (Furumoto et al., 2007). In addition, doxorubicin-loaded and albumin-modified liposomes demonstrated enhanced pharmacokinetics and tissue distribution of doxorubicin (Yokoe et al., 2008). Tumor accumulation and therapeutic index of albumin-modified PEGylated liposomal doxorubicin was significantly higher than non-modified PEGylated liposomal doxorubicin indicating that surface modification of nanoparticles with albumin, enhances their safety and effectiveness.

In addition, nanoparticle surface can be modified with ligands that recognize and bind to specific receptors. Also, monoclonal antibodies can be conjugated onto nanoparticle surface to provide specificity. For instance, nanoparticles modified with HER2 specific

antibody, delivers the drug, particularly HER2 expressing cells (Kirpotin et al., 2006). Torchilin's group has also designed different approaches for active targeted delivery to the tumor with liposomes and micellar delivery systems. They have developed monoclonal antibody 2C5-modified doxorubicin loaded liposomes to enhance the therapeutic activity of the payload in brain tumor xenografts (Gupta and Torchilin, 2007) These studies demonstrate that surface characteristics are fundamentally important for nanoparticles to avoid their rapid clearance from the blood circulation before reaching the tumor site, and to provide active targeting through surface modifications with antibodies or ligands.

Release characteristics

The release properties of nanoparticles determine the efficiency of the treatment at target sites. Conventional drugs used in clinic have a narrow therapeutic window due to rapid increase and decrease of plasma drug levels after systemic administration, resulting in bordering doses with subsequent side effects (Figure 1A). However, drug delivery systems aims at delivering the desired concentration of the drug within the therapeutic range at target site, culminating minimized side effects and discomfort in patients (Figure 1B).

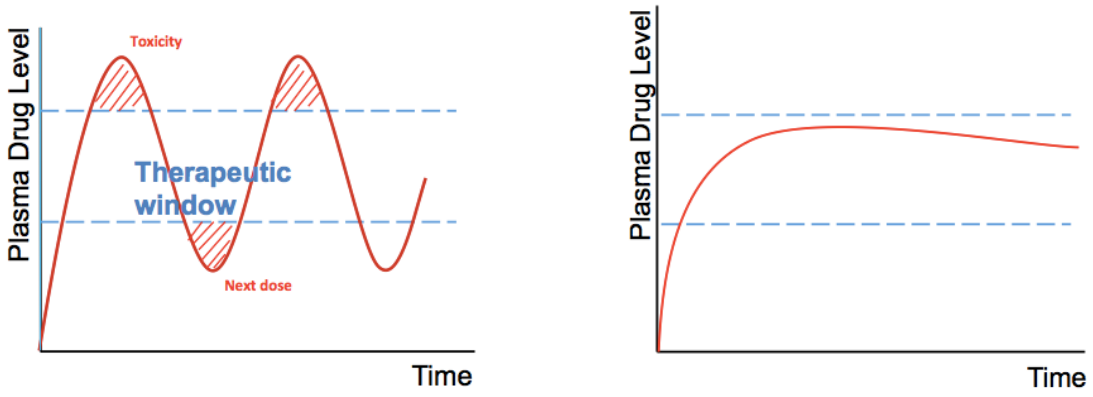

Figure 1. Drug levels in plasma after systemic administration
Graphs representing the drug levels in plasma over time after administration of (A) conventional drugs and (B) drug delivery for sustained release.

Constant plasma drug levels over a long period of time can be attained through zero-order release kinetics that can be achieved by using osmotic pressure, mechanical pumping, and electrokinetic transportation (Sakamoto et al., 2010). Besides, biocompatible polymeric nanoparticles are also used to prolong the period of drug release due to their long biodegration time in a range from days to months. Particularly, molecular weight is a major parameter in biodegradation rate of polymers. For instance, poly lactide-co-glycolide (PLGA) and poly lactic acid (PLA) were both used in order to study the sustained release of docetaxel after intravenous administration (Musumeci et al., 2006). Release rate of the drug has been shown to highly associate with molecular weight of the polymers. Furthermore, polymer with high molecular weight led to slower degradation of the material, compared to the polymer with low molecular weight, resulting in sustained release of the payload.

Multistage delivery system is an additional alternative approach providing sustained release of the payload where mesoporous silicon particles (MSP) offer unique opportunities for drug delivery (Tanaka et al., 2010). MSPs size, charge, shape, porosity are among the characteristics that can be tailored for particular applications and objectives of its use. We have used MSPs loaded with nanoliposomes carrying small interfering RNA (siRNA) that leads to target mRNA degradation. In this study, degradation of silicon particles allowed for the long-term release of siRNA to the target site (Shen et al., 2013a, Tanaka et al., 2010).

Another strategy to control the release of the payload can be using the environment of target site as a driving mechanism. Environment responsive nanocarriers offer a unique strategy, in particular, when the stimulus is specific to the disease pathology (Ganta et al., 2008). The approach seems promising since the stimuli trigger the payload to diffuse out of the particles through a controlled drug release. The biological stimuli include pH, temperature, and redox microenvironment (Shenoy et al., 2005), (Kommareddy and Amiji, 2005). Recently, Chen and colleagues have designed dual responsive- doxorubicin loaded polymeric micelles that release the payload in response to temperature and pH (Chen et al., 2012). In this study, drug release was analyzed at different pH conditions such as physiological condition (pH 7.4), endosomal (pH 6.6 and 6.0), lysosomal (pH 5.4), and different temperature conditions. Doxorubicin release rate was associated with increased temperature and decreased pH. Furthermore, they have demonstrated enhanced antitumor activity in tumor bearing mice that were generated by subcutaneously injected HeLa cells. On the other hand, external stimuli can be used to

trigger the release such as magnetic field, mild temperature increase or ultrasound (MacEwan et al., 2010). For instance, ultrasound triggers the degradation of polymers, slightly increases the temperature and cell membrane permeability, ultimately resulting in the release of the drug at target site (Mitragotri, 2005). Cisplatin release upon low frequency ultrasound has been demonstrated by Schroeder and colleagues (Schroeder et al., 2009). In this study, cisplatin-loaded liposomes were intraperitoneally administered into tumor bearing mice and the release of cisplatin was triggered by ultrasound at tumor site. Despite the tremendous progress in the design and development of nanoparticles, further preclinical studies are still required to conduct clinical trials for cancer therapy.

Advances in nanomedicine offer new opportunities to improve the anticancer armamentarium. Targeted and nontargeted nanoparticles are currently in preclinical and clinical phases indicating the impact of delivery systems on the field. Further studies in nanomedicine will improve therapeutic window of drugs with immensely reduced side effects leading to improved patient outcomes.

Ovarian Cancer

Ovarian cancer (OC) has the highest mortality rate among gynecologic malignancies. In the United States in 2014, over 21,000 women will be diagnosed with OC, and more than 14,000 women will die (Siegel et al., 2014). The poor survival rate in patients is due to the late-stage presentation of the disease. Despite the ongoing studies on screening strategies, only 20% of ovarian cancers can be diagnosed at stage 1, in which the disease is still limited to ovaries. When it metastasizes to the pelvic organs (stage 2), the abdomen (stage 3) or the peritoneal cavity (stage 4), the five-year median survival rate decreases down to 40 % (Vaughan et al., 2011).

Ovarian cancers are notably heterogeneous at cellular level and different ovarian tumors arise from distinct cell types. The normal ovary contains three major cell types: germ cells, endocrine and interstitial cells, and epithelial cells. Tumors that arise from germ cells constitute 3-5% of ovarian cancers whereas sex-cord-stromal tumors account for 7% of all ovarian malignancies. However, approximately 90% of the malignant ovarian tumors originate from the surface epithelium and in general, cancer develops after age 40 (Romero and Bast Jr, 2012). Number of ovulatory cycles and a family history of ovarian, breast, uterine, or colon cancer are major risk factors for patients.

OC can be classified into two major groups based on histological grade, molecular phenotype, and genotype; Type II and I. Type I cancers are often diagnosed in early

stages (I and II) and grow slowly whereas Type II cancers usually characterized by its late stage presentation (III-IV) and aggressive growth (Romero and Bast Jr, 2012).

The histotypes of OC are: serous, endometrioid, mucinous and clear cell (Figure 2). These histotypes are associated with *HOXA9*, *HOXA10*, and *HOXA11* genes that control the normal gynecological differentiation (Cheng et al., 2005). Tumor histotypes and grades are critical factors in order to determine the diagnosis and the prognosis (Soslow, 2008),(Silverberg, 2000). Numerous invasive mucinous ovarian cancers are metastases to the ovary, often from the gastrointestinal tract, including the colon, appendix or stomach. Endometrioid and clear cell ovarian cancers originate in endometriosis, which is linked to menstruation from the endometrium (Figure 2) (Vaughan et al., 2011).

The most common histological subtype is high-grade serous OC (HGSOC), and the poor survival rate associated with this subtype is primarily due to the advanced stage of disease and widespread metastases, at the time of diagnosis. The rapid spread of HGSOC is based on its propensity to seed the peritoneal cavity, leading to ascites formation and metastases (Naora and Montell, 2005) (Kipps et al., 2013). Ascites formation occurs through the blockage of diaphragmatic lymphatics that restrains the outflow of the fluid from the peritoneal cavity, leading to the accumulation of ascites fluid abdominal swelling in advanced stages (Romero and Bast Jr, 2012).

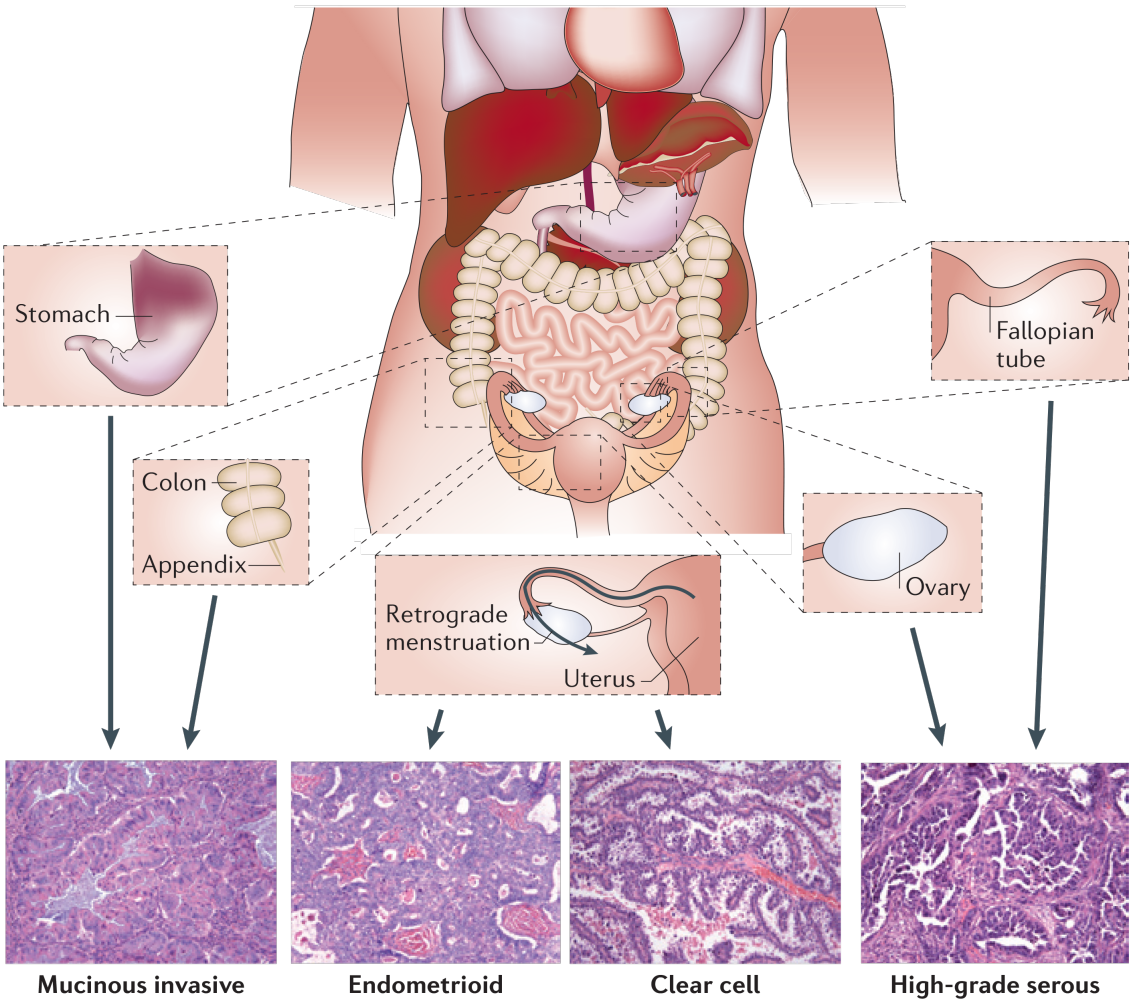

Figure 2. Origin and histotypes of ovarian cancer
This figure is used with permission and originally published by Vaughan, S., Coward, J. I., Bast, R. C., Berchuck, A., Berek, J. S., Brenton, J. D., Coukos, G., Crum, C. C.,Drapkin, R. & Etemadmoghadam, D in 2011 in Nature Cancer Reviews

Molecular alterations are also critical in the development and progression of OC. *TP53* is mostly mutated in high-grade tumors whereas *BRAF* and *KRAS* mutations are more frequent in low-grade serous tumors. Clear cell and endometrioid tumors commonly exhibit mutations in PI3K pathway (*PTEN, PIK3CA*) and *RAS* mutations are mostly

assessed in mucinous OC (Coleman et al., 2013). Inherited *BRCA1* and *BRCA2* mutation mostly lead to Type II tumors (Sessa and Del Conte, 2010).

In the treatment of ovarian cancer, surgery has a pivotal role for the extended survival of the patient. It is then followed by a combination of carboplatin- and taxane-based therapy. Although 70 % of patients respond to the initial therapy at this stage, drug resistant cells can remain dormant in the peritoneal cavity and lead to recurrent disease (Bast et al., 2009).

Carboplatin is an alkylating agent that binds covalently to DNA; thereby creating adducts that form intrachain or interchain crosslinks. Paclitaxel increases microtubule stability through non-covalent interaction and prevents the mitotic spindle formation. Platinum-based cancer therapy was first introduced in late 1970s with cisplatin. Then it was replaced with carboplatin that has lower toxic effects in combination with other agents such as taxanes (Figure 3) (Vaughan et al., 2011). The combination therapy can improve survival rather than single agent treatment. For instance, combination of carboplatin with paclitaxel (Parmar et al., 2003, Gonzalez-Martin et al., 2005), gemcitabine (Pfisterer et al., 2006), or liposomal doxorubicin (Pujade-Lauraine et al., 2010) leads to better survival than single carboplatin treatment (Bast and Markman, 2010).

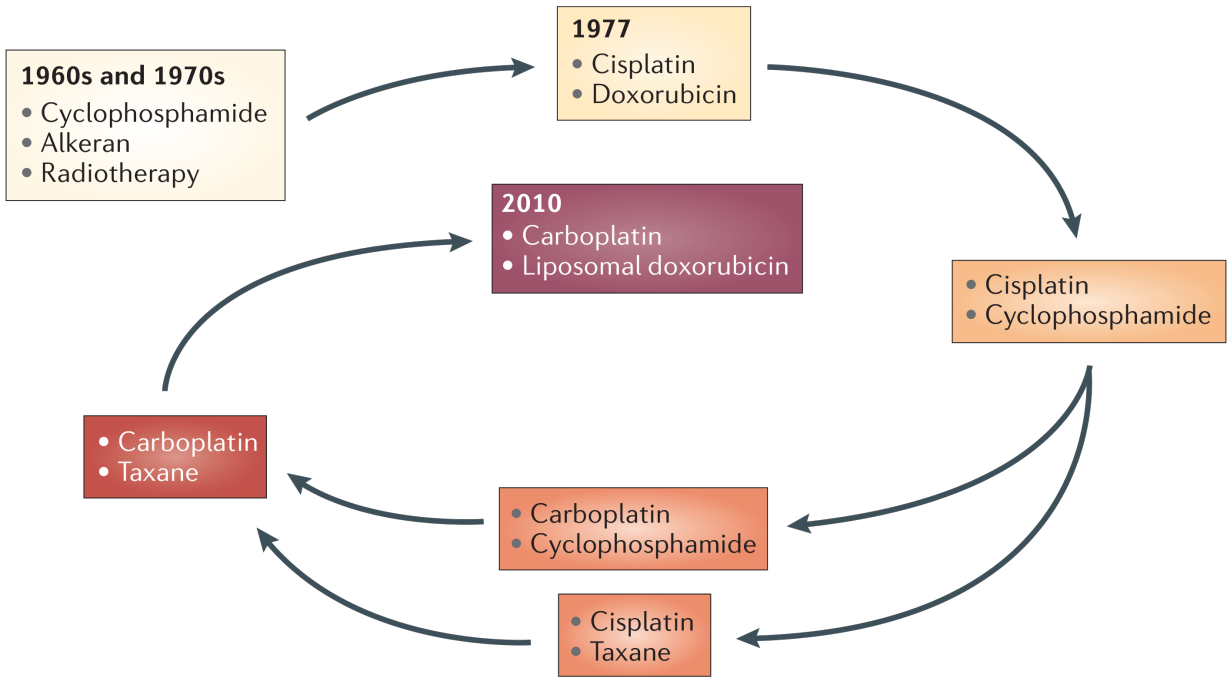

Figure 3. Evolution of chemotherapy for ovarian cancer
This figure is used with permission and originally published by Vaughan, S., Coward, J. I., Bast, R. C., Berchuck, A., Berek, J. S., Brenton, J. D., Coukos, G., Crum, C. C.,Drapkin, R. & Etemadmoghadam, D in 2011 in Nature Cancer Reviews

Overall, chemotherapy improves the survival of patients however the tumor relapse in most cases and long-term survival rate is relatively low. The primary reason of the treatment failure is the development of drug resistance. Thus, identification of new targets and a better understanding of the biology behind the tumor growth and survival are required.

Given the heterogeneity of OC at molecular level, extensive characterization of cancer specimens is required in order to find out the altered genes and/or proteins that can be targeted in patients. DNA sequencing of relevant genes, high-resolution comparative genomic hybridization, single nucleotide polymorphism analysis, expression arrays,

reverse phase protein arrays can be carried out for further characterization of the tumors (Bast et al., 2009). In addition, The Cancer Genome Atlas (TCGA) database reveals the expression of relevant genes in a variety of tumor types and the correlation with survival in patients.

RNAi-based screenings are carried out not only to find out new targets in ovarian cancer cells but also to knockdown the relevant genes *in vitro* and *in vivo*. RNAi based therapies offer a unique opportunity to knockdown specific genes and paves the way to personalized medicine in cancer therapy. In order to achieve sufficient delivery of RNAi, biological barriers have to be overcome. This emphasizes the crucial role of nanotechnology-based carriers in the development of novel strategies.

Early-phase RNAi based therapy trials drew the attention to the feasibility of siRNA delivery into tumors and the selective knockdown of target of interest at tumor site (Tabernero et al., 2013, Davis et al., 2010). These studies showed the potential of RNAi-based therapy as a promising strategy in cancer management. However, there are still critical steps to be taken in the development of RNAi based therapeutics. These include the delivery (accumulation, uptake, and intracellular trafficking) and siRNA target selection and validation (Wu et al., 2014).

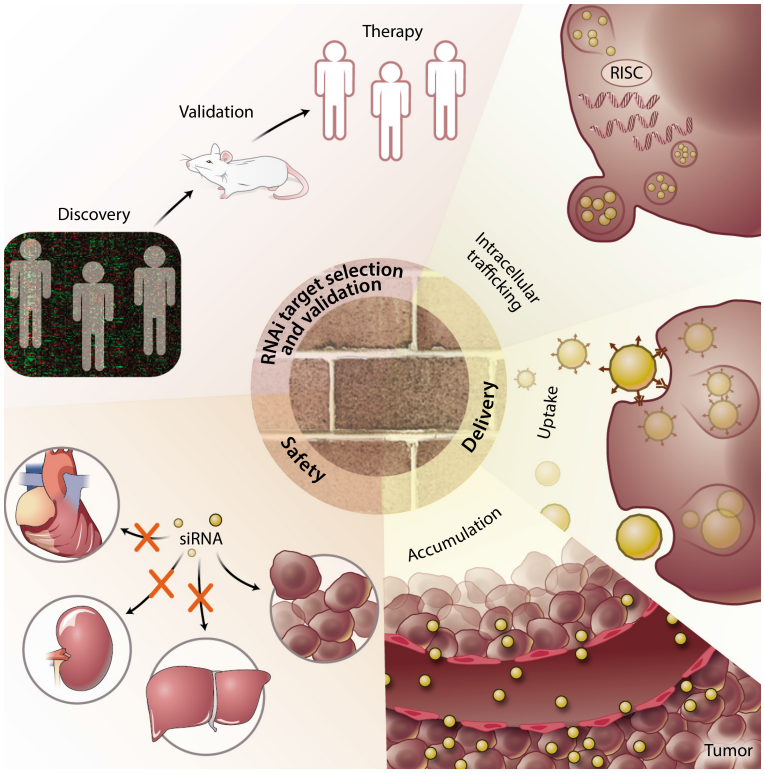

Figure 4. Overcoming obstacles in RNAi delivery
This figure is used with permission and originally published by Wu, S. Y., Lopez-Berestein, G., Calin G. A., Sood A. K., in 2014 in Science Translational Medicine

Wu and her colleagues summarize the overall strategy in five sub-aims (Figure 4). Target selection and validation are as critical as nanocarrier characterization. In addition, relevant toxicology, pharmacology, and pharmacokinetics should be considered and toxic immune mediated reactions should be assessed in the early steps of the development. In this study, we also aimed to take the initial steps of the development and characterization of a novel RNAi-based therapeutic agent.

Metastasis

Metastasis is a multistep process that requires the acquisition of genetic and epigenetic alterations within a tumor cell (Valastyan and Weinberg, 2011). Initially, tumor cells detach from the extracellular matrix and invade through the surrounding tissue. Next, the cells migrate towards a vascular supply and penetrate into the vessels, followed by gaining access to the systemic circulation. The last step is the extravasation of these tumor cells into organ parenchyma and their proliferation in the distant organs in an appropriate microenvironment (Figure 5) (Talmadge and Fidler, 2010).

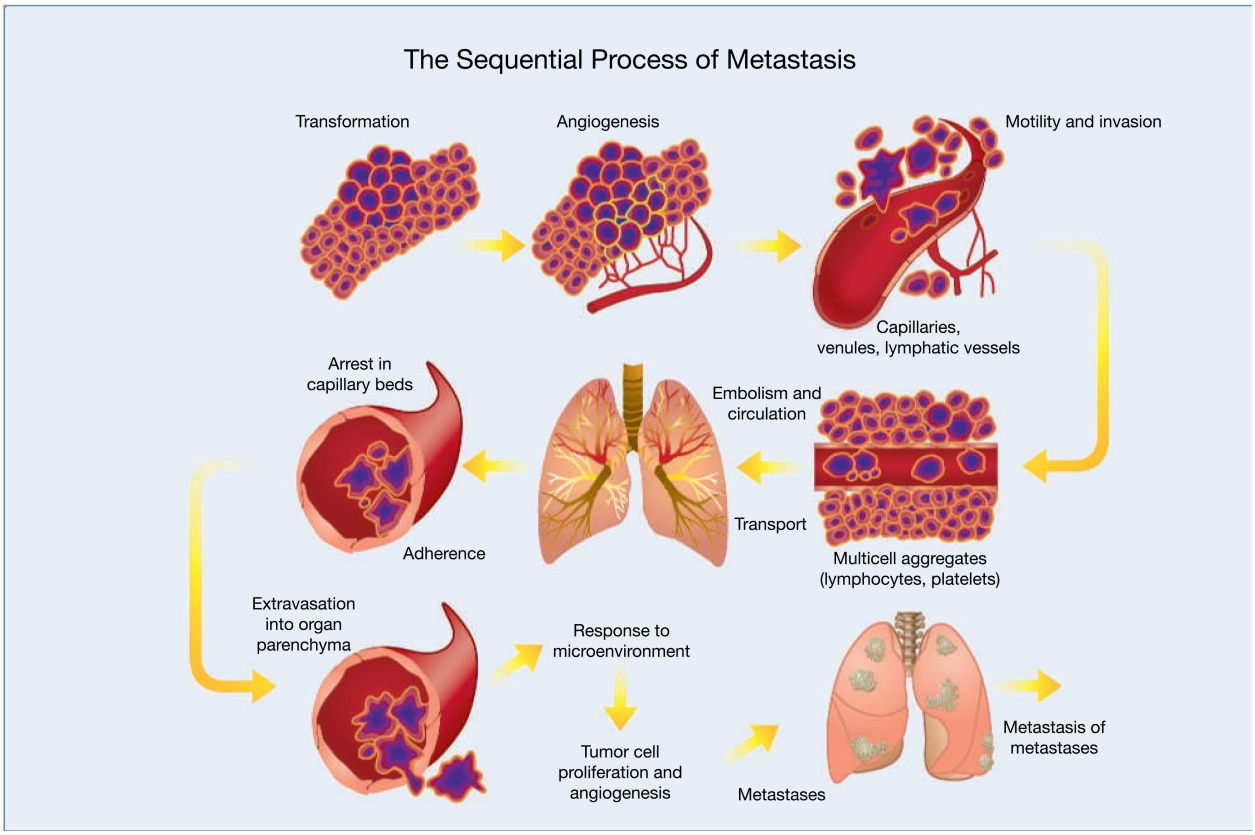

Figure 5. Invasion-metastasis cascade
This figure is used with permission and originally published by Talmadge JE and Fidler IJ in 2010

Hence, the tumor cells can repeat the entire cascade that can lead to additional metastases (Langley and Fidler, 2011).

Historically, metastasis was thought to be a random case. However, in 1889, Stephen Paget declared that the organ distribution of metastases in breast cancer patients was not random and he suggested that some tumor cells (seed) tend to grow in the microenvironment of selected organs (soil) (Paget, 1889). Schackert and Fidler also demonstrated that some tumor cells metastasize to specific regions within an organ (Langley and Fidler, 2011, Schackert and Fidler, 1988).

Ovarian cancer has the propensity to spread to the abdominal cavity and forms nodules on the surface of peritoneum including omentum. But the mechanism of spread was not known. However in a recent study, Sunila Pradeep and her colleagues demonstrated that circulating tumor cells localize and proliferate in the omentum and spread to the other peritoneal surfaces. They used a parabiosis model where the skins of two mice were surgically fused (Pradeep et al., 2014). The study showed that an increased level of ErbB3 in ovarian cancer cells and NRG1 in the omentum is responsible for the hematogenous omental metastasis.

Anoikis

Anoikis is a form of cell death subsequent to loss of contact with extracellular matrix or neighboring cells. However cancer cells develop resistance to anoikis and survive in the absence of this contact. Therefore, disrupting the anoikis resistance in tumor cells may be an effective strategy to prevent metastasis (Young et al., 2013).

Epithelial cells require adhesion to extracellular matrix through cell surface receptors known as integrins. Integrins are heterodimers that consists of α and β subunits. There are 18 α and 8 β subunits of integrins. The integrin ligation leads to cell adhesion, migration and survival through tranducing the signals whereas unligated integrins induce apoptosis and prevent non-tumorigenic cells to survive in an inappropriate environment (Desgrosellier and Cheresh, 2010). Integrins serve as a mechanosensor through monitoring the extracellular environment and become activated via tensional forces and mechanical stress (Nagano et al., 2012). The cytoplasmic β tail is essential in transducing the signaling that can be initiated either outside or inside the cell. Intracellular proteins that are known to bind this region include talin, kindlins and filamins (Harburger and Calderwood, 2009).

Integrins activate multiple oncogenic pathway that also activates cell survival and motility (Guo and Giancotti, 2004). Integrin ligation activates Focal Adhesion Kinase (FAK) – a nonreceptor tyrosine kinase that can phosphorylate both itself at Y397 and other cellular proteins such as Src and p85 subunit of PI3K, mediating cell survival and

migration (Figure 6). In addition, integrin signaling can induce BCL2, which is anti-apoptotic to prevent the cells from undergoing apoptosis (Zhang et al., 1995)

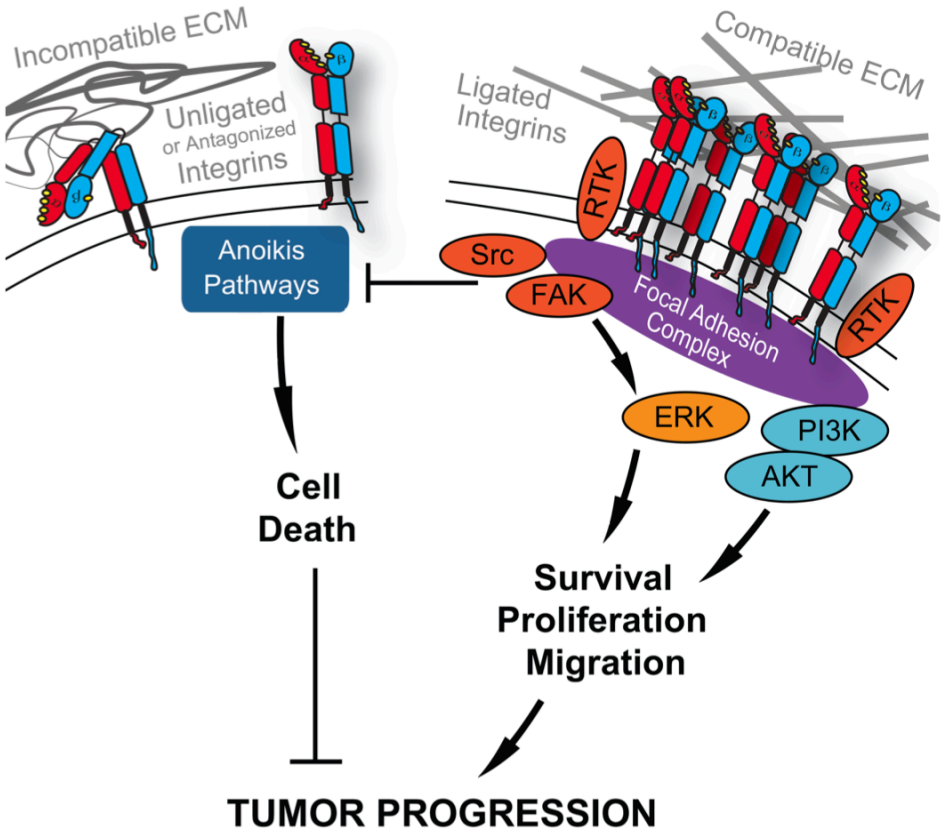

Figure 6. Anoikis and integrins
This figure is used with permission and originally published by Young, S. A., Graf, R. & Stupack, D. G. in 2013, in Neuroblastoma Integrins.

Hypothesis and Aims of The Study

The poor survival of ovarian cancer patients is associated with advanced disease at the time of diagnosis. However, few effective strategies to target this metastatic process currently are known; this highlights the need for a deeper understanding of the molecular mechanisms that regulate OC growth and progression. To identify new therapeutic targets and strategies, we carried out an integrated analysis of The Cancer Genome Atlas (TCGA) HGSOC dataset and gene profiles of ovarian and breast tumors to identify genes that are important for cancer metastasis. Among the genes identified, zinc finger protein 304 (ZNF304) was found to be highly associated with overall survival in HGSOC patients. ZNF304 is a transcription factor that belongs to the C2H2 zinc finger family. The member genes of this family represent the largest class of transcription factors in humans and, indeed, one of the largest gene families in mammals (Tadepally et al., 2008). ZNF304 can be upregulated by activated Kirsten rat sarcoma viral oncogene homolog (KRAS) in KRAS-positive colorectal cancer cells and binds at the promoters of INK4-ARF and other CpG island methylator phenotype genes in colorectal cancer cells and in human embryonic stem cells (Serra et al., 2014). However, the role of ZNF304 in metastasis and its downstream effectors are not well understood.

Synthetic siRNAs are an effective gene-silencing tool. However, its disadvantage is its rapid degradation by serum nucleases, poor cellular uptake and rapid renal clearance following systemic administration. Nanomedicine provides for safe and effective for the systemic administration of siRNA. In the nanotechnology component of the project, a

novel dual assembly nanoparticle system (DANP) is developed and characterized for the *in vivo* delivery of ZNF304 siRNA. The goal was to improve functional applications of DANP to maintain a constant siRNA level by releasing at a predetermined rate over an extended period of time with minimum side effects. Here, we aimed to unravel the mechanisms by which ZNF304 promotes cancer metastasis and to evaluate its role as a potential therapeutic target using siRNA and Dual Assembly Nanoparticles (DANP).

Overall hypothesis of the present study is:

Dual assembly nanoparticles (DANP) loaded with ZNF304 siRNA will lead to prolonged silencing of the target gene and antitumor activity in orthotopic models of OC.

We tested this hypothesis with the following specific aims:

Specific Aim 1. To identify a novel target gene and determine its mechanism of action in OC

Specific Aim 2. To develop and characterize siRNA loaded DANP and to demonstrate that DANP-siRNA leads to sustained silencing of target genes in an orthotopic model of ovarian cancer.

Specific Aim 3. To demonstrate the antitumor activity of DANP siRNA in orthotopic models of ovarian cancer.

CHAPTER II: Methods

Integrative computational analysis and patient data selection

Clinical and expression data (Level 3 Illumina HiSeqv2) for 260 patients were downloaded from The Cancer Genome Atlas portal and were used to analyze the relationship between expression of ZNF304 and overall survival as well as between expressions of ZNF304 and ITGB1. The Spearman's rank-order correlation test was applied to measure the strength of the association between ZNF304 and ITGB1 levels in patient samples in TCGA dataset.

Cell lines and culture. The immortalized non-transformed human ovarian surface epithelial cell line HIO-180 and the human epithelial OC cell lines HeyA8, MDAH 2774, SKOV3IP1, A2780PAR, and A2780CP20 were maintained as described previously (Kamat et al., 2007, Lu et al., 2007b, Lu et al., 2007a, Sood et al., 2001, Thaker et al., 2004). Taxane resistant HeyA8MDR and SKOV3-TR cells were maintained in Roswell Park Memorial Institute 1640 medium supplemented with 10% fetal bovine serum and 0.1% gentamicin sulfate (Gemini Bio-Products) with or without paclitaxel (300 ng/ml for HeyA8-MDR; 150 ng/ml for SKOV3-TR). The A2780CP20 cell line was developed by sequential exposure of the A2780 cell line to increasing concentrations of cisplatin. All of the cell lines are routinely screened for Mycoplasma species (Mycoalert Mycoplasma Detection Kit, Lonza). All in vitro and in vivo experiments were conducted when cells were 70% to 80% confluent.

Western blot analysis. Western blot analysis was performed as previously reported (Landen et al., 2005, Halder et al., 2006). All antibodies used in this study and vendors are listed in Appendix in Table 3.

SiRNA constructs and delivery. SiRNAs were purchased from Qiagen or Sigma-Aldrich. A non-silencing siRNA that did not share sequence homology with any known human mRNA was used as a control for target siRNA. In vitro transient transfection was performed as described previously (Landen et al., 2005). The ZNF304 siRNA sequences are listed in Appendix in Table 2.

Invasion and migration assays. Cell migration and invasion assays have been described previously (Spannuth et al., 2009). For migration assays, cells were treated with either control or ZNF304 siRNA for 72 hours. Then, cells were re-suspended in serum-free medium (5×10^4 cells/ml), and 1 ml of the cell solution was added to gelatin-coated inserts. The inserts were then transferred to wells filled with serum-containing medium. Cells were allowed to migrate for 6 hours at 37°C. Migrated cells on the bottom of the wells were collected, fixed, stained, and counted by light microscopy. Cells were counted in 10 random fields (× 200 final magnification), and the average number of migrated cells was calculated; the percentage of migration was determined by setting control siRNA-treated samples as 100% migration.

For invasion assays, cells were treated with control or ZNF304 siRNA for 48 hours. Then, cells were resuspended in serum-free medium (5×10^4 cells/ml), and 1 ml of the cell solution was added to inserts coated with a defined matrix consisting of

human laminin, type IV collagen, and gelatin (Kim et al., 2011). Inserts were then transferred to wells filled with serum-containing medium. Cells were then allowed to invade for 24 hours at 37°C. Migrated cells on the bottom of the wells were collected, fixed, stained, and counted by light microscopy. Cells were counted in 10 random fields (× 200 final magnification), and the average number of migrated cells was calculated; the percentage of migration was determined by setting the control siRNA-treated samples as 100% invasion.

RPPA. This study was conducted in The University of Texas MD Anderson Cancer Center Institution RPPA Core Facility, and the method was described previously (Tibes et al., 2006). In brief, cellular proteins were denatured by 1% sodium dodecyl sulfate (with beta-mercaptoethanol) and were diluted in 5 2-fold serial dilutions in dilution buffer (lysis buffer containing 1% sodium dodecyl sulfate). Serial diluted lysates were arrayed on nitrocellulose-coated slides (Grace Bio-Labs) with an Aushon 2470 arrayer (Aushon BioSystems). A total of 5808 array spots were arranged on each slide, including the spots corresponding to positive and negative controls prepared from mixed cell lysates or dilution buffer, respectively. Each slide was probed with a validated primary antibody plus a biotin-conjugated secondary antibody. In the RPPA analysis, the antibodies were used if only the Pearson correlation coefficient between RPPA and Western blotting was greater than 0.7. Antibodies with a single or dominant band on Western blotting were further assessed by direct comparison to RPPA using cell lines with differential protein expression or modulated with ligands/inhibitors or siRNA for phospho- or structural proteins, respectively. The signal obtained was amplified using a Dako

Cytomation-catalyzed system and was visualized by diaminobenzidine colorimetric reaction. The slides were scanned, analyzed, and quantified using customized software (MicroVigene, VigeneTech Inc.) to generate spot intensity. Each dilution curve was fitted with a logistic model ("Supercurve Fitting" developed by the Department of Bioinformatics and Computational Biology in MD Anderson Cancer Center, "http://bioinformatics.mdanderson.org/OOMPA"). This model fits a single curve using all the samples (i.e., dilution series) on a slide, with the signal intensity as the response variable and the dilution steps as independent variables. The fitted curve was plotted with the signal intensities—both observed and fitted—on the y-axis, and the log2-concentration of proteins plotted on the x-axis for diagnostic purposes. The protein concentrations of each set of slides were then normalized by Tukey's median polish, which was corrected across samples by the linear expression values using the median expression levels of all antibody experiments to calculate a loading correction factor for each sample (Adapted from UT MD Anderson Cancer Center RPPA Core Facility website).

Cell-cycle analysis. Cells were transfected with either control siRNA or ZNF304 siRNA, trypsinized and collected 72 hours post transfection. Samples were washed in phosphate-buffered saline solution (PBS) and were fixed in 75% ethanol overnight. Cells were then centrifuged, washed twice in PBS, and reconstituted in PBS with propidium iodide (PI; 50 μg/ml), as previously described (Landen et al., 2010). PI fluorescence was assessed by flow cytometry, and the percentage of cells in each cycle was analyzed by FlowJo software.

Chromatin immunoprecipitation assay. HeyA8 cells were cultured in 10% fetal bovine serum to ~75% confluence, and cells were cross-linked with 37% formaldehyde for 20 minutes and were incubated with glycine (0.125 M) for 5 minutes to stop the cross-linking, as previously described (Cheema et al., 2003). Cells were lysed, and chromatin was sonicated according to the protocol provided by the kit (EZ ChIP, Upstate Biotechnology; cat #17-371). Possible binding sites of ZNF304 in the *ITGB1* promoter were predicted using an online tool (http://compbio.cs.princeton.edu/zf/). Six primer pair sets were designed using basic local alignment search tool software (National Center for Biotechnology Information). Primers used for amplification of the DNA in quantitative PCR are shown in Appendix Table 6. Anti-ZNF304 antibody (Table 3) was used for the chromatin immunoprecipitation assays. The Bio-Rad DNA Engine Dyad Thermal Cycler was used with the following cycling conditions: 2 minutes at 94°C, followed by 35 cycles of 30 seconds at 94°C, 30 seconds at 58°C, and 1 minute at 68°C, followed by 1 minute at 68°C.

Plasmid construction and luciferase reporter assay. Fragments containing the predicted binding sites (BS1, BS2, and BS3) were amplified from HeyA8 cell genomic DNA by PCR using primers containing SacI or HindIII restriction enzyme sites. The PCR products were purified, digested, and subsequently cloned into the same restriction site of the pGL3 control vector (Promega) downstream of the firefly luciferase reporter gene. Sequences were analyzed with a DNA BigDye Terminator sequencing kit, version 3.1 (Life Technologies) HeyA8 cells were plated in 24-well plates (60,000 cells per well) 24

hours prior to transfection with either ZNF304 siRNA or ZNF304-expressing vector (Promega). Twenty-four hours after the first transfection, cells were transfected with the luciferase reporter vectors containing BS1, BS2, or BS3 together with *Renilla* luciferase construct, which was used as a normalization reference. Transfections were performed with Attractene transfection reagent (Qiagen) according to the manufacturer's instructions. Cells were lysed 48 hours after luciferase vector transfection, and activity was measured using a dual-luciferase reporter assay system (Promega) in the Veritas microplate luminometer (Turner BioSystems). Two independent experiments were performed in triplicate.

In vitro anoikis. Cells were transfected with control or ZNF304 siRNA and transferred to 6-well tissue culture plates that were coated with polyhydroxyethylmethacrylate, and cells were cultured in these plates for 72 hours at 37°C in a 5% carbon dioxide atmosphere. After incubation, cells were detached with 0.5% trypsin/0.1% ethylenediaminetetraacetic acid in PBS. Cells were suspended in Roswell Park Memorial Institute 1640 medium and were centrifuged at 500 *g* for 10 minutes. Pellets were washed with PBS and were stained with PI solution (50 μg/ml) containing RNase A (25 μg/ml). After incubating the pellets for 30 minutes at 37°C, we analyzed cell viability by flow cytometry.

Preparation of DANP. DANPs were prepared via ionic gelation of anionic tripolyphosphate and siRNA. Briefly, predetermined tripolyphosphate (0.25% weight/volume) and siRNA (1 μg/μl) were added to chitosan solution, and the

siRNA/chitosan nanoparticles spontaneously formed under constant stirring at room temperature. After incubating the nanoparticles at 4°C for 40 minutes, we collected the siRNA/DANP by centrifugation (Thermo Biofuge) at 13,000 rpm for 40 minutes at 4°C. Chitosan nanoparticles were coated with polylactic acid polymer under probe sonication, and the organic solvent was evaporated. The pellet was washed in sterile water 3 times to isolate siRNA/DANP, which was stored at 4°C until used. For the biodistribution study, DANPs were labeled with rhodamine 6G (Sigma-Aldrich). Rhodamine 6G (0.1% weight/volume) was added to the polymer solution (chloroform) in the simple emulsion. The particles were collected and were washed 3 times to eliminate the nonencapsulated marker.

Orthotopic in vivo models of OC and tissue processing. Female athymic nude mice (NCr-nu) (8-12 weeks old) were purchased from the National Cancer Institute-Frederick Cancer Research and Development Center (Frederick, MD) and were maintained as previously described (Landen et al., 2005). The MD Anderson Cancer Center Institutional Animal Care and Use Committee approved and supervised all animal studies. Mice were cared for in accordance with guidelines set forth by the American Association for Accreditation of Laboratory Animal Care and the United States Public Health Service Policy on Human Care and Use of Laboratory Animals. To generate tumors, SKOV3IP1 cells (1×10^6) or HeyA8 cells (2.5×10^5) were injected into the peritoneal cavity, as previously described (Lu et al., 2008). For therapy experiments, 10 mice were assigned randomly to each group. This sample size was sufficient to provide 80% power for a test at significance level of 0.05. As part of preliminary analysis, we validated the normality assumption and proceeded with a non-parametric test as

appropriate. Treatments with control or ZNF304 siRNA incorporated in DANP were intravenously administered either weekly (150 μg/kg body weight) or biweekly (300 μg/kg body weight). Paclitaxel (100 μg/mouse for the HeyA8 model and 75 μg/mouse for the SKOV3 model) was injected intraperitoneally once weekly. Mice were euthanized 6 weeks after first administration in SKOV3 model and 4 weeks after first administration in HeyA8 model. After euthanasia, we recorded mouse and tumor weight, number of nodules, and distribution of tumors. Individuals who performed the necropsies were blinded to the treatment group assignments. Tissue specimens were fixed with either formalin or optimal cutting temperature medium (Miles) or were snap-frozen in liquid nitrogen.

For the biodistribution study of DANP, mice were injected intraperitoneally with HeyA8 cells (2.5×10^5) for tumor inoculation. When tumors were palpable, rhodamine 6G–labeled particles that contained control siRNA (150 μg/kg) were administered intravenously. After 24 hours, mice were euthanized; tumors and the major organs (brain, heart, kidney, spleen, liver, and lungs) were removed and fixed in optimal cutting temperature medium and sectioned. The organ and tumor distribution of particles was assessed by fluorescence microscopy.

For the toxicity study of DANP-siRNA, C57 mice were treated: DANP alone (n=6), DANP-Control siRNA (n=6), DANP-ZNF304 siRNA (n=6). Two mice were kept without any treatment. 72 hours after the single iv administration mice were anesthetized and blood samples were taken through cardiac puncture. Samples (n=3 mice/group) were analyzed to determine Blood Urea Nitrogen (BUN), Creatinine, Alanine Transaminase (ALT), alkaline phosphatase levels and cytokine levels (n=6

mice/ group) in blood. Furthermore, 4 organs (brain, spleen, kidney and liver) were removed from each mouse. Our pathologist analyzed the hematoxylin and eosin (H&E) stained slide of sectioned paraffin tissue specimens in order to determine whether the organs exhibit any treatment-related clinical signs of toxicity.

In vivo anoikis. Viability of tumor cells from ascites fluid was determined by dual staining with PI and epithelial cell adhesion molecule tagged with fluorescein isothiocyanate. MDAH 2774 cells (2×10^6) were injected intraperitoneally into nude mice, and treatments started when mice developed detectable ascites. Mice were divided into 2 groups, (n=3/group) receiving a single administration of either DANP-control siRNA or DANP-ZNF304 siRNA (300 μg/kg). After 7 days, ascites fluid was drawn from the peritoneal cavity and rapidly centrifuged at 500 *g* for 10 minutes. Pellets were washed with a red blood cell lysis buffer and reconstituted in PBS. Suspended cells were then incubated with excited state absorption-fluorescein isothiocyanate (1:30 dilution) for 30 minutes at room temperature. After incubation, cells were washed and stained with a PI solution (50 μg/ml). Cells were then incubated for 30 minutes at 37°C and analyzed on a Gallios flow cytometer (Beckman Coulter).

Immunohistochemical analysis. Analyses of tumors cell proliferation and microvessel density were conducted by following procedures described previously (Landen et al., 2006, Langley et al., 2003, Lu et al., 2010). Two investigators quantified the number of positive cells in a blinded fashion. The antibodies used and the vendors are listed in Appendix Table 3.

Statistical analysis. Unless specified otherwise, all data are presented as the mean values ± the standard error of the mean from at least 3 independent experiments. Two-sided *t* tests were used to test the relationships between the means of data sets, and *P* values indicate the probability of the means compared, being equal with $*P < 0.05$, $**P < 0.01$ and $***P < 0.001$. Student's *t* tests and analysis of variance were calculated with GraphPad software. Statistical analyses were performed in R (version 3.0.1) (http:///www.r-project.org/), and *P* values less than 0.05 were considered statistically significant. For the analysis of RPPA results, we used the Benjamini-Hochberg multiple testing correction (Benjamini and Hochberg, 1995) to estimate the false discovery rate.

CHAPTER III: Results

Discovery of ZNF304 and its role in human HGSOC

We first carried out an integrative computational analysis to identify genes that are important for cancer metastasis and that are upregulated in ovarian cancer (OC). Since N-cadherin has been reported to play a critical role in invasion and anoikis resistance of cancer cells (Suyama et al., 2002, Abdul Azis, 2013), we first identified gene signatures in tumors with high N-cadherin expression in The Cancer Genome Atlas (TCGA) HGSOC dataset. Of 16,869 genes that were upregulated in OC, 493 genes had a positive correlation with tumoral N-cadherin expression (Figure 7A). Of these 493 genes, ciliary neurotrophic factor receptor (*CNTFR*); melanoma antigen family D, 1 (*MAGED1*); nuclear receptor subfamily 2, group F, member 2 (*NR2F2*), and *ZNF304* were upregulated in invasive ovarian and breast tumor epithelium compared with normal ovarian (Bowen et al., 2009) and breast epithelium (Casey et al., 2009), respectively.

We then assessed the effect of tumoral expression on patient survival for these 4 genes using TCGA HGSOC dataset. For each gene, we randomly split the entire OC patient population into training (2/3 of cases) and validation cohorts (1/3 of cases). In both cohorts, patients were divided into sextiles according to mRNA expression, and the first and last sextiles were contrasted. Importantly, the relationships between overall survival and known prognostic factors such as age or residual disease were examined in both the training and the validation cohorts using a Cox proportional hazards model. Only *ZNF304* was a significant factor in this analysis (Figure 7B and 7C). In contrast, *CNTFR*, *MAGED1*, and *NR2F2* expression levels were not correlated with patient survival (Figure 8). Patients with high tumoral ZNF304 expression had significantly

lower median overall survival than patients with low tumoral ZNF304 expression (Figure 7B [training set, 22.2 versus 48.7 months, *P* = 0.031]; and Figure 7C [validation set, 40.4 versus 26.9 months, *P* = 0.039]). Therefore, ZNF304 was selected for additional studies.

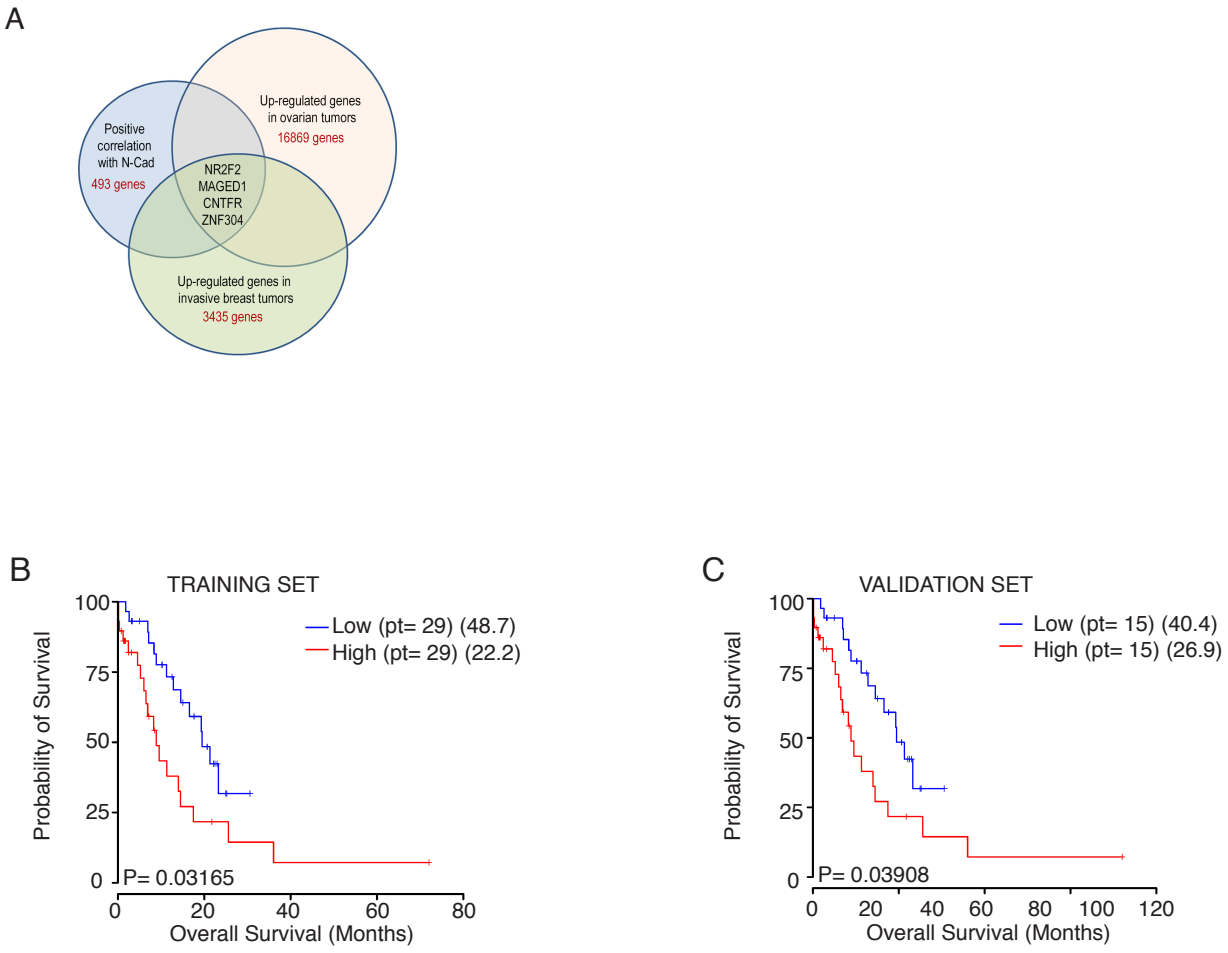

Figure 7. Increased ZNF304 expression is associated with poor survival in HGSOC patients

(A) Graphical representation of computational analysis using TCGA dataset

(B) Kaplan- Meier curves for ovarian carcinoma patients based on ZNF304 expression in Training set and (C) Validation set. Kaplan- Meier curves indicate that high ZNF304 expression is a predictor of poor overall survival in OC patients. (n =88, P= 0.03)

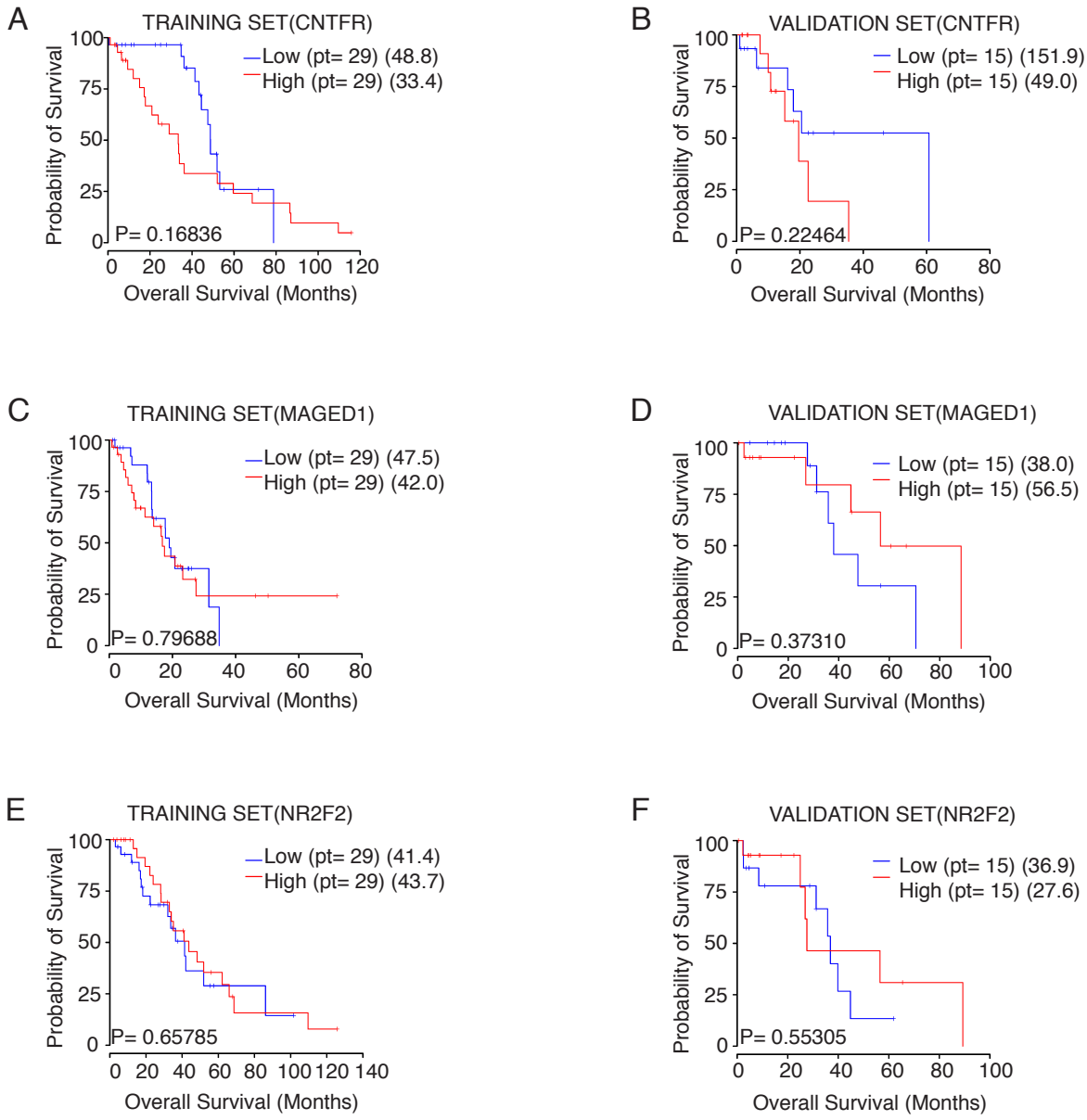

Figure 8. *CNTFR*, *MAGED1*, and *NR2F2* expression levels are not correlated with patient survival in HGSOC patients

(A) CNTFR expression in Training set (left), and (B) Validation set (right); (C) MAGED1 expression in Training set (left), and (D) Validation set (right); (E) NR2F2 expression in Training set(left), and (F) Validation set (right)

Next, we examined protein expression levels of ZNF304 (75 kDa) by Western blot analysis in 6 OC tumor cell lines and in HIO180 non-transformed ovarian epithelial cells (Figure 9A). ZNF304 protein was highly expressed in all OC cells tested, but a lower expression was observed in the HIO180 cells. ZNF304 mRNA basal levels were high in 4 of the 6 OC cell lines

(Figure 9B).

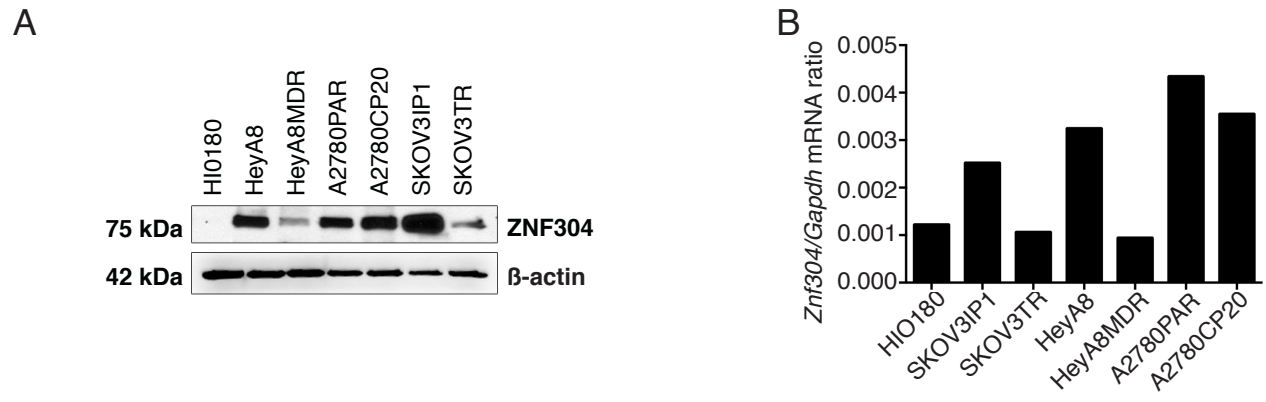

Figure 9. ZNF304 is expressed in ovarian cell lines
(A) Western Blot analysis of ZNF304 protein expression and (B) RT-PCR analysis of ZNF304 mRNA levels in 7 ovarian cell lines

Downregulation of ZNF304 inhibits invasion, migration, and proliferation of OC cells

Given the potential role of ZNF304 in cancer metastasis, we next investigated whether silencing this target would affect invasion and migration. We first tested the knockdown efficiency of 3 siRNA sequences of ZNF304 in HeyA8 cells (Figure 10). Two of the 3 siRNA sequences tested (ZNF304 siRNA-1 and ZNF304 siRNA-3) showed more than 65% inhibition of ZNF304 in HeyA8 cells. Therefore, these 2 siRNA sequences were selected for further studies.

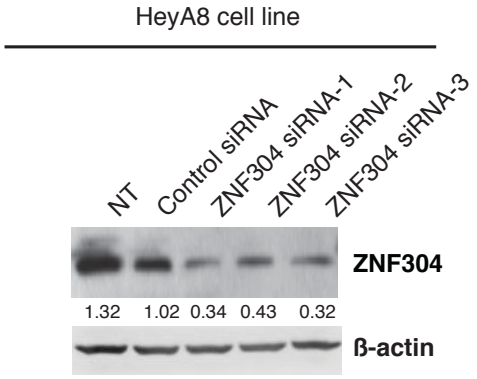

Figure 10. ZNF304 siRNA decreases the ZNF304 levels in HeyA8 cells

Western Blot analysis of ZNF304 protein expression 72 hours after Control siRNA or ZNF304 siRNA transfection in HeyA8 cells.

Next, we performed invasion and migration assays in HeyA8 and SKOV3IP1 cell lines with the selected siRNA sequences, resulting in 40% inhibition of invasion and 45% inhibition of migration in HeyA8 cells (Figure 11, A and B, respectively) and 27% inhibition of migration in SKOV3IP1 cells (Figure 11C).

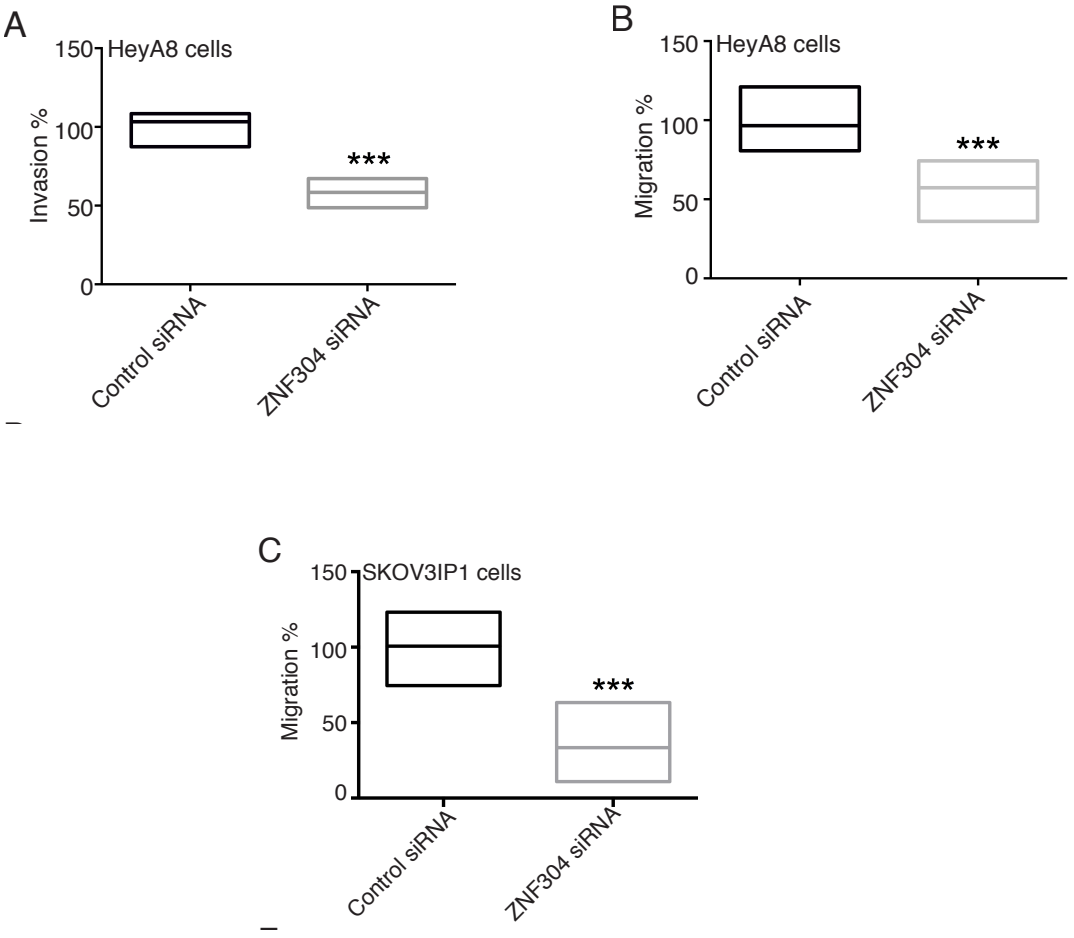

Figure 11. Silencing ZNF304 inhibits invasion and migration

(A) Invasion %, B) migration % of HeyA8 cells, and (C) migration % of SKOV3IP1 cells. Migration and invasion percentages in ZNF304 siRNA treated samples were calculated after normalization with control siRNA treated samples. Data presented as mean ± SEM.

To determine the potential signaling pathways in which ZNF304 is involved, we performed a reverse phase protein array (RPPA) analysis of control siRNA-treated and ZNF304 siRNA-treated HeyA8 cells. Samples were probed with 214 proteins, including total and phospho-proteins. Silencing ZNF304 led to reduced expression of caveolin-1, fibronectin, MYH9 (myosin II), and the effectors of the Ras signaling pathway (BRAF, RAF1) (Figure 12). Focal adhesion and integrin signaling pathways were significantly deregulated in ZNF304-silenced HeyA8 cells. This last finding guided us to further analyze the link between ZNF304 and integrin signaling. In addition, ZNF304 mRNA expression was highly correlated with β1 integrin expression in HGSOC patient samples ($r = 0.20$, $P = 0.0015$; Figure 13).

To further understand the role of ZNF304, we validated the RPPA data and determined the levels of focal adhesion complex members after ZNF304 siRNA transfection in HeyA8 cells. Silencing ZNF304 decreased phosphorylation of Src and FAK, which are adaptor proteins of focal adhesion and major markers of cell migration (Figure 14, A and B, respectively). To further analyze pathways related to migration and invasion, we investigated the effects of ZNF304 silencing on paxillin and β1 integrin (Figure 14C). ZNF304 silencing inhibited both paxillin phosphorylation at tyrosine sites 31 and 118 and β1 integrin expression in the cell lines tested.

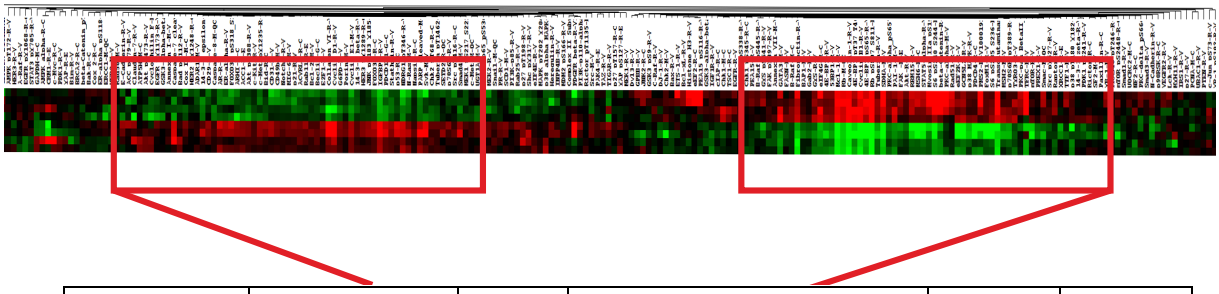

Database	PATHWAY	Count	GENES	*P* Value	FDR
KEGG	Focal adhesion	7	*CAV1, BRAF, PAK4, MET, RAF1, ITGA2, MAPK8, FN1*	9.72E-04	1.0069
KEGG	Insulin signaling	7	*EIF4EBP1, BRAF, TSC2, RAF1, MAPK8, RPS6KB1, RPS6*	8.41E-05	0.0875
PANTHER	PDGF signaling	7	*BRAF, STAT5A, RAB11B, RAF1, RAB11A, MAPK8, RPS6KB1*	0.0026	2.3630
PANTHER	Integrin signaling	6	*CAV1, BRAF, RAF1, ITGA2, MAPK8, FN1*	0.0275	22.5233
KEGG	Actin cytoskeleton	6	*BRAF, PAK4, RAF1, ITGA2, MYH9, FN1*	0.0069	6.9846
PANTHER	Interleukin signaling	6	*CDKN1B, BRAF, FOXM1, STAT5A, RAF1, FOXO3*	0.0238	19.8068
REACTOME	Insulin receptor signaling	6	*EIF4EBP1, TSC2, EEF2K, RAF1, RPS6KB1, RPS6*	4.80E-07	3.76E-04
KEGG	p53 signaling	6	*CCNB1, BID, CCNE1, TSC2, CASP8, TP53, CHEK1*	1.42E-05	0.0148
KEGG	Cell cycle	6	*CCNB1, CCNE1, CDKN1B, SMAD4, TP53, CHEK1, RB1*	4.35E-04	0.4514

Figure 12. RPPA analysis revealed the link between ZNF304 and integrin signaling

Integrated function and pathway analysis were performed using DAVID bioinformatics resources (http://david.abcc.ncifcrf.gov/), and significant features were clustered

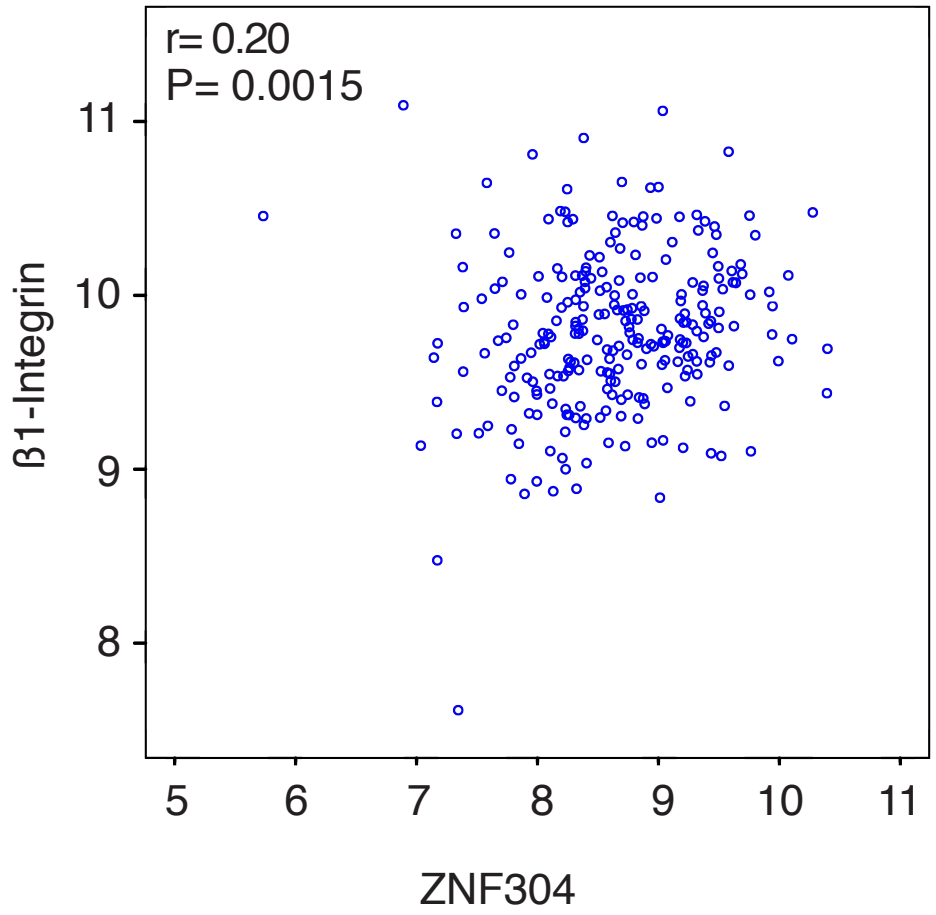

Figure 13. ZNF304 and β1 integrin mRNA levels highly correlates in HGSOC patients

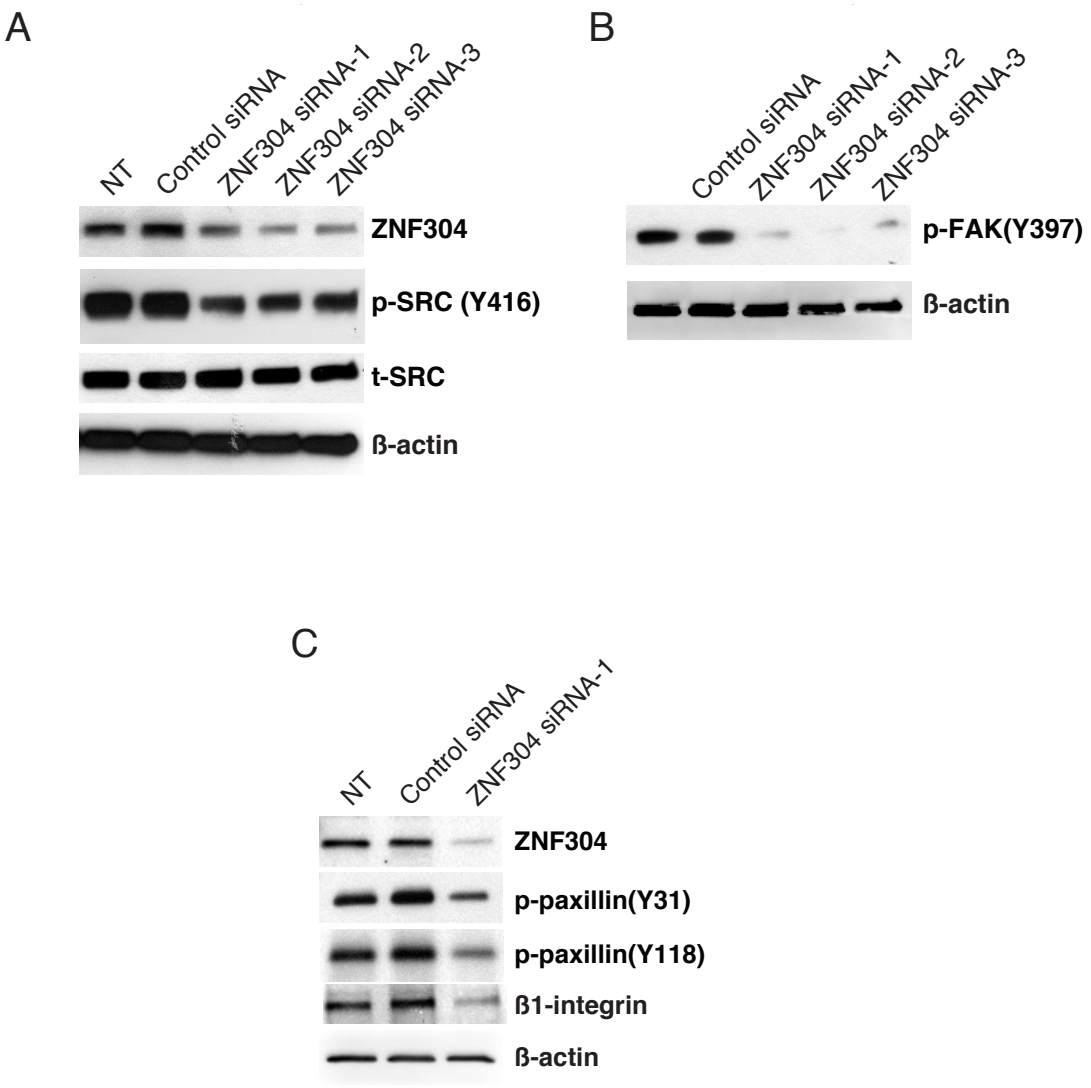

Figure 14. Silencing ZNF304 leads to reduction in focal adhesion complex members

(A) p-src (Y416) and total src levels, (B) Western Blot analysis of FAK phosphorylation

(C) β1 integrin levels and paxillin phosphorylation levels at tyrosine 31 and tyrosine 118 sites upon 72 hours ZNF304 siRNA treatment.

In the RPPA results, forkhead box M1 (FOXM1) and cyclin B1 levels were also decreased in ZNF304-silenced samples, suggesting that ZNF304 might play a role in the cell cycle. To determine the effects of ZNF304 silencing on proliferation, we performed cell-cycle analysis in HeyA8, SKOV3IP1, A2780PAR, and A2780CP20 cell lines after 72 hours of ZNF304 siRNA transfection (Figure 15, A–D, respectively). All cell lines treated with ZNF304 siRNA showed significant arrest in the G2 phase, confirming the decreases in cyclin B**1** and FOXM1 levels found in the RPPA analysis.

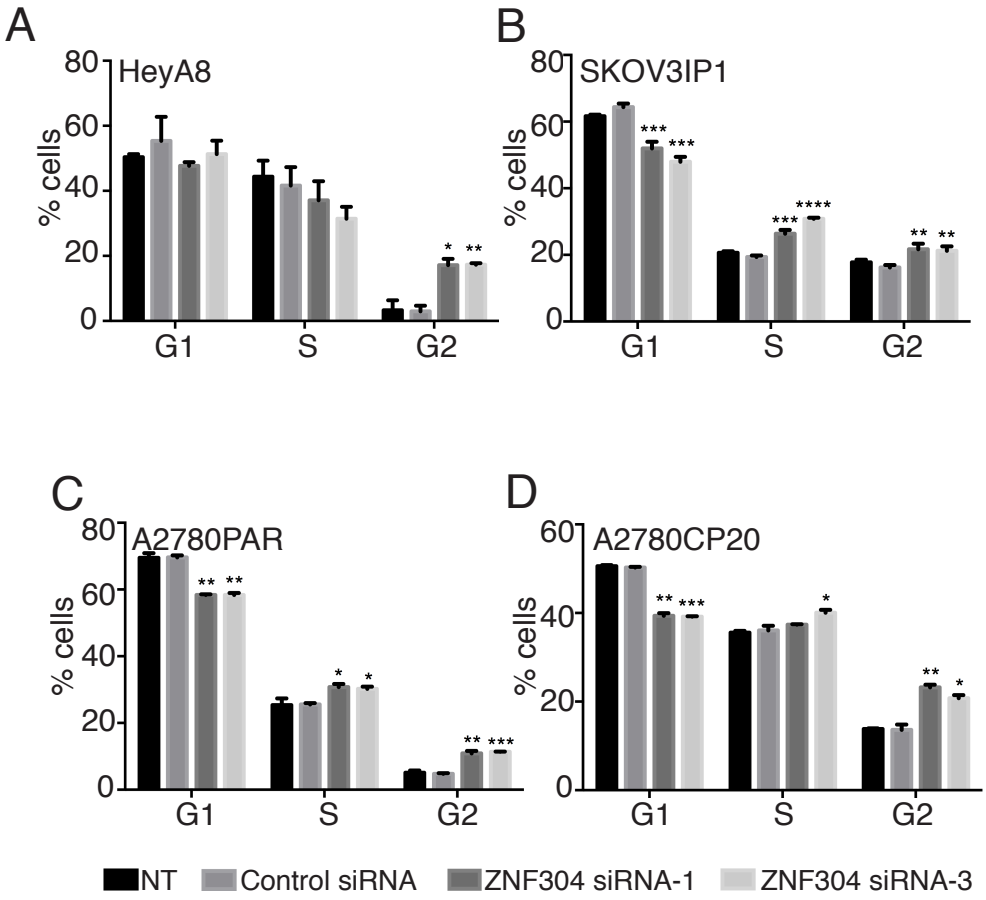

Figure 15. Silencing ZNF304 reduces proliferation through cell cycle arrest
(A) Cell cycle analysis after 72 hours transfection with Control siRNA or ZNF304 siRNA in HeyA8 (B). SKOV3IP1 (C), A2780PAR (D), and A2780CP20 cells (n=3, **P* < 0.05, ***P* < 0.01, ****P* < 0.001).

ZNF304 transcriptionally regulates β1 integrin

The *ZNF304* gene is located at chromosome 19q13.43 (www.genome.ucsc.edu). The ZNF304 protein consists of a Kruppel-associated box domain and 16 zinc finger proteins (UniProt) (Figure 16). To explore the mechanism by which ZNF304 silencing downregulates migration, we determined protein and mRNA levels of β1 integrin upon ZNF304 siRNA treatment in HeyA8 and SKOV3IP1 cells. Silencing ZNF304 reduced β1 integrin mRNA levels in these cells (Figure 17). We determined the basal protein levels of β1 integrin and observed that it was expressed in the cell lines tested (Figure 18).

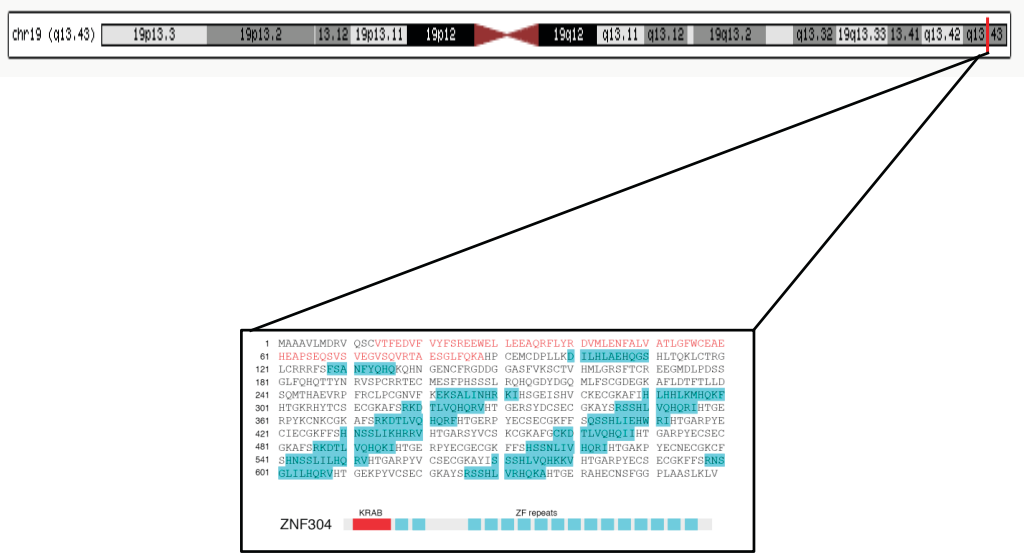

Figure 16. *ZNF304* gene is located at chromosome 19q13.43 and ZNF304 protein consists of 16 zinc fingers.

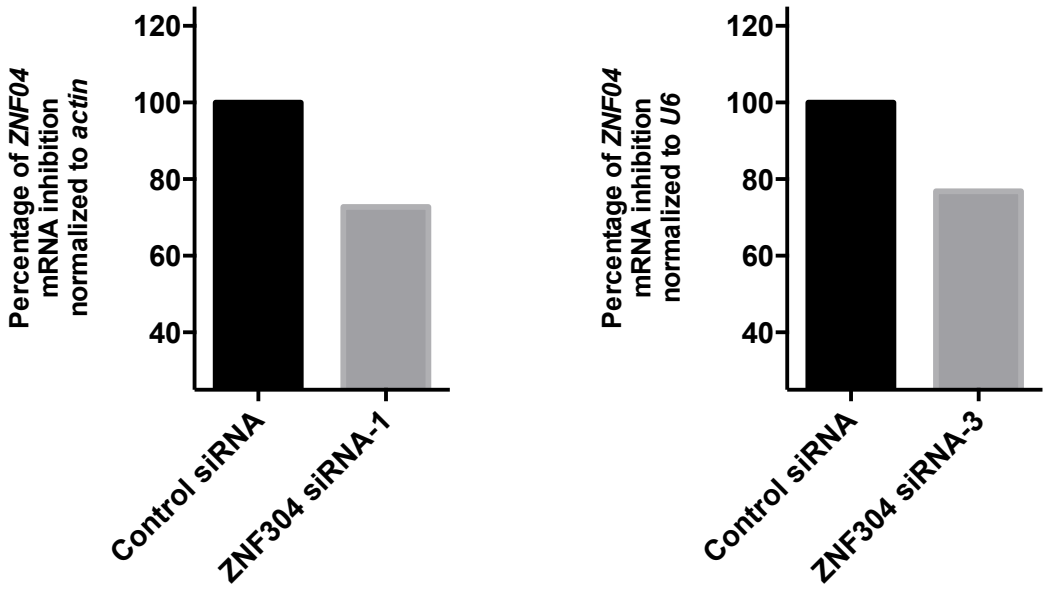

Figure 17. Silencing ZNF304 decreases β1 integrin mRNA levels
Quantification of mRNA levels by Real Time RT-PCR in Control siRNA and ZNF304 siRNA transfected HeyA8 cells (n=2).

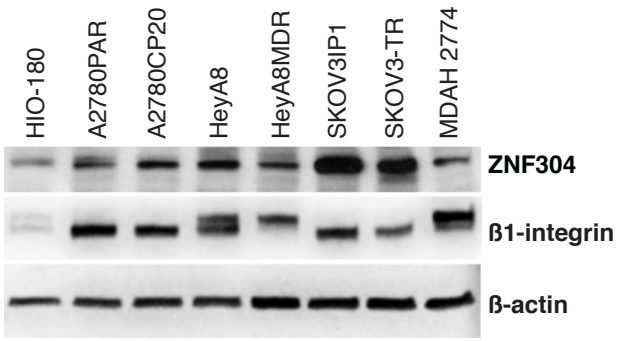

Figure 18. β1 integrin is expressed in all cell lines tested
Western Blot analysis of basal protein expression of ZNF304 and Integrin β-1

We next investigated whether ZNF304 transcriptionally regulates β1 integrin. ZNF304-DNA binding sites were predicted on the basis of support vector machines (Persikov et al., 2009). We identified ten possible ZNF304 binding sites in the β1 integrin promoter by using support vector machine scores that ranged from 24.25 to 18.9 (Figure 19A). The transcription start site was predicted by the ensemble and was compared with the β1 integrin transcript sequence and the binding locations in the β1 integrin promoter region (Figure 19B). Six primer sets containing the segments for the 10 binding sites were designed (Figure 19C). DNA segments were amplified, cloned, sequenced, and confirmed with a standard nucleotide-nucleotide basic local alignment search tool (National Center for Biotechnology Information). To determine whether ZNF304 binds to the β1 integrin promoter, we performed chromatin immunoprecipitation assays (ChIP) in HeyA8 cells with ZNF304 antibody. Subsequent polymerase chain reaction (PCR) results confirmed the interaction of β1 integrin promoter and 5 of the 6 predicted ZNF304 binding sites (BS1, BS2, BS3, BS5, and BS6) (Figure 19D). A densitometric analysis of input and immunoprecipitation results for each binding site revealed that BS1, BS2, and BS3 had an affinity of > 50% (Figure 19E). Owing to their affinity, BS1, BS2, and BS3 were selected for further studies.

A

Primary and complementary DNA regions	SVM score
agttctcctgcctcagcctccggagtagctgggactacaggcacccacga tcaagaggacggagtcggaggcctcatcgaccctgatgtccgtgggtgct	24.2562
agaccagtgtagacaactgtttctaggtctttgaccgtgaagaggagaca tctggtcacatctgttgacaaagatccagaaactggcacttctcctctgt	23.3080
tcgcctgcttccgggtttggagctcttccggaggcacaagggtttcagaa agcggacgaaggcccaaacctcgagaaggcctccgtgttcccaaagtctt	20.9709
tggcttgcttccctcaggccacttctaactgtggtctcctctccgccccc accgaacgaagggagtccggtgaagattgacaccagaggagaggcgggggg	20.7479
cttgtttcgcctgcttccgggtttggagctcttccggaggcacaagggtt gaacaaagcggacgaaggcccaaacctcgagaaggcctccgtgttcccaa	20.5850
tcaggtgatctgcctgcctcagcctcccaaagtgctgagattccaggcgt agtccactagacggacggagtcggagggtttcacgactctaaggtccgca	20.4998
agtctcgctctttcgccaggctagagtacagtggcgcgatcttggctcac tcagagcgagaaaagcggtccgatctcatgtcaccgcgctagaaccgagtg	20.2544
gtcgcaggatcgttgacatctgtcattaaactgtttccagctgctggcct cagcgtcctagcaactgtagacagtaatttgacaaaggtcgacgaccgga	19.2742
gaggctccctggccctctgcctctcctttcctgtccgggtctctgtggct ctccgagggaccgggagacggagaggaaaggacaggcccagagacaccga	19.0826
atttaagtatttccttagggtaaattcccagtagctggattattagaggg taaattcataaaggaatcccatttaagggtcatcgacctaataatctccc	18.9303

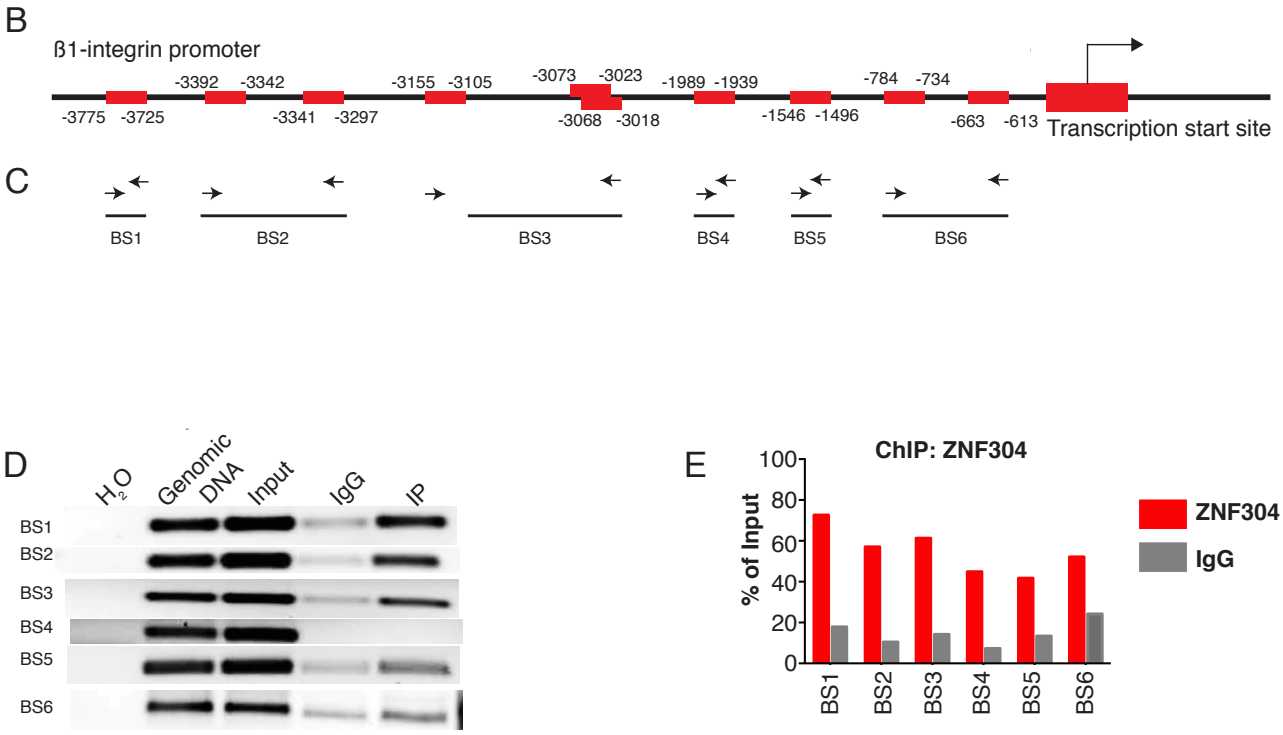

Figure 19. ZNF304 binds to β1 integrin promoter

(A) Predicted binding sites of ZNF304 in ITGB1 promoter based on SVM scores using an online tool, which is available at http://compbio.cs.princeton.edu/zf/
(B) ITGB1 promoter with 10 predicted binding sites,
(C) Six primer sets that were designed for ten predicted sites
(D) ChIP analyses with ZNF304 antibody from HeyA8 cells. Relevant sequences were quantified by PCR with pre-designed six sets of primers subsequent to ChIP assay, (E) densitometric analysis of ChIP analysis. Sequence and antibody specificity controls are included. Data are presented as percentage of input.

To identify the role of ZNF304 in the regulation of β1 integrin gene transcription, we developed 3 constructs that each contained one of the binding sites and inserted them into pGL3-basic vector. HeyA8 cells were transfected with the constructs, and the activity of each binding site was determined by a dual-luciferase reporter assay in cells with basal ZNF304 expression and in cells in which ZNF304 had been knocked down by siRNA. As shown in Figure 20A, overall luciferase activity increased in cells transfected with the binding site constructs compared with cells transfected with empty vector. Cells transfected with BS1-vector had 2 times more luciferase expression than empty vector cells, whereas BS2-vector–transfected cells had 6 times more luciferase expression than did the empty vector cells. Cells transfected with BS3-vector showed the highest luciferase activity (approximately 70 times more expression than empty vector cells). ZNF304 silencing led to a decrease in luciferase activity in all 3 binding sites. The most significant was BS2-transfected cells, which had a 40.3% inhibition of luciferase activity (P = 0.02). We found a 13.8% decrease in luciferase activity for cells transfected with BS1-vector and a 7.8% decrease for cells transfected with BS3-vector, compared with control cells (P = 0.0173 and P = 0.2630, respectively). Co-transfection of ZNF304-expressing vector significantly induced the luciferase activity of BS1-, BS2-, and BS3-vector–transfected cells (Figure 20B). These results indicate that ZNF304 is a positive regulator of the active β1 integrin promoter and that ZNF304 increases its transcription by binding to BS2.

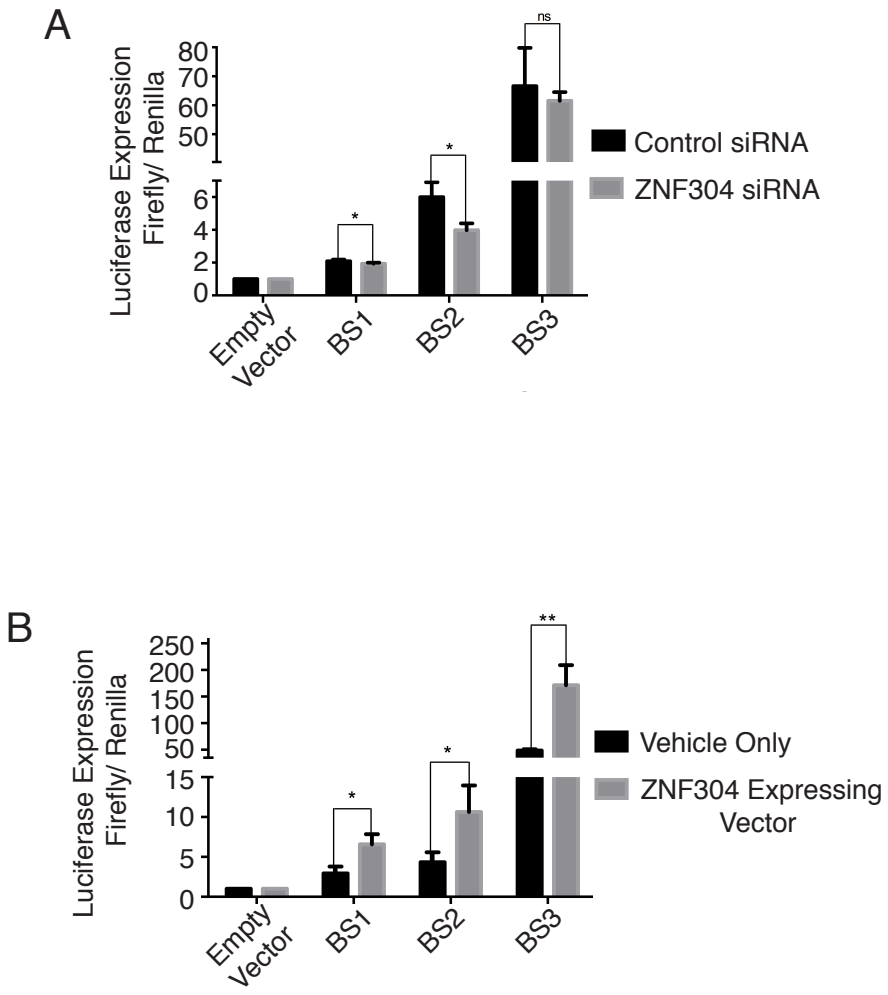

Figure 20. ZNF304 regulates β1 integrin

(A) Luciferase activity upon control siRNA (black) or ZNF304 siRNA (grey) treatment in HeyA8 cells. Fold of induction was calculated after normalization with empty vector. Data presented as mean ± SEM.

(B) Luciferase activity upon ZNF304-expressing vector transfection in BS-1, BS2, and BS-3 vector transfected HeyA8 cells. Data presented as mean ± SEM.

ZNF304 protects tumor cells from anoikis

β1 integrin confers a survival advantage to tumor cells (Vachon, 2011). As a regulator of β1 integrin, ZNF304 can also inhibit anoikis through β1 integrin downregulation. Therefore, we examined detached HeyA8 cells in vitro using polyhydroxyethylmethacrylate (poly-HEMA)-coated tissue culture plates that promote anchorage-independent cell growth (Sood et al., 2010). Cells transfected with either of the ZNF304 siRNAs for 72 hours had a significantly higher (*[ZNF304 siRNA-1, P <0.0001]; [ZNF304 siRNA-3, P <0.0005])* rate of anoikis (75%-80%), than control untreated or control siRNA-treated cells (60%) (Figure 21A). Consistent with these results, immunoblotting from these samples showed that silencing ZNF304 also increased poly ADP ribose polymerase (PARP) cleavage (Figure 21B), which supports our observation of increased anoikis in cells transfected with ZNF304 siRNA.

To determine the link between ZNF304-mediated β1 integrin and anoikis, we also performed a rescue experiment. HeyA8 and SKOV3IP1 cells were transfected with either control siRNA or ZNF304 siRNA. Next, cells were transiently transfected with either empty vector or β1 integrin–expressing vector and transferred to anoikis plates. Both HeyA8 and SKOV3IP1 cells that were transfected with β1 integrin–expressing vector showed increased survival and decreased anoikis rates (Figure 21C). Furthermore, silencing ZNF304 increased the anoikis sensitivity and death rate of HeyA8 cells even in the presence of high β1 integrin expression.

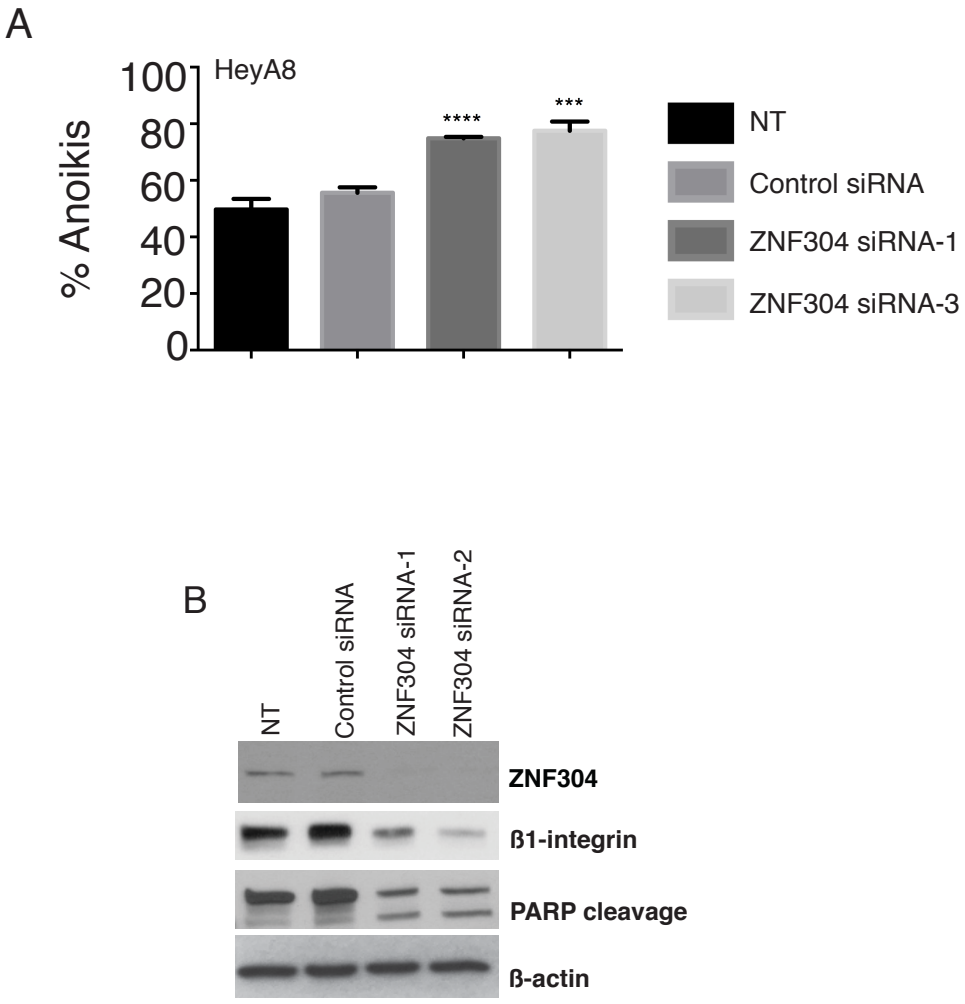

Figure 21. ZNF304 mediates inside-out signaling

(A) The anoikis rate of HeyA8 cells in suspension condition at 24, 48, and 72 hours *in vitro (n=3)*
(B) PARP cleavage in ZNF304 siRNA and control siRNA (72 hours) treated samples in suspension condition.

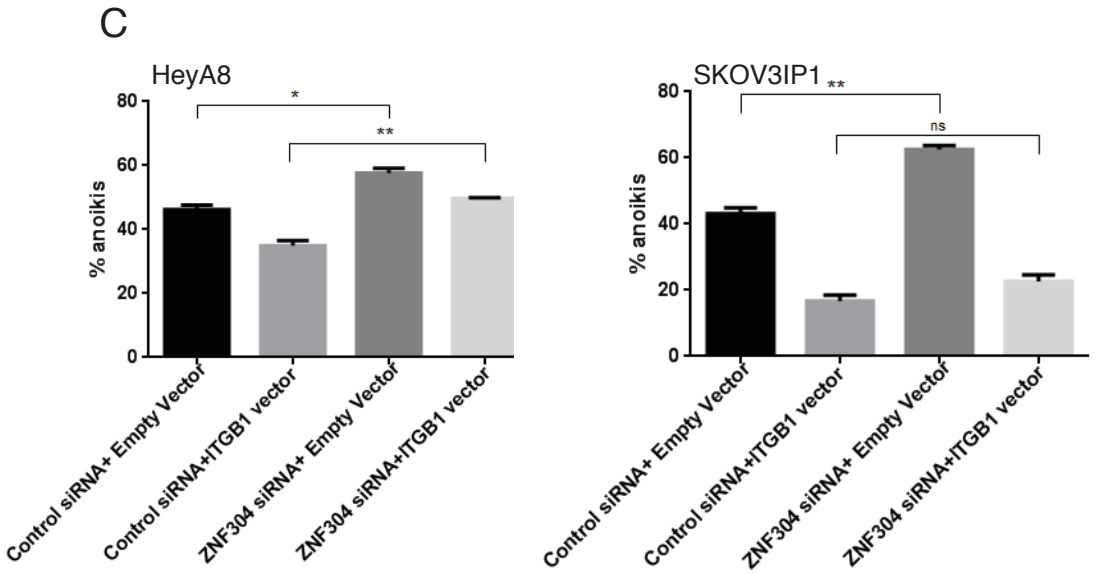

Figure 21 (continued). ZNF304 mediates inside-out signaling
(C) The anoikis rate of HeyA8 and SKOV3IP1 cells in suspension condition after ZNF304 silencing and β1 integrin overexpression *(n=2)*

Development and characterization of DANP

Size, charge and morphology

On the basis of our in vitro findings, we next investigated whether ZNF304 gene silencing would be effective in treating orthotopic murine models of OC. For the in vivo experiments, we developed and characterized a novel delivery system designed for sustained and prolonged gene silencing. Dual assembly nanoparticles (DANP) were prepared by using a chitosan core coated with polylactic acid (PLA). These particles had a diameter of 150-200 nm and a zeta potential of -10 mV, which corresponded to a neutral range (Figure 22, A and B, respectively). Atomic force microscopy images demonstrated the spherical morphology and size distribution of the DANP (Figure 23). This optimized nanoparticle formulation was used for all subsequent experiments owing to their small size, slight negative charge, and high efficiency at incorporating siRNA. We incorporated siRNA in the chitosan core by using chitosan/tripolyphosphate at a 3:1 ratio, which yielded more than 75% loading efficiency, as previously described (Lu et al., 2010).

Biodistribution

We next determined the tissue distribution of the DANP by labeling the particles with rhodamine 6G and administering these red fluorescence–labeled particles as a single dose intravenously to HeyA8 tumor–bearing mice. Twenty-four hours later, the mice were euthanized, and their major organs and the tumors were removed, processed, and sectioned. The number of particles in each field was assessed by fluorescence microscopy (Figure 24).

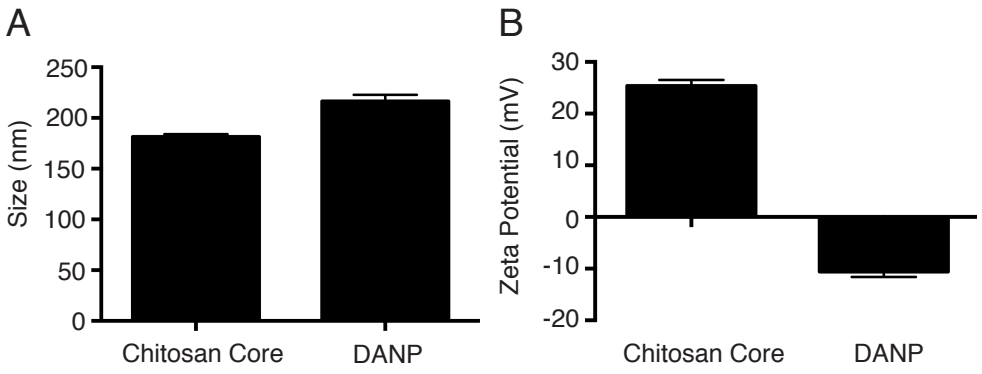

Figure 22. Size and and zeta potential characteristics of DANP

(A) Size and (B) zeta potential of DANP determined by Zeta Sizer (Dynamic Light Scattering).

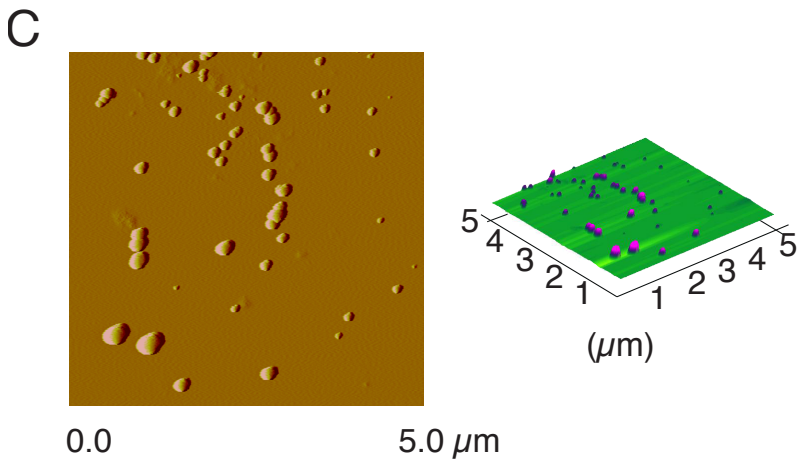

Figure 23. DANP exhibits spherical morphology

C) Atomic Force Microscopy images of DANP showing the morphology and size distribution of particles

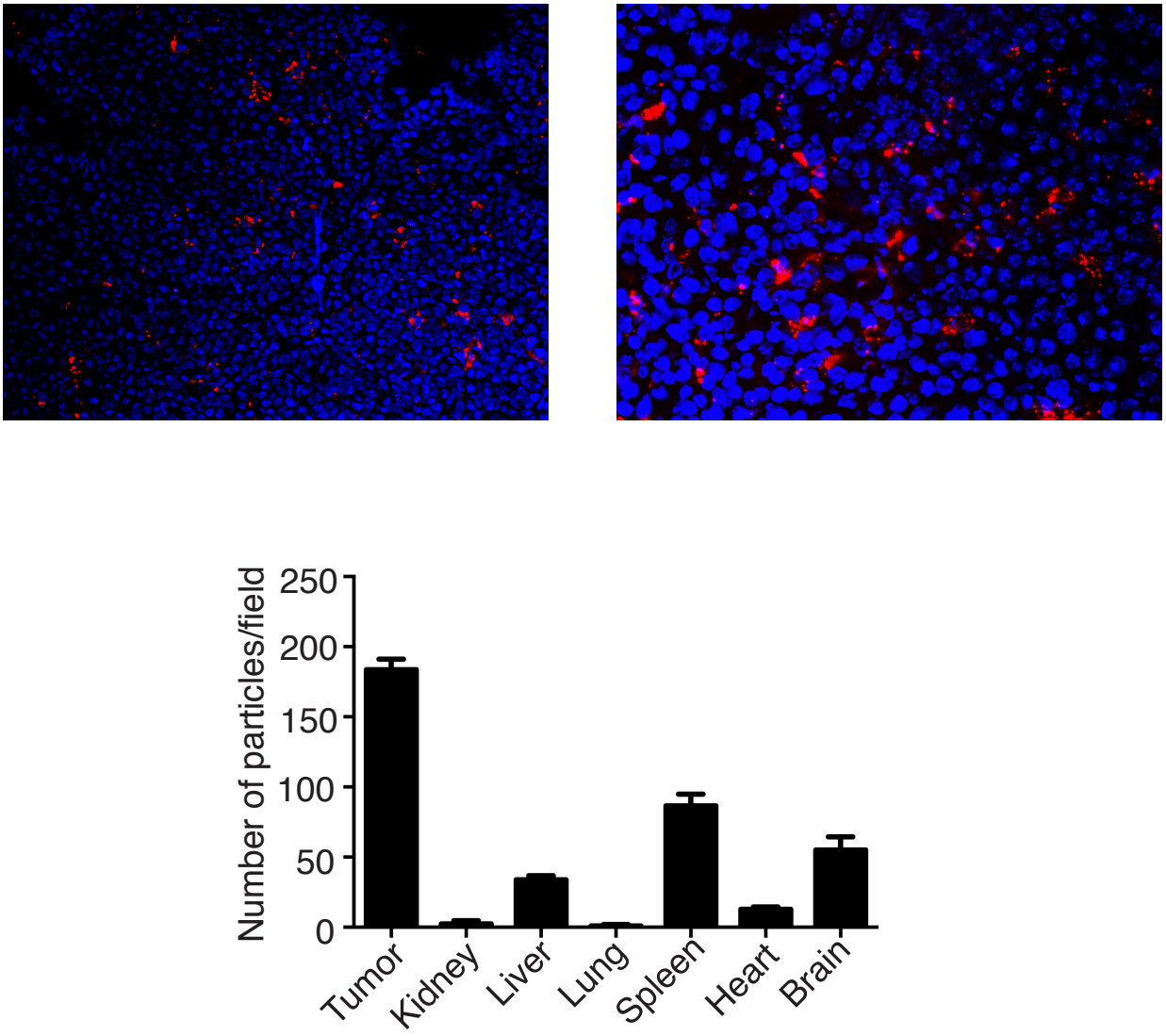

Figure 24. DANP accumulates in tumor
Biodistribution of rhodamine 6G-labeled DANP in vivo. Tumor and the major organs were removed 24 hours after a single administration of rhodamine 6G labeled DANP. The nanoparticles were monitored using fluorescent microscopy and representative images were taken at 10X (left) and 20X magnification (right). Number of nanoparticles was counted at 5 fields per slide (center). Data are presented as means ± standard error of the mean (SEM).

Duration of in vivo gene silencing

In our first set of experiments, we determined the duration of in vivo DANP-mediated *ZNF304* silencing in an orthotopic HeyA8 mouse model. ZNF304-siRNA-DANP (300 µg/Kg body weight) was administered as a single intravenous injection 2 weeks after tumor inoculation. Groups of mice were euthanized on day 3, 7, and 14 after injection. Tumors were collected and analyzed by immunoblotting to determine ZNF304 protein expression levels. We demonstrated that ZNF304 protein silencing started at day 3 and continued up to 14 days after a single administration of ZNF304-siRNA-DANP (Figure 25).

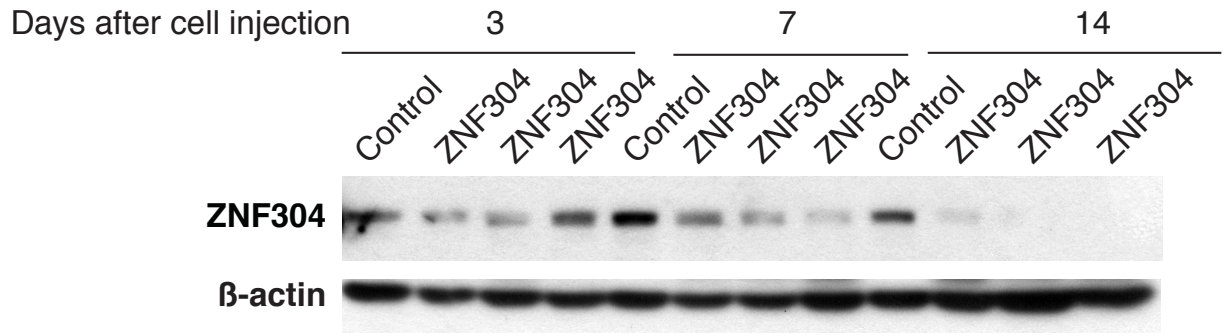

Figure 25. DANP-ZNF304 siRNA downregulates ZNF304 *in vivo* up to 14 days after a single IV injection

Tumors were removed and analyzed by immunoblotting at 3, 7, and 14 days after a single administration of ZNF304 siRNA-DANP.

Toxicity

To determine whether DANP particles alone or containing siRNA will cause toxicity, we assessed the blood chemistries 72 hours after a single IV administration of DANP with or without siRNA incorporation. The groups were: NT (n=1), DANP alone (n=3), DANP-Control siRNA (n=3), DANP-ZNF304 siRNA (n=3). The levels of Alanine Transaminase (ALT), Blood Urea Nitrogen (BUN), Creatinine and Alkaline Phosphatase were and hematologic parameters in normal range at 72 hours after a single intravenous administration of DANP, DANP-Control siRNA, and ZNF304 siRNA (Figure 26, Table 1 respectively) (Schnell et al., 2002). Plasma samples were also analyzed in order to determine whether the treatment caused an inflammatory response. No significant difference was observed in cytokine levels at 72 hours after a single systemic administration (Figure 27).

Additionally, we removed the major organs (liver, kidney, spleen and brain) in order to assess the potential toxicity 72 hours after a single systemic administration. Hematoxylin and eosin stained tissues were analyzed by our pathologist and no sign of toxicity was observed in any of the groups during the analyses (Figure 28). No clinical findings/ abnormalities were observed during animal studies

		NT (n=1)	Empty DANP (n=4)				DANP- ControL siRNA (n=4)				DANP- ZNF304 siRNA (n=4)			
Parameter	**Units**	**Mean**	**Mean**	**Min**	**Max**	**SD**	**Mean**	**Min**	**Max**	**SD**	**Mean**	**Min**	**Max**	**SD**
White Blood Cell Count	10.e3/uL	1.0	2.8	2.0	4.0	0.9	4.1	2.0	5.6	1.5	4.3	2.3	5.8	1.5
Red Blood Cell Count	10.e6/uL	10.7	10.1	9.7	10.4	0.4	10.5	10.0	11.0	0.5	10.1	9.7	10.7	0.5
Hemoglobin	g/dL	15.4	14.8	14.1	15.5	0.6	15.1	14.3	15.5	0.6	14.5	14.0	15.2	0.5
Hematocrit	%	52.9	50.4	49.4	52.0	1.3	51.9	49.6	54.4	2.2	49.8	48.7	52.6	49.8
MCV	fL	49.5	49.7	49.1	51.0	49.7	49.2	48.0	50.1	0.8	49.3	48.4	50.1	0.7
MCH	pg	14.4	14.6	14.4	14.9	0.2	14.4	14.2	14.6	0.2	14.4	14.1	14.9	0.4
MCHC	g/dL	29.0	29.3	29.2	29.9	29.3	29.2	28.6	29.6	0.4	29.2	28.7	29.1	0.5
RDW	%	13.3	13.5	13.0	13.9	0.5	13.0	12.7	13.2	0.2	13.4	13.2	13.6	0.2
Platelet Count	10.e3/uL	582.0	705.0	425.0	833.0	188.3	889.6	834.0	1094.0	889.6	981.3	990.0	1047.0	60.7
MPV	fL	6.3	6.7	6.1	7.4	0.5	6.3	6.1	6.6	0.2	6.2	6.1	6.3	0.1
Segs	%	17.2	12.7	11.6	14.0	1.0	9.2	7.4	12.3	2.0	13.7	9.7	16.5	3.2
Lymphs	%	71.7	78.6	72.0	83.0	4.9	86.3	83.0	88.7	2.1	82.2	79.0	86.3	3.6
Monos	%	1.7	4.2	1.6	9.0	3.4	1.9	1.1	3.1	0.8	1.5	1.0	1.9	0.4
Eos	%	8.3	3.5	3.0	5.0	1.1	1.5	1.6	2.6	0.7	1.4	0.9	1.8	0.5
Basos	%	0.5	0.8	0.2	2.0	1.1	0.2	0.1	0.3	0.1	0.4	0.1	0.6	0.2
LUC	%	0.7	0.9			0.0	0.8	0.5	1.0	0.2	1.0	0.6	1.6	0.4

Table 1. Summary data of hematology parameters after administration of Empty DANP, DANP-Control siRNA, DANP-ZNF304 siRNA

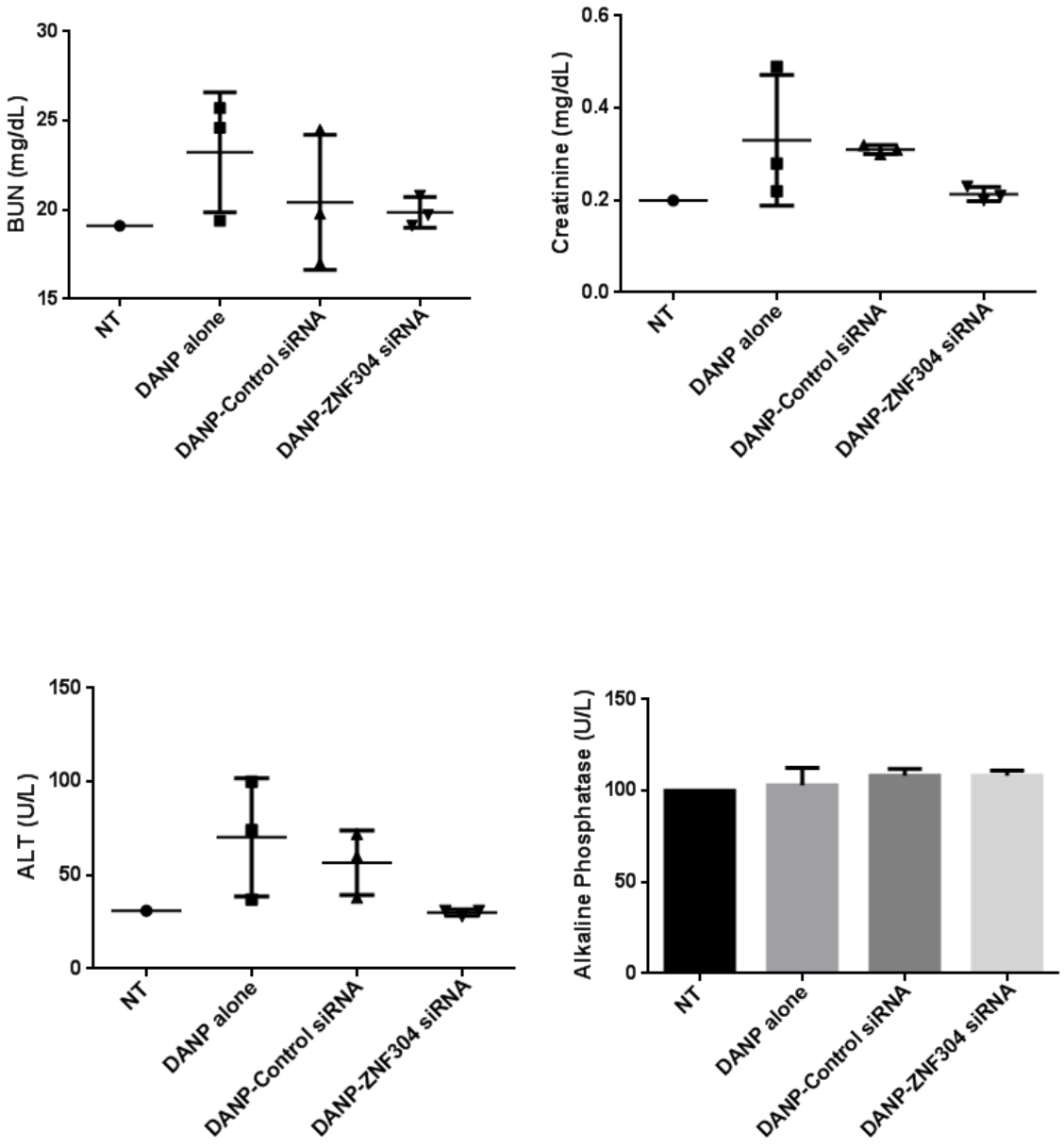

Figure 26. BUN, Creatinine, ALT and alkaline phosphatase levels remain in normal range in blood after DANP-ZNF304 siRNA administration

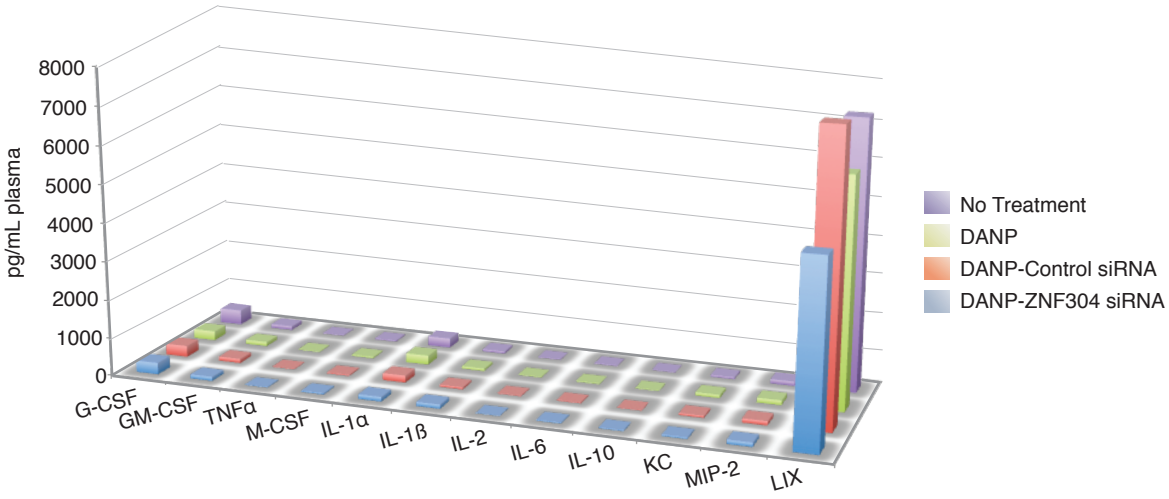

Figure 27. No sign of inflammatory response in plasma after DANP-ZNF304 siRNA administration

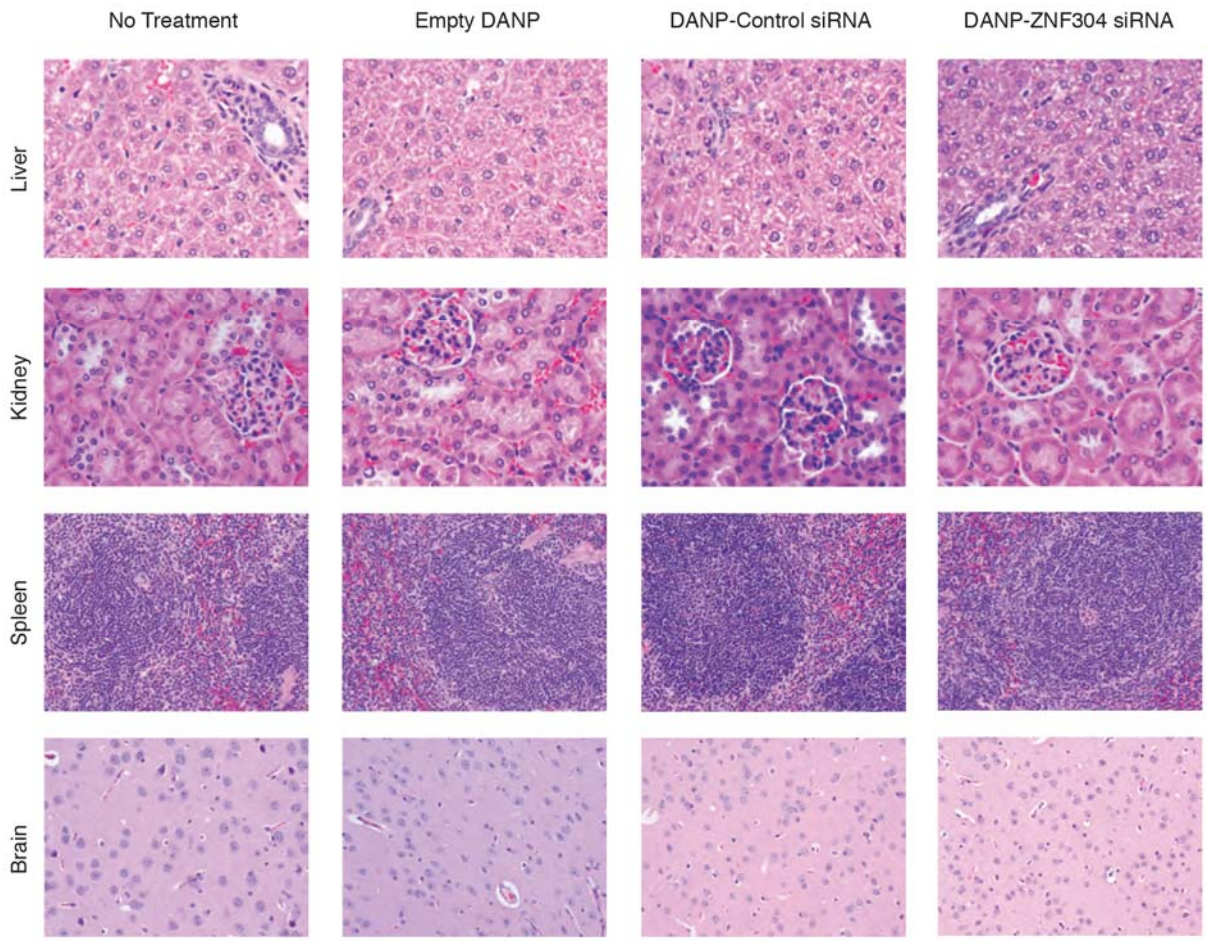

Figure 28. No sign of toxicity in liver, kidney, spleen and brain tissues after DANP-ZNF304 siRNA administration

Effects of ZNF304 gene silencing on antitumor activity in orthotopic models of OC

On the basis of these findings, we examined the antitumor activity of weekly or biweekly *ZNF304* silencing in 2 orthotopic OC mouse models, HeyA8 and SKOV3IP1. In the first model, mice were injected with HeyA8 cells to induce tumors and 1 week later were randomly assigned to 6 treatment groups (10 mice in each group): DANP alone, control siRNA-DANP, ZNF304-siRNA-DANP (150 μg/Kg body weight) administered weekly, and ZNF304-siRNA-DANP (300 μg/Kg body weight) administered biweekly, or, since paclitaxel is commonly used for OC treatment and combines effectively with many biologically targeted agents, paclitaxel only or a combination of paclitaxel plus ZNF304 siRNA-DANP (300 μg/Kg body weight, biweekly administration) (Figure 29). Significant reductions in tumor weight were observed in the groups treated with ZNF304 siRNA-DANP weekly or biweekly. Mice treated with ZNF304 siRNA-DANP had a significantly lower tumor burden (62% reduction in tumor weight; $P < 0.01$) (Figure 29, first panel) and had 50% fewer nodules than did mice treated with control siRNA-DANP ($P < 0.05$) (Figure 29, second panel). Moreover, the ZNF304 siRNA-DANP treatment group had significantly fewer nodules than did the control group (P=0.0001, weekly administration; P=0.0001, biweekly administration; student's *t*-test).

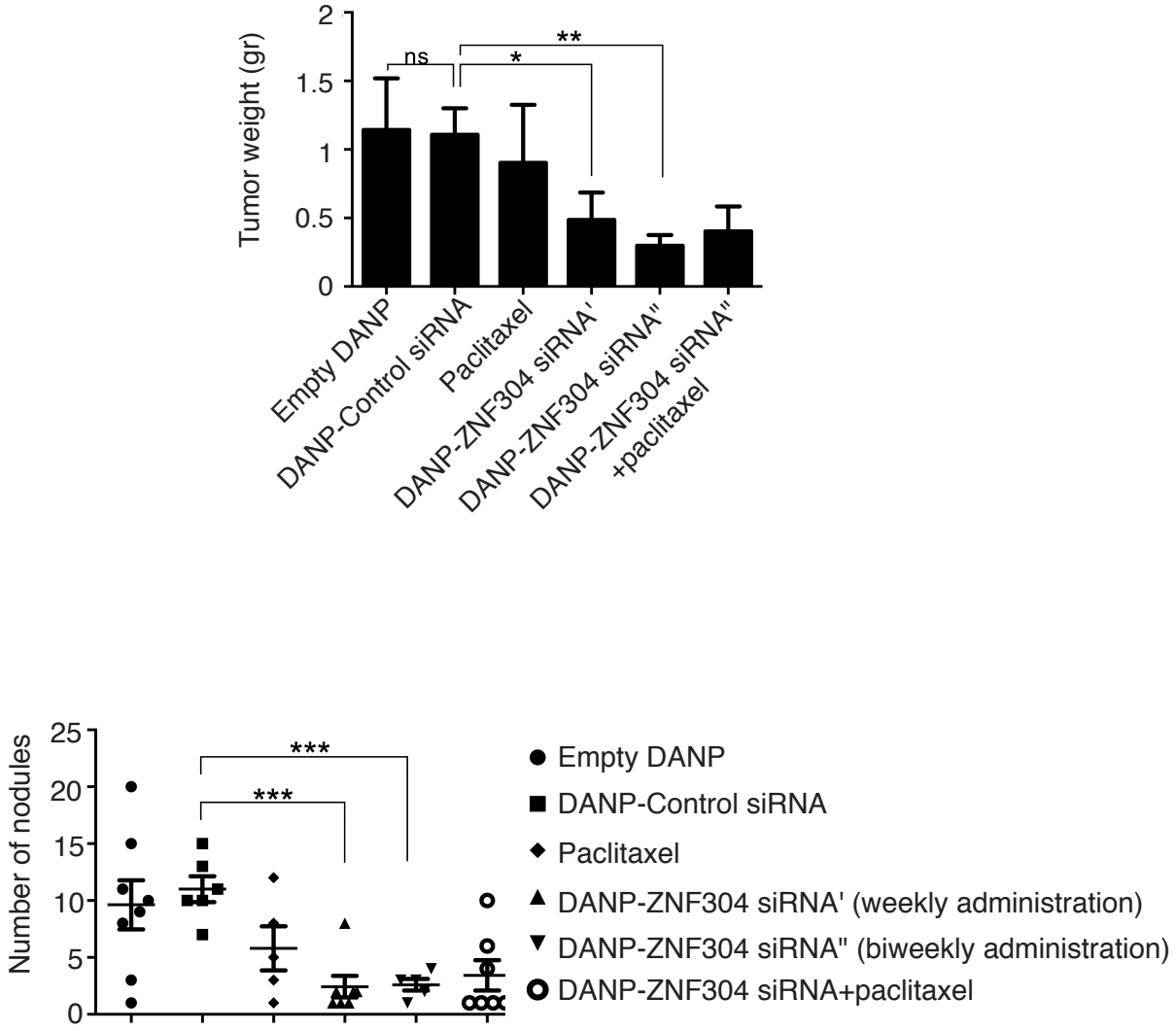

Figure 29. Silencing ZNF304 leads to increased antitumor activity in HeyA8 orthotopic murine model of OC
Data presented as mean ± SEM (n=10 mice/group)

In the second orthotopic model (SKOV3IP1), the treatment groups were (1) control siRNA-DANP, (2) ZNF304 siRNA-DANP, (3) control siRNA-DANP plus paclitaxel, and (4) ZNF304 siRNA-DANP plus paclitaxel (n=10/group). siRNA-DANP was administered intravenously every 2 weeks in all treatment groups. Tumors removed from mice treated with ZNF304 siRNA-DANP alone weighed 60% less than those of mice treated with DANP-control siRNA. (Figure 30, first row). Number of nodules was dramatically reduced in mice treated with either ZNF304 siRNA-DANP or ZNF304 siRNA-DANP plus paclitaxel (Figure 30, below). The greatest reduction was observed in the group treated with both DANP-ZNF304 siRNA and paclitaxel. None of the groups in either mouse model showed decreased body weight, which indicates that the treatments were not toxic (Figure 31). These data indicate that inhibiting ZNF304 results in antitumor activity in mouse models of OC and that the DANP delivery system is an efficient tool for in vivo gene silencing.

Given the in vitro effects of ZNF304 silencing, we performed Ki67 and CD31 staining to examine the biological effects of silencing ZNF304 on tumor cell proliferation and angiogenesis, respectively. Mice treated with ZNF304 siRNA-DANP showed significant reduction in cell proliferation compared to control group (*P<0.0001)* (Figure 32, first panel). Given that ZNF304 transcriptionally regulates β1 integrin, which is required for endothelial cell adhesion, migration, and survival (Carlson et al., 2008, Weis and Cheresh, 2011), we also examined the effects of ZNF304 siRNA treatment on angiogenesis. The ZNF304 siRNA-DANP treatment group had significantly reduced microvessel density compared with the control (*P=0.0252)* (Figure 32, second panel).

These data showed that downregulation of ZNF304 was highly associated with decreased cell proliferation and decreased microvessel density.

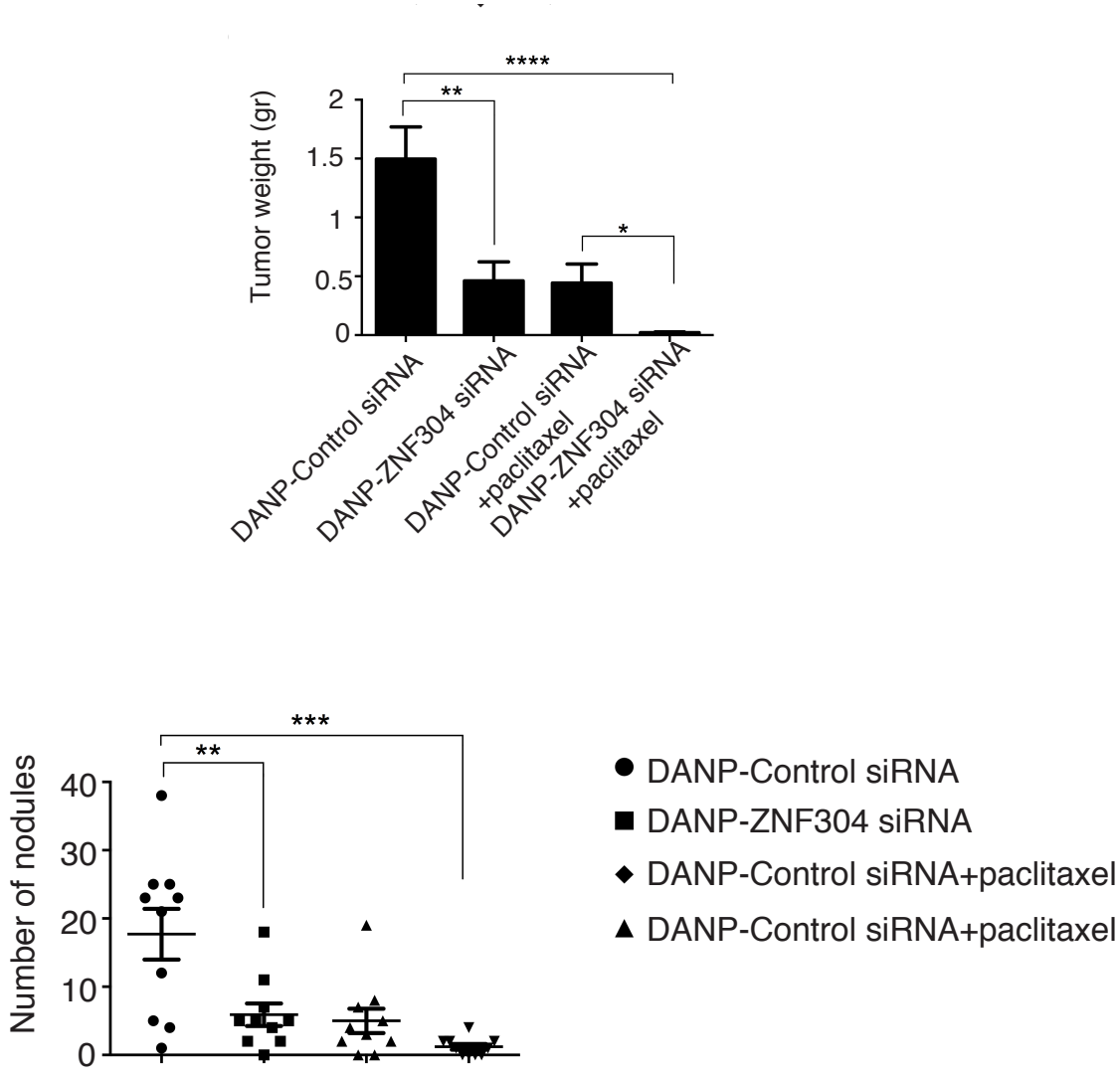

Figure 30. Targeting ZNF304 leads to increased antitumor activity in SKOV3 orthotopic murine model of OC
Data presented as mean ± SEM (n=10 mice/group)

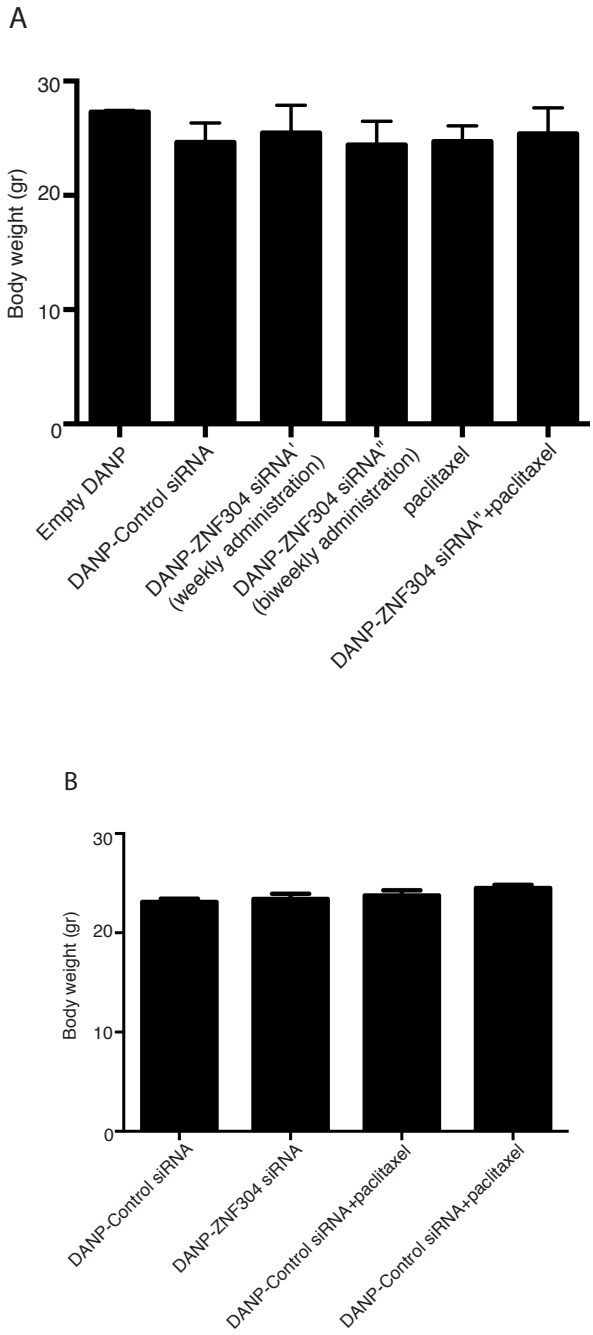

Figure 31. DANP-siRNA treatment does not affect body weight indicating no toxicity
Data presented as mean ± SEM (n=10 mice/group)

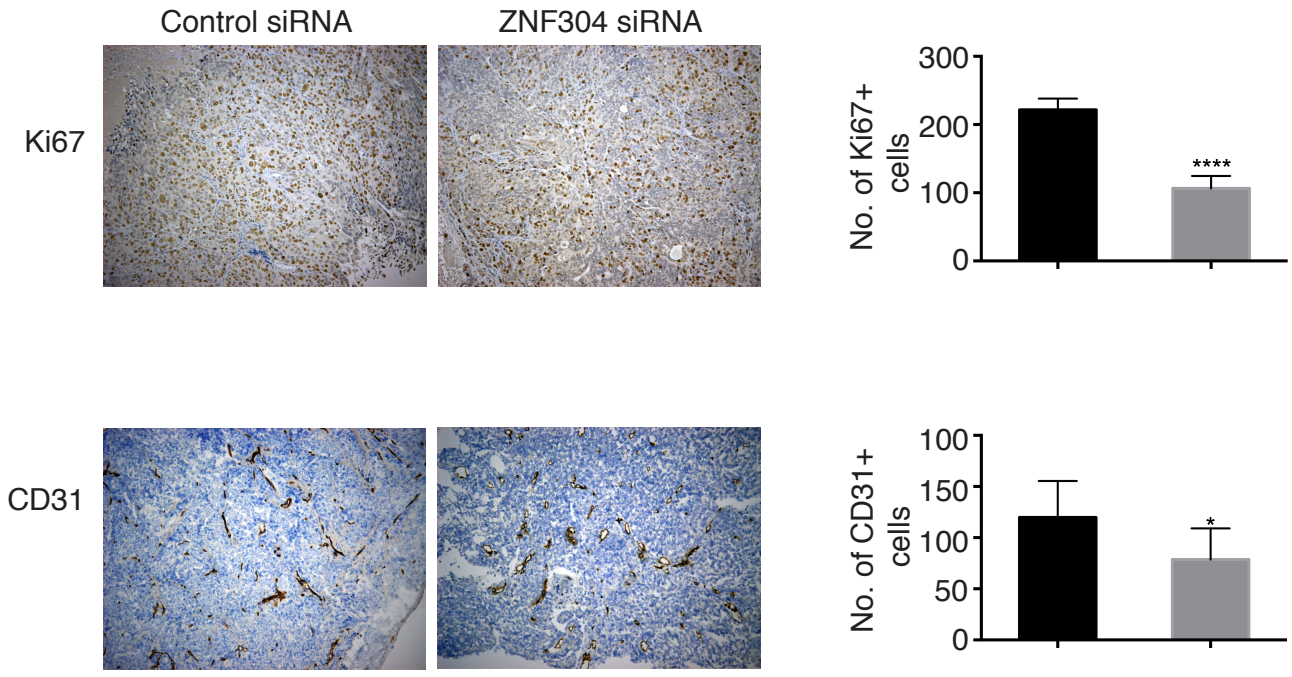

Figure 32. Silencing ZNF304 decreases proliferation and angiogenesis *in vivo*
Data presented as mean ±SEM (n=5 slides /group)

Next, we addressed whether ZNF304 silencing could directly increase the rates of anoikis *in vivo*. For this question, we use the OC MDAH 2774 cell line since it causes mice to develop ascites (Sood et al., 2010). MDAH 2774 cells were implanted into the peritoneal cavity of nude mice, and ascites production was observed 4-6 weeks post-inoculation. Next, we analyzed the ascites for viable tumor epithelial cells using fluorescein isothiocyanate (FITC)-labeled anti-epithelial cellular adhesion molecule antibody followed by flow cytometry analysis (Figure 33). The control group showed 40% epithelial cell death in ascites, whereas mice treated with intravenous ZNF304 siRNA-DANP had up to 80% epithelial cell death. These results show that silencing ZNF304 significantly decreased the ability of OC cells to survive in ascites (P=0.0001, Student's *t*-test).

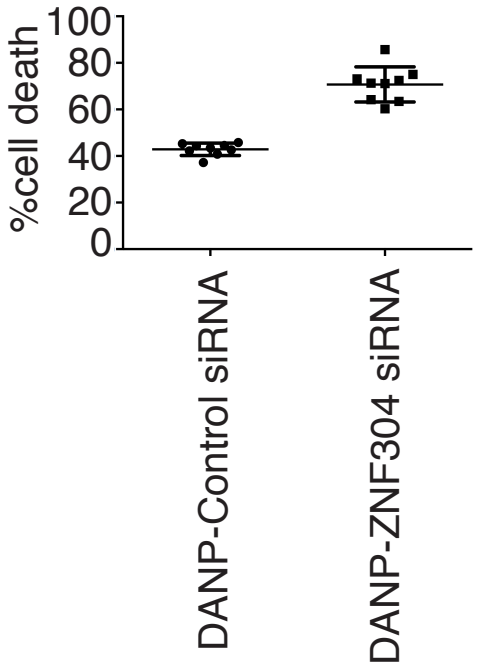

Figure 33. Silencing ZNF304 culminate in enhanced anoikis in vivo
Data presented as mean ±SEM (n=3 mice/group)

CHAPTER IV: Discussion

Summary

Ovarian cancer (OC) is lethal. According to statistical estimations, 21980 women will be newly diagnosed in 2014 and 14270 women will die due to OC (Siegel et al., 2014). Primary reason of elevated death rate is the late-stage presentation of the disease with multiple tumor nodules. Hence, more than 70 % of patients with advanced disease develop resistance to chemotherapy and experience disease recurrence, which generates the second limitation (Romero and Bast Jr, 2012, Bast and Markman, 2010).

Personalized cancer therapy gives the hope of enabling tailored therapies to ameliorate survival rates, overcome resistance and decrease toxicity through administration of the right drug combination for individuals (Meric-Bernstam and Mills, 2012). It requires detailed molecular characterization of patient tumor and its microenvironment that can be achieved by rapid identification of novel targets and generation of databases for extensive information about markers that predict prognosis, treatment response and resistance.

In this current study, we combined the opportunities that were provided by high-throughput screening technologies supported with bioinformatics, proteomic technology, and nanotechnology. We identified ZNF304, through an extensive computational analysis and validated its functional significance in OC using Reverse Phase Protein Array (RPPA) with subsequent analysis of the potential pathways and downstream effectors. We also developed an RNAi delivery system that carry RNAi safely,

accumulate at tumor site and release RNAi in a sustained manner leading to decreased administration frequency. One of the key findings from this study is that ZNF304 is a novel transcriptional regulator of β1 integrin. Silencing ZNF304 with siRNA that is incorporated in our delivery system DANP resulted in antitumor activity in orthotopic models of OC.

Overall, we have identified a novel zinc finger protein as a contribution in the biology of cancer that could open up new avenues not only for OC, but also in a broad range of other types of cancer. We also developed and characterized a novel RNAi delivery system that will move forward to translational applications in the near future.

Discovery of ZNF304

Elevated metastatic rate and the resistance to chemotherapy are two major issues that require improvement for better outcomes in OC patients. The ability for the prediction of clinical response should be advanced in order to identify the right combination of drugs for individuals. Given the heterogeneity of OC at molecular level, tumors should be screened in details using high-resolution comparative genomic hybridization, single nucleotide polymorphism analysis, gene and protein expression arrays, and immunohistochemistry of relevant markers for an appropriate individually designed therapy selection (Meric-Bernstam and Mills, 2012). Besides overcoming the logistic challenges, further understanding of the biology is essential that can be only achieved by identifying novel targets that have a critical role in survival and metastasis.

Therefore, we embarked on a study of identifying a novel target that is significant in survival and metastasis. We mined The Cancer Genome Atlas (TCGA), which was generated using extensive information and comprehensive analyses of all somatic alterations in the cancer genomes (Chin et al., 2011a, Chin et al., 2011b). We identified 16,869 upregulated genes in OC, and found out the ones that were positively correlated with tumoral N-cadherin expression since N-cadherin is crucial in metastasis (Suyama et al., 2002, Cavallaro and Christofori, 2004). We were guided to study ZNF304 since out of four target genes; only ZNF304 was associated with overall survival in OC patients. The inhibition of invasion and migration of cells after ZNF304 silencing *in vitro,* strengthen the potential of our target selection and led us to perform a protein analysis using RPPA technology. RPPA is a fast and sensitive platform that provided us the proteomic analysis to understand the potential role of ZNF304 *in vitro* after silencing ZNF304 (Tibes et al., 2006, Stemke-Hale et al., 2008). The comprehensive analysis of the RPPA data unraveled the link between ZNF304 and integrin signaling.

Functional Significance of ZNF304 in OC

Integrins are crucial for normal functions of multicellular organisms and critical at each step of cancer: tumorigenesis, progression, and metastasis (Desgrosellier and Cheresh, 2010). Integrins are regulated and activated by conformational changes, clustering, and trafficking (Margadant et al., 2011). These transmembrane proteins are an essential link

between the extracellular matrix (ECM) and cytoplasm, and the signaling can be in 2 directions: outside-in or inside-out through the cytoplasmic β tail (Margadant et al., 2011).

Outside-in signaling. β1 integrin is a subunit of heterodimeric membrane adhesion receptors, and it can form heterodimers with integrin α subunits and interact with extracellular matrix proteins. For example, α4β1, α8β1, and αvβ1 are fibronectin-binding integrins; α3β1, α6β1, and α7β1 interact with laminin and nectin; and α1β1, α2β1, α10β1, and α11β1 bind to collagens (Brakebusch and Fässler, 2005, Giancotti, 2000). Integrin promotes cell survival and regulates focal adhesion through β1 tail, leading to tumor metastasis in many types of cancer including OC (Caccavari et al., 2010, Guo and Giancotti, 2004, Grzesiak et al., 2011, Mitra et al., 2011). Furthermore, Schiller and colleagues demonstrated that expression of α5β1 integrins is essential to sense the stiffness of fibronectin-based ECM via acting as a mechano-sensor in metastasis (Minton, 2013, Schiller et al., 2013). Additionally, several β1 integrin-targeting strategies, such as monoclonal antibodies and peptide inhibitors, showed activity in clinical trials for cancer therapy (Desgrosellier and Cheresh, 2010, Barkan and Chambers, 2011, Jahangiri et al., 2014). However, targeting ZNF304—the regulator of β1 integrin expression—may offer greater efficacy than targeting only activation of β1 integrin.

Inside-out signaling. The first study showing the inside-out regulation of β1 integrin unraveled the control by R-Ras of the ligand-binding affinity of β1 integrin and

fibronectin (Zhang et al., 1996). Thus, the regulation of integrin activation and affinity was known as a transcription-independent function of the Ras-linked mitogen-activated protein kinase pathway (Hughes et al., 1997, Kinbara et al., 2003). However, the transcriptional regulation of β1 integrin remained unknown. Here, we elucidated that the regulation of β1integrin expression through ZNF304 at the transcriptional level.

RPPA analysis revealed that ZNF304 regulates integrin signaling through inhibiting the expression of caveolin-1, fibronectin, myosin II, and the effectors of the Ras signaling pathway (BRAF, and RAF1). The reduction in β1 integrin and the phosphorylated levels of focal adhesion–associated adaptor proteins indicated that ZNF304 may be a master regulator of migration (Huttenlocher and Horwitz, 2011). Previous studies showed that fibronectin and β1 integrin ligation, followed by activation of cytoplasmic β subunit, promotes the invasive migration of OC cells through the ECM (Caswell et al., 2007). Myosin II and FAK mediate the phosphorylation of paxillin, reinforcing the cytoskeletal ECM linkage and driving focal adhesion maturation (Pasapera et al., 2010). Additionally, β1 integrin-FAK signaling directs the initial proliferation of micrometastatic cancer cells disseminated in the lungs, which indicates the role of integrin-FAK signaling in the metastatic cascade (Shibue and Weinberg, 2009). Thus, ZNF304 may be a regulator of this metastatic process. Correspondingly, we provide evidence that silencing the key regulator ZNF304 decreased nodule formation and tumor growth in orthotopic mouse models of OC.

The functional crosstalk between cell adhesion receptors and receptor tyrosine kinases contributes to cancer cell survival (Guo and Giancotti, 2004). The interaction between ErbB1 and β1 integrin induces tumor cell detachment, migration and metastatic potential. β1 integrin was also shown to regulate epidermal growth factor receptor signaling in lung cancer cells (Morello et al., 2011) and to mediate epidermal growth factor-induced cell invasion in OC cells (Lau et al., 2012). Morello and colleagues demonstrated that silencing β1 integrin

led to decreased proliferation, impaired migration and invasive behavior. Hence, silencing β1 integrin leads to a defective activation of EGFR signaling cascade and increases EGFR on the surface of the cell, indicating that β1 integrin is essential for EGFR turnover on the cell membrane. Therefore silencing ZNF304—the regulator of β1 integrin—may also inhibit epidermal growth factor receptor signaling, inhibiting cancer cell survival and slowing tumor progression.

The interaction between ECM and integrins play a critical role in cell migration by providing an essential step for cell motility. Adherent cells require anchorage of the cell for survival (Meredith et al., 1993, Frisch and Francis, 1994). All communications within the microenvironment are in most cases mutually beneficial. Thus, its combination with ECM provide life support for the cells (Liotta and Kohn, 2004). Dr. Steven Frisch discovered and named this phenomenon as the term “anoikis,” that means “homelessness,” and refers to a form of programmed cell death as a result of inadequate cell-ECM interaction or absence of cell-ECM attachment (Meredith et al.,

1993, Frisch and Francis, 1994, Liotta and Kohn, 2004). However, malignant cells develop resistance to anoikis, and survive in absence in these signals, leading to an elevated metastatic spread (Simpson et al., 2008, Jenning et al., 2013). A recent study showed that activated integrins enhance the metastatic potential of prostate cancer cells by decreasing their sensitivity to anoikis during tumor dissemination and by increasing their interactions with ECM ligands during extravasation (Lee et al., 2013). This study suggested that in prostate cancer cells, β1 integrin is activated through an inside-out signaling, which also enhances its affinity for ligand binding. The interaction of β1 integrin with ECM ligands further activates β1 integrin through outside-in signaling, suggesting the bidirectional interactions can follow each other leading to further activation of integrins, subsequently followed by growth signals. Our *in vitro* and *in vivo* anoikis results showed that silencing ZNF304 enhances the anoikis rate through inhibiting inside-out integrin signaling and accordingly blocking outside-in signaling.

Development and characterization of Dual Assembly Nanoparticles for RNAi delivery and sustained down-regulation of targets

In recent years, there has been an explosion in knowledge regarding non-coding RNAs. At present, there are several small and long coding RNAs including siRNA, microRNA, pyknons, long non-coding RNAs and others (Rigoutsos, 2010, Hansji et al., 2014, Sana et al., 2012). We currently know that protein-coding genes represent less than 2% of the total genome and non-coding RNAs can regulate DNA, RNA and protein expression governing multiple pathways.

Given the fact that RNAi based therapies offer a unique opportunity to knockdown specific genes and paves the way to personalized medicine in cancer therapy, sufficient RNAi delivery is essential. However, a number of pharmacological, physiological and biological barriers have to be overcome. This emphasizes the crucial role of nanotechnology-based delivery in the development of novel strategies. Early-phase RNAi based therapy trials drew the attention to the feasibility of siRNA delivery into tumors and the selective knockdown of target of interest at tumor site (Tabernero et al., 2013, Davis et al., 2010). These studies showed the potential of RNAi-based therapy as a promising strategy. However, there are still critical steps to be taken in the development of RNAi based therapeutics including the delivery, relevant toxicology, pharmacology, and pharmacokinetics that should be assessed in the early steps of the development (Wu et al., 2014). In this study, we took the initial steps of the development and characterization of DANP-siRNA therapeutic agent. Our group has previously developed and characterized chitosan nanoparticles for systemic delivery of siRNA (Lu et al., 2010, Han et al., 2010). Although chitosan nanoparticles is an efficient RNA interference delivery system, weekly administration is required since the target downregulation lasts only for 7 days after a single administration. Our results demonstrate that DANP, a combination of 2 biocompatible and biodegradable polymers, led to sustained silencing of ZNF304 and antitumor activity with a single administration every 2 weeks. Furthermore, according to the level of silencing at 14 days after a single DANP-siRNA administration; we expect the silencing of the gene of interest, beyond 14 days. Thus, DANP is a powerful therapeutic tool that leads to long-term silencing of genes and could enhance the use of siRNA and patient compliance.

There have been similar attempts in the development of nanoparticles for sustained release of the drugs. Ferrari and colleagues designed multistage vector system (MSV) that is composed of porous silicon particles loaded with nanoparticles that leads to the slow-rate release of siRNA in murine orthotopic models of OC (Tanaka et al., 2010). MSV/EphA2 siRNA was administered biweekly for 6 week leading to remarkable tumor reduction *in vivo* (Shen et al., 2013b). They also showed that the carriers highly accumulate at tumor site with biodistribution studies and demonstrated that no inflammatory response was created after systemic administration (Tanaka et al., 2010).

The toxicity of nanoparticles is crucial in evaluating the potential of carriers at development stages of drug delivery systems (Wu et al., 2014). However, there are no standards in order to determine the toxicity of nanocarriers. In this study, we studied the potential toxicity of DANP in serum 72 hours after a single systemic administration and no clinical abnormality was found (Schnell et al., 2002). In addition, following a single administration of DANP; no sign of toxicity was observed in the liver, kidney, brain, and spleen after a single iv administration, in compliance with no significant difference in inflammatory cytokine levels. We similarly observed no significant difference in inflammatory cytokines. These data indicate that DANP is a safe and non-toxic.

In vivo validation of target selection and DANP

The treatment of ovarian cancer is still limited to surgery followed by chemotherapy especially with platinum and taxane based regimens (Romero and Bast Jr, 2012).

Cisplatin is an alkylating agent that leads to inter- or intrachain crosslinks through covalently binding to DNA. Paclitaxel increases microtubule stability through non-covalent interaction and prevents the mitotic spindle formation. Given the fact that ZNF304 silencing leads to remarkable reduction in focal adhesion members such as FAK and Src, we combined our ZNF304 siRNA treatment with weekly intraperitoneal paclitaxel administration in our *in vivo* antitumor activity studies since focal adhesion kinase (FAK) and Src inhibition are shown to be critical for chemotherapy sensitivity, previously. FAK inhibition has been shown to sensitize ovarian cancer cells to taxanes *in vitro* and *in vivo* (Kang et al., 2013). In addition, Huang and his colleagues showed that Src inhibitor dasatinib in combination with paclitaxel is sufficient in reduction of tumor weight and number of nodules in orthotopic *in vivo* models of uterine cancer (Huang et al., 2014). Additionally, this combination showed its feasibility in Phase I studies in breast cancer patients (Gil et al., 2014, Cadoo et al., 2013, Huang et al., 2014). However; since ZNF304 is a transcription factor and platinum based drugs lead to the crosslink of DNA, a combination treatment of ZNF304 siRNA and carboplatin can also show enhanced antitumor activity *in vivo*. Additionally, our data demonstrated that ZNF304 silencing caused cell cycle arrest in four ovarian cancer cell lines. Therefore, a combination treatment with ZNF304 siRNA and carboplatin may extent the DNA damage and increase the chemo sensitivity of cells *in vitro*. Therefore, the effects of ZNF304 silencing with or without carboplatin treatment can be studied in future studies in order to unravel whether ZNF304 is linked to platinum resistance.

CHAPTER V: Future Directions

Translational Application of Dual Assembly Nanoparticles

This project provided basis for a number of future studies. In particular, we demonstrated that DANP is a safe and sufficient delivery system for siRNA. Hence, the particles are currently under evaluation by the Nanotechnology Characterization Laboratory (NCL). NCL works with the National Institute of Standards and Technology (NIST) and the U.S. Food and Drug Administration (FDA), serving as a national resource to facilitate the regulatory review for nanotechnology applications. Long-term goal of this project is to take DANP-siRNA to clinic and further characterization is required for the transition to clinical trials.

In addition, given the fact that DANP is a polymeric particle, surface chemistries can be studied in order to chemically conjugate specific ligands on the surface of DANP for active targeting purposes. DANP passively accumulates at tumor site owing to the Enhanced Permeability and Retention (EPR) effect; however the presence of specific ligands on the nanoparticle will lead to selective uptake of nanoparticles by only tumor cells.

Further investigation of the mechanism of ZNF304

In this study, we showed that ZNF304 regulates β1 integrin, however since it is a novel transcription factor, its alternative downstream effectors are currently not known. Therefore ChIP sequencing can be performed and effectively analyzed in order to identify its additional targets and uncover the biological mechanisms that ZNF304 is involved in; not only for OC, but also in other types of cancer. A recent study has shown

the link between KRAS and ZNF304 in colorectal cancer, suggesting that KRAS promotes silencing through up-regulation of ZNF304, which also regulates transcriptional silencing of INK4A-ARF in human embryonic stem cells (Serra et al., 2014). Further investigation should be performed for the effects of ZNF304 silencing in KRAS-driven cancers such as lung and pancreatic cancer.

Determining the role of ZNF304 in chemotherapy resistance

The worse survival in OC patients is highly associated with chemo-resistance since more than 70 % of patients with advanced disease develop resistance to chemotherapy and experience disease recurrence, which generates the second limitation (Romero and Bast Jr, 2012, Bast and Markman, 2010). We have examined the effect of combination treatment with paclitaxel and ZNF304 silencing in our antitumor activity studies, however we have not studied the effect of platinum drugs in combination with ZNF304 silencing. Proliferation assays can be performed and followed by RPPA array within samples that are treated with platinum alone and platinum in combination with ZNF304 siRNA to find out the relevant downstream targets that ZNF304 might be regulating in the resistance mechanism. This project can contribute to the field in terms of identifying targets that are significant in chemotherapy resistance.

Appendix

Table 2. siRNA sequences used in zinc finger protein 304 (ZNF304) transfection experiments

Name	Target Sequence	Source	Cat #
ZNF304 siRNA-1	5′-GAUCACACCUUACACAGAA-3′	Sigma-Aldrich	SASI_HS01_00189770
ZNF304 siRNA-2	5′-CUUAUUGAGCACUGGAGAA -3′	Sigma-Aldrich	SASI_HS01_00189771
ZNF304 siRNA-3	5′-GCAACAUAAUGGAGAGAAU-3′	Sigma-Aldrich	SASI_HS01_00189772
Control siRNA	5′-UUCUCCGAACGUGUCACGUUU-3′	Sigma-Aldrich	WD00909801

Table 3. Antibodies used in the Western blotting, chromatin immunoprecipitation, and immunohistochemical analyses

Target Protein	Source	Cat #	Applications
Actin-beta	Sigma-Aldrich	A5316	WB
ZNF304	Sigma-Aldrich	SAB2106472	WB, ChIP
β1 integrin	Cell Signaling Technology	4706S	WB
Akt (pS473)	Cell Signaling Technology	4060S	WB
Akt	Cell Signaling Technology	9272	WB
FAK (pY397)	BD Biosciences	611722	WB
FAK	BD Biosciences	610087	WB
PARP	Cell Signaling Technology	9542	WB
Src (p416)	Cell Signaling Technology	6943	WB
Src	Cell Signaling Technology	2123	WB
Paxillin (pY118)	Cell Signaling Technology	2541	WB
Paxillin (pY31)	Epitomics	1228-1	WB
Paxillin	Cell Signaling Technology	2542	WB
Ki67	Thermo Scientific	RB9043-P	IHC
CD31	BD Biosciences	53370	IHC

Table 4. Oligonucleotide sequences for quantitative reverse transcription polymerase chain reaction

Target Gene	Forward Sequence	Reverse Sequence
ZNF304 -set 1	5′-GCACAGAGATTCCTGTACCGT-3′	5′-TTTCAAGAGTGGGTCACACATC-3′
ZNF304 -set 2	5′-GTGTGACCCACTCTTGAAAGAC-3′	5′-CCCTCTGAAGCAATTCTCTCCAT-3′
ZNF304 -set 3	5′-TGGAGGGGCCTCATTTGTG-3′	5′-CTCCCTGCACGTAAAGGATCT-3′
ITGB1-set 1	5′-CCTACTTCTGCACGATGTGATG-3′	5′-CCTTTGCTACGGTTGGTTACATT-3′
ITGB1-set 2	5′-GTAACCAACCGTAGCAAAGGA-3′	5′-TCCCCTGATCTTAATCGCAAAAC-3′
ITGB1-set 3	5′-CAAGAGAGCTGAAGACTATCCCA-3′	5′-TGAAGTCCGAAGTAATCCTCCT-3′

Table 5. Oligonucleotide sequences for quantitative polymerase chain reaction analysis of chromatin immunoprecipitation assays

Gene	Amplicon location	Forward sequence	Reverse sequence
ITGB1	3775-3725	GGGTTGAGGAGAGGGAAGGTA	TGCCTTTCAGTTGCTGTCCTAA
ITGB1	3392-3297	AAGGCCAGCAGCATTGAAAG	AGAACACAGAAGAGCTACAGGAC
ITGB1	3155-3108	TCTGTTTCTTGCCAGTGCCC	CCTTCTGAAACCCTTGTGCC
ITGB1	1989-1939	TTTGCCTTGAGAAAGTCACG	TCCTGTAATCCCAGCTTCTCA
ITGB1	1546-1496	TGTGTGTGTATATGTGTGTCACCTT	TGCGAGAAACCAACTGGTAG
ITGB1	784-613	TCCCAGGTTCAAGCAGTTCTC	GCTCACGCCTGGAATCTCA

Bibliography

ABDUL AZIS, T. Role of cell adhesion molecules in invasion, anoikis resistance and drug resistance: An in vitro analysis using multiple phenotyping approach. Qatar Foundation Annual Research Conference, 2013.

ALBANELL, J. & BASELGA, J. 1999. Trastuzumab, a humanized anti-HER2 monoclonal antibody, for the treatment of breast cancer. *Drugs Today (Barc),* 35**,** 931-946.

ALEXIS, F., PRIDGEN, E., MOLNAR, L. K. & FAROKHZAD, O. C. 2008. Factors affecting the clearance and biodistribution of polymeric nanoparticles. *Molecular pharmaceutics,* 5**,** 505-515.

BANGHAM, A. & HORNE, R. 1964. Negative staining of phospholipids and their structural modification by surface-active agents as observed in the electron microscope. *Journal of molecular biology,* 8**,** 660-IN10.

BANGHAM, A., STANDISH, M. & WATKINS, J. 1965. Diffusion of univalent ions across the lamellae of swollen phospholipids. *Journal of molecular biology,* 13**,** 238-IN27.

BARKAN, D. & CHAMBERS, A. F. 2011. β1-integrin: a potential therapeutic target in the battle against cancer recurrence. *Clinical Cancer Research,* 17**,** 7219-7223.

BAST, R. C., HENNESSY, B. & MILLS, G. B. 2009. The biology of ovarian cancer: new opportunities for translation. *Nature Reviews Cancer,* 9**,** 415-428.

BAST, R. C. & MARKMAN, M. 2010. Chemotherapy: A new standard combination for recurrent ovarian cancer? *Nature Reviews Clinical Oncology,* 7**,** 559-560.

BAWA, R., A SIEGEL, R., MARASCA, B., KAREL, M. & LANGER, R. 1985. An explanation for the controlled release of macromolecules from polymers. *Journal of Controlled Release,* 1**,** 259-267.

BENJAMINI, Y. & HOCHBERG, Y. 1995. Controlling the false discovery rate: a practical and powerful approach to multiple testing. *Journal of the Royal Statistical Society. Series B (Methodological)***,** 289-300.

BLAGOSKLONNY, M. V. 2004. Analysis of FDA approved anticancer drugs reveals the future of cancer therapy. *Cell Cycle,* 3**,** 1033-1040.

BOWEN, N. J., WALKER, L. D., MATYUNINA, L. V., LOGANI, S., TOTTEN, K. A., BENIGNO, B. B. & MCDONALD, J. F. 2009. Gene expression profiling supports the hypothesis that human ovarian surface epithelia are multipotent and capable of serving as ovarian cancer initiating cells. *BMC medical genomics,* 2**,** 71.

BRAKEBUSCH, C. & FÄSSLER, R. 2005. β 1 integrin function in vivo: adhesion, migration and more. *Cancer and Metastasis Reviews,* 24**,** 403-411.

BRAY, F., JEMAL, A., GREY, N., FERLAY, J. & FORMAN, D. 2012. Global cancer transitions according to the Human Development Index (2008–2030): a population-based study. *The Lancet Oncology*.

CACCAVARI, F., VALDEMBRI, D., SANDRI, C., BUSSOLINO, F. & SERINI, G. 2010. Integrin signaling and lung cancer. *Cell adhesion & migration,* 4**,** 124.

CADOO, K., MORRIS, P., LAKE, D., D'ANDREA, G., DICKLER, M., GILEWSKI, T., DANG, C., MCARTHUR, H., BROMBERG, J. & GOLDFARB, S. 2013. Abstract P2-16-12: An exploratory analysis of the role of dasatinib in preventing progression of disease in bone in patients with metastatic breast cancer. *Cancer Research,* 73**,** P2-16-12-P2-16-12.

CAI, X., HU, J., XIAO, J. & CHENG, Y. 2013. Dendrimer and cancer: a patent review (2006-present). *Expert opinion on therapeutic patents***,** 1-15.

CARLSON, T. R., HU, H., BRAREN, R., KIM, Y. H. & WANG, R. A. 2008. Cell-autonomous requirement for β1 integrin in endothelial cell adhesion, migration and survival during angiogenesis in mice. *Development,* 135**,** 2193-2202.

CASALUCE, F., SGAMBATO, A., ROSSI, A. & MULSHINE, J. L. 2012. The US FDA has approved Abraxane® for the treatment of non-small-cell lung cancer Aurora: a new light for targeted therapy in small-cell lung cancer. *Lung Cancer,* 1**,** 251-254.

CASEY, T., BOND, J., TIGHE, S., HUNTER, T., LINTAULT, L., PATEL, O., ENEMAN, J., CROCKER, A., WHITE, J. & TESSITORE, J. 2009. Molecular signatures suggest a major role for stromal cells in development of invasive breast cancer. *Breast cancer research and treatment,* 114**,** 47-62.

CASWELL, P. T., SPENCE, H. J., PARSONS, M., WHITE, D. P., CLARK, K., CHENG, K. W., MILLS, G. B., HUMPHRIES, M. J., MESSENT, A. J. & ANDERSON, K. I. 2007. Rab25 associates with α5β1 integrin to promote invasive migration in 3D microenvironments. *Developmental cell,* 13**,** 496-510.

CAVALLARO, U. & CHRISTOFORI, G. 2004. Cell adhesion and signalling by cadherins and Ig-CAMs in cancer. *Nature Reviews Cancer,* 4**,** 118-132.

CHAMPION, J. A., KATARE, Y. K. & MITRAGOTRI, S. 2007. Particle shape: a new design parameter for micro-and nanoscale drug delivery carriers. *Journal of Controlled Release,* 121**,** 3-9.

CHEEMA, S. K., MISHRA, S. K., RANGNEKAR, V. M., TARI, A. M., KUMAR, R. & LOPEZ-BERESTEIN, G. 2003. Par-4 transcriptionally regulates Bcl-2 through a WT1-binding site on the bcl-2 promoter. *Journal of Biological Chemistry,* 278**,** 19995-20005.

CHEN, J., HESSLER, J. A., PUTCHAKAYALA, K., PANAMA, B. K., KHAN, D. P., HONG, S., MULLEN, D. G., DIMAGGIO, S. C., SOM, A. & TEW, G. N. 2009. Cationic nanoparticles induce nanoscale disruption in living cell plasma membranes. *The Journal of Physical Chemistry B,* 113**,** 11179-11185.

CHEN, Y.-C., LIAO, L.-C., LU, P.-L., LO, C.-L., TSAI, H.-C., HUANG, C.-Y., WEI, K.-C., YEN, T.-C. & HSIUE, G.-H. 2012. The accumulation of dual pH and temperature responsive micelles in tumors. *Biomaterials*.

CHENG, W., LIU, J., YOSHIDA, H., ROSEN, D. & NAORA, H. 2005. Lineage infidelity of epithelial ovarian cancers is controlled by HOX genes that specify regional identity in the reproductive tract. *Nature medicine,* 11**,** 531-537.

CHIN, L., ANDERSEN, J. N. & FUTREAL, P. A. 2011a. Cancer genomics: from discovery science to personalized medicine. *Nature medicine,* 17**,** 297-303.

CHIN, L., HAHN, W. C., GETZ, G. & MEYERSON, M. 2011b. Making sense of cancer genomic data. *Genes & development,* 25**,** 534-555.

CHOI, H. S., LIU, W., MISRA, P., TANAKA, E., ZIMMER, J. P., IPE, B. I., BAWENDI, M. G. & FRANGIONI, J. V. 2007. Renal clearance of quantum dots. *Nature biotechnology,* 25**,** 1165-1170.

CHONN, A. & CULLIS, P. R. 1995. Recent advances in liposomal drug-delivery systems. *Current opinion in Biotechnology,* 6**,** 698-708.

COLEMAN, R. L., MONK, B. J., SOOD, A. K. & HERZOG, T. J. 2013. Latest research and treatment of advanced-stage epithelial ovarian cancer. *Nature Reviews Clinical Oncology,* 10**,** 211-224.

DAVIS, M. E., ZUCKERMAN, J. E., CHOI, C. H. J., SELIGSON, D., TOLCHER, A., ALABI, C. A., YEN, Y., HEIDEL, J. D. & RIBAS, A. 2010. Evidence of RNAi in humans from systemically administered siRNA via targeted nanoparticles. *Nature,* 464**,** 1067-1070.

DECUZZI, P., GODIN, B., TANAKA, T., LEE, S.-Y., CHIAPPINI, C., LIU, X. & FERRARI, M. 2010. Size and shape effects in the biodistribution of intravascularly injected particles. *Journal of Controlled Release,* 141**,** 320-327.

DECUZZI, P., PASQUALINI, R., ARAP, W. & FERRARI, M. 2009. Intravascular delivery of particulate systems: does geometry really matter? *Pharmaceutical research,* 26**,** 235-243.

DESGROSELLIER, J. S. & CHERESH, D. A. 2010. Integrins in cancer: biological implications and therapeutic opportunities. *Nature Reviews Cancer,* 10**,** 9-22.

DUNNE, M., CORRIGAN, O. & RAMTOOLA, Z. 2000. Influence of particle size and dissolution conditions on the degradation properties of polylactide-< i> co</i>-glycolide particles. *Biomaterials,* 21**,** 1659-1668.

ELLINGTON, A. D. & SZOSTAK, J. W. 1990. In vitro selection of RNA molecules that bind specific ligands. *Nature,* 346**,** 818-822.

FERNANDES, J. C., WANG, H., JREYSSATY, C., BENDERDOUR, M., LAVIGNE, P., QIU, X., WINNIK, F. M., ZHANG, X., DAI, K. & SHI, Q. 2008. Bone-protective Effects of Nonviral Gene Therapy With Folate–Chitosan DNA Nanoparticle Containing Interleukin-1 Receptor Antagonist Gene in Rats With Adjuvant-induced Arthritis. *Molecular Therapy,* 16**,** 1243-1251.

FERRARA, N. 2005. VEGF as a therapeutic target in cancer. *Oncology,* 69**,** 11-16.

FRISCH, S. M. & FRANCIS, H. 1994. Disruption of epithelial cell-matrix interactions induces apoptosis. *The Journal of cell biology,* 124**,** 619-626.

FURUMOTO, K., YOKOE, J.-I., OGAWARA, K.-I., AMANO, S., TAKAGUCHI, M., HIGAKI, K., KAI, T. & KIMURA, T. 2007. Effect of coupling of albumin onto surface of PEG liposome on its in vivo disposition. *International journal of pharmaceutics,* 329**,** 110-116.

GANTA, S., DEVALAPALLY, H., SHAHIWALA, A. & AMIJI, M. 2008. A review of stimuli-responsive nanocarriers for drug and gene delivery. *Journal of Controlled Release,* 126**,** 187-204.

GENG, Y., DALHAIMER, P., CAI, S., TSAI, R., TEWARI, M., MINKO, T. & DISCHER, D. E. 2007. Shape effects of filaments versus spherical particles in flow and drug delivery. *Nature Nanotechnology,* 2**,** 249-255.

GIANCOTTI, F. G. 2000. Complexity and specificity of integrin signalling. *Nature Cell Biology,* 2.

GIL, M., MARTIN, M., ANTOLIN, S., TRIGO, J., GUERRERO, A., VIDAL, L., URRUTICOECHEA, A., PANDIELLA, A., HERNANDO, A. & OCANA, A. Phase I study of dasatinib in combination with trastuzumab and paclitaxel in patients with HER2 positive metastatic breast cancer. EUROPEAN JOURNAL OF CANCER, 2014. ELSEVIER SCI LTD THE BOULEVARD, LANGFORD LANE, KIDLINGTON, OXFORD OX5 1GB, OXON, ENGLAND, S180-S180.

GODIN, B., CHIAPPINI, C., SRINIVASAN, S., ALEXANDER, J. F., YOKOI, K., FERRARI, M., DECUZZI, P. & LIU, X. 2012. Drug Delivery: Discoidal Porous Silicon Particles: Fabrication and Biodistribution in Breast Cancer Bearing Mice (Adv. Funct. Mater. 20/2012). *Advanced Functional Materials,* 22**,** 4186-4186.

GONZALEZ-MARTIN, A., CALVO, E., BOVER, I., RUBIO, M., ARCUSA, A., CASADO, A., OJEDA, B., BALAÑÁ, C., MARTÍNEZ, E. & HERRERO, A. 2005. Randomized phase II trial of carboplatin versus paclitaxel and carboplatin in platinum-sensitive recurrent advanced ovarian carcinoma: a GEICO (Grupo Espanol de Investigacion en Cancer de Ovario) study. *Annals of oncology,* 16**,** 749-755.

GRADISHAR, W. J., TJULANDIN, S., DAVIDSON, N., SHAW, H., DESAI, N., BHAR, P., HAWKINS, M. & O'SHAUGHNESSY, J. 2005. Phase III trial of nanoparticle albumin-bound paclitaxel compared with polyethylated castor oil–based paclitaxel in women with breast cancer. *Journal of clinical oncology,* 23**,** 7794-7803.

GRAGOUDAS, E. S., ADAMIS, A. P., CUNNINGHAM JR, E. T., FEINSOD, M. & GUYER, D. R. 2004. Pegaptanib for neovascular age-related macular degeneration. *New England Journal of Medicine,* 351**,** 2805-2816.

GRATTON, S. E., ROPP, P. A., POHLHAUS, P. D., LUFT, J. C., MADDEN, V. J., NAPIER, M. E. & DESIMONE, J. M. 2008. The effect of particle design on cellular internalization pathways. *Proceedings of the National Academy of Sciences,* 105**,** 11613-11618.

GRILLO-LÓPEZ, A. J. 2002. Zevalin: the first radioimmunotherapy approved for the treatment of lymphoma. *Expert review of anticancer therapy,* 2**,** 485-493.

GRZESIAK, J. J., CAO, H. S. T., BURTON, D. W., KAUSHAL, S., VARGAS, F., CLOPTON, P., SNYDER, C. S., DEFTOS, L. J., HOFFMAN, R. M. & BOUVET, M. 2011. Knockdown of the β1 integrin subunit reduces primary tumor growth and inhibits pancreatic cancer metastasis. *International Journal of Cancer,* 129**,** 2905-2915.

GUO, W. & GIANCOTTI, F. G. 2004. Integrin signalling during tumour progression. *Nature reviews Molecular cell biology,* 5**,** 816-826.

GUPTA, B. & TORCHILIN, V. P. 2007. Monoclonal antibody 2C5-modified doxorubicin-loaded liposomes with significantly enhanced therapeutic activity against intracranial human brain U-87 MG tumor xenografts in nude mice. *Cancer Immunology, Immunotherapy,* 56**,** 1215-1223.

GUTIÉRREZ-PUENTE, Y., TARI, A. M., STEPHENS, C., ROSENBLUM, M., GUERRA, R. T. & LOPEZ-BERESTEIN, G. 1999. Safety, pharmacokinetics, and tissue distribution of liposomal P-ethoxy antisense oligonucleotides targeted to Bcl-2. *Journal of Pharmacology and Experimental Therapeutics,* 291**,** 865-869.

HALDER, J., KAMAT, A. A., LANDEN, C. N., HAN, L. Y., LUTGENDORF, S. K., LIN, Y. G., MERRITT, W. M., JENNINGS, N. B., CHAVEZ-REYES, A. & COLEMAN, R. L. 2006. Focal adhesion kinase targeting using in vivo short interfering RNA delivery in neutral liposomes for ovarian carcinoma therapy. *Clinical Cancer Research,* 12**,** 4916-4924.

HAN, H. D., MANGALA, L. S., LEE, J. W., SHAHZAD, M. M., KIM, H. S., SHEN, D., NAM, E. J., MORA, E. M., STONE, R. L. & LU, C. 2010. Targeted gene silencing using RGD-labeled chitosan nanoparticles. *Clinical Cancer Research,* 16**,** 3910-3922.

HANSJI, H., LEUNG, E. Y., BAGULEY, B. C., FINLAY, G. J. & ASKARIAN-AMIRI, M. E. 2014. Keeping abreast with long non-coding RNAs in mammary gland development and breast cancer. *Frontiers in genetics,* 5.

HARBURGER, D. S. & CALDERWOOD, D. A. 2009. Integrin signalling at a glance. *Journal of cell science,* 122**,** 159-163.

HAWKINS, M. J., SOON-SHIONG, P. & DESAI, N. 2008. Protein nanoparticles as drug carriers in clinical medicine. *Advanced Drug Delivery Reviews,* 60**,** 876-885.

HERBRECHT, R. 1996. The changing epidemiology of fungal infections: are the lipid-based forms of amphotericin B an advance? *European Journal of Haematology,* 56**,** 12-17.

HUANG, J., HU, W., BOTTSFORD-MILLER, J., LIU, T., HAN, H. D., ZAND, B., PRADEEP, S., ROH, J.-W., THANAPPRAPASR, D. & DALTON, H. J. 2014. Cross-talk between EphA2 and BRaf/CRaf Is a Key Determinant of Response to Dasatinib. *Clinical Cancer Research,* 20**,** 1846-1855.

HUGHES, P. E., RENSHAW, M. W., PFAFF, M., FORSYTH, J., KEIVENS, V. M., SCHWARTZ, M. A. & GINSBERG, M. H. 1997. Suppression of integrin activation: a novel function of a Ras/Raf-initiated MAP kinase pathway. *Cell,* 88**,** 521-530.

HUTTENLOCHER, A. & HORWITZ, A. R. 2011. Integrins in cell migration. *Cold Spring Harbor perspectives in biology,* 3**,** a005074.

HUWYLER, J., DREWE, J. & KRÄHENBÜHL, S. 2008. Tumor targeting using liposomal antineoplastic drugs. *International journal of nanomedicine,* 3**,** 21.

JAHANGIRI, A., AGHI, M. K. & CARBONELL, W. S. 2014. β1 Integrin: Critical Path to Antiangiogenic Therapy Resistance and Beyond. *Cancer research,* 74**,** 3-7.

JAMES, J. & DUBS, G. 1997. FDA approves new kind of lymphoma treatment. Food and Drug Administration. *AIDS treatment news***,** 2.

JATZKEWITZ, H. 1954. Incorporation of physiologically-active substances into a colloidal blood plasma substitute. I. Incorporation of mescaline peptide into polyvinylpyrrolidone]. *Hoppe-Seyler's Zeitschrift für physiologische Chemie,* 297**,** 149.

JENNING, S., PHAM, T., KALE IRELAND, S., RUOSLAHTI, E. & BILIRAN, H. 2013. Bit1 in anoikis resistance and tumor metastasis. *Cancer letters*.

KAMAT, A. A., KIM, T. J., LANDEN, C. N., LU, C., HAN, L. Y., LIN, Y. G., MERRITT, W. M., THAKER, P. H., GERSHENSON, D. M. & BISCHOFF, F. Z. 2007. Metronomic chemotherapy enhances the efficacy of antivascular therapy in ovarian cancer. *Cancer Research,* 67**,** 281-288.

KANG, Y., HU, W., IVAN, C., DALTON, H. J., MIYAKE, T., PECOT, C. V., ZAND, B., LIU, T., HUANG, J. & JENNINGS, N. B. 2013. Role of focal adhesion kinase in regulating YB–1–mediated paclitaxel resistance in ovarian cancer. *Journal of the National Cancer Institute***,** djt210.

KIM, H.-S., HAN, H. D., ARMAIZ-PENA, G. N., STONE, R. L., NAM, E. J., LEE, J.-W., SHAHZAD, M. M., NICK, A. M., LEE, S. J. & ROH, J.-W. 2011. Functional roles of Src and Fgr in ovarian carcinoma. *Clinical Cancer Research,* 17**,** 1713-1721.

KINBARA, K., GOLDFINGER, L. E., HANSEN, M., CHOU, F.-L. & GINSBERG, M. H. 2003. Ras GTPases: integrins' friends or foes? *Nature Reviews Molecular Cell Biology,* 4**,** 767-778.

KIPPS, E., TAN, D. S. & KAYE, S. B. 2013. Meeting the challenge of ascites in ovarian cancer: new avenues for therapy and research. *Nature Reviews Cancer*.

KIRPOTIN, D. B., DRUMMOND, D. C., SHAO, Y., SHALABY, M. R., HONG, K., NIELSEN, U. B., MARKS, J. D., BENZ, C. C. & PARK, J. W. 2006. Antibody targeting of long-circulating lipidic nanoparticles does not increase tumor localization but does increase internalization in animal models. *Cancer research,* 66**,** 6732-6740.

KOMMAREDDY, S. & AMIJI, M. 2005. Preparation and evaluation of thiol-modified gelatin nanoparticles for intracellular DNA delivery in response to glutathione. *Bioconjugate chemistry,* 16**,** 1423-1432.

LANDEN, C. N., CHAVEZ-REYES, A., BUCANA, C., SCHMANDT, R., DEAVERS, M. T., LOPEZ-BERESTEIN, G. & SOOD, A. K. 2005. Therapeutic EphA2 gene targeting in vivo using neutral liposomal small interfering RNA delivery. *Cancer research,* 65**,** 6910-6918.

LANDEN, C. N., GOODMAN, B., KATRE, A. A., STEG, A. D., NICK, A. M., STONE, R. L., MILLER, L. D., MEJIA, P. V., JENNINGS, N. B. & GERSHENSON, D. M. 2010. Targeting aldehyde dehydrogenase cancer stem cells in ovarian cancer. *Molecular cancer therapeutics,* 9**,** 3186-3199.

LANDEN, C. N., LU, C., HAN, L. Y., COFFMAN, K. T., BRUCKHEIMER, E., HALDER, J., MANGALA, L. S., MERRITT, W. M., LIN, Y. G. & GAO, C. 2006. Efficacy and antivascular effects of EphA2 reduction with an agonistic antibody in ovarian cancer. *Journal of the National Cancer Institute,* 98**,** 1558-1570.

LANGLEY, R. R. & FIDLER, I. J. 2011. The seed and soil hypothesis revisited—The role of tumor-stroma interactions in metastasis to different organs. *International Journal of Cancer,* 128**,** 2527-2535.

LANGLEY, R. R., RAMIREZ, K. M., TSAN, R. Z., VAN ARSDALL, M., NILSSON, M. B. & FIDLER, I. J. 2003. Tissue-specific microvascular endothelial cell lines from H-2Kb-tsA58 mice for studies of angiogenesis and metastasis. *Cancer research,* 63**,** 2971-2976.

LAU, M.-T., SO, W.-K. & LEUNG, P. C. 2012. Integrin β1 mediates epithelial growth factor-induced invasion in human ovarian cancer cells. *Cancer letters,* 320**,** 198-204.

LEE, C. C., MACKAY, J. A., FRÉCHET, J. M. & SZOKA, F. C. 2005. Designing dendrimers for biological applications. *Nature biotechnology,* 23**,** 1517-1526.

LEE, Y.-C., JIN, J.-K., CHENG, C.-J., HUANG, C.-F., SONG, J. H., HUANG, M., BROWN, W. S., ZHANG, S., YU-LEE, L.-Y. & YEH, E. T. 2013. Targeting constitutively activated β1 integrins inhibits prostate cancer metastasis. *Molecular Cancer Research,* 11**,** 405-417.

LEROUEIL, P. R., BERRY, S. A., DUTHIE, K., HAN, G., ROTELLO, V. M., MCNERNY, D. Q., BAKER, J. R., ORR, B. G. & BANASZAK HOLL, M. M. 2008. Wide varieties of cationic nanoparticles induce defects in supported lipid bilayers. *Nano letters,* 8**,** 420-424.

LIOTTA, L. A. & KOHN, E. 2004. Anoikis: cancer and the homeless cell. *Nature,* 430**,** 973-974.

LU, C., BONOME, T., LI, Y., KAMAT, A. A., HAN, L. Y., SCHMANDT, R., COLEMAN, R. L., GERSHENSON, D. M., JAFFE, R. B. & BIRRER, M. J. 2007a. Gene alterations identified by expression profiling in tumor-associated endothelial cells from invasive ovarian carcinoma. *Cancer research,* 67**,** 1757-1768.

LU, C., HAN, H. D., MANGALA, L. S., ALI-FEHMI, R., NEWTON, C. S., OZBUN, L., ARMAIZ-PENA, G. N., HU, W., STONE, R. L. & MUNKARAH, A. 2010. Regulation of tumor angiogenesis by EZH2. *Cancer cell,* 18**,** 185-197.

LU, C., KAMAT, A. A., LIN, Y. G., MERRITT, W. M., LANDEN, C. N., KIM, T. J., SPANNUTH, W., ARUMUGAM, T., HAN, L. Y. & JENNINGS, N. B. 2007b. Dual targeting of endothelial cells and pericytes in antivascular therapy for ovarian carcinoma. *Clinical cancer research,* 13**,** 4209-4217.

LU, C., THAKER, P. H., LIN, Y. G., SPANNUTH, W., LANDEN, C. N., MERRITT, W. M., JENNINGS, N. B., LANGLEY, R. R., GERSHENSON, D. M. & YANCOPOULOS, G. D. 2008. Impact of vessel maturation on antiangiogenic therapy in ovarian cancer. *American journal of obstetrics and gynecology,* 198**,** 477. e1-477. e10.

MACEWAN, S. R., CALLAHAN, D. J. & CHILKOTI, A. 2010. Stimulus-responsive macromolecules and nanoparticles for cancer drug delivery. *Nanomedicine,* 5**,** 793-806.

MAEDA, H., GREISH, K. & FANG, J. 2006. The EPR effect and polymeric drugs: a paradigm shift for cancer chemotherapy in the 21st century. *Polymer Therapeutics II.* Springer.

MARGADANT, C., MONSUUR, H. N., NORMAN, J. C. & SONNENBERG, A. 2011. Mechanisms of integrin activation and trafficking. *Current opinion in cell biology,* 23**,** 607-614.

MATSUMURA, Y. & MAEDA, H. 1986. A new concept for macromolecular therapeutics in cancer chemotherapy: mechanism of tumoritropic accumulation of proteins and the antitumor agent smancs. *Cancer research,* 46**,** 6387-6392.

MCGINNIS, A. C., CHEN, B. & BARTLETT, M. G. 2012. Chromatographic methods for the determination of therapeutic oligonucleotides. *Journal of Chromatography B,* 883**,** 76-94.

MEREDITH, J., FAZELI, B. & SCHWARTZ, M. 1993. The extracellular matrix as a cell survival factor. *Molecular biology of the cell,* 4**,** 953-961.

MERIC-BERNSTAM, F. & MILLS, G. B. 2012. Overcoming implementation challenges of personalized cancer therapy. *Nature Reviews Clinical Oncology,* 9**,** 542-548.

MIELE, E., SPINELLI, G. P., MIELE, E., TOMAO, F. & TOMAO, S. 2009. Albumin-bound formulation of paclitaxel (Abraxane® ABI-007) in the treatment of breast cancer. *International journal of nanomedicine,* 4**,** 99.

MINTON, K. 2013. Cell adhesion: Integrating the integrin response. *Nature Reviews Molecular Cell Biology,* 14**,** 401-401.

MITRA, A., SAWADA, K., TIWARI, P., MUI, K., GWIN, K. & LENGYEL, E. 2011. Ligand-independent activation of c-Met by fibronectin and α5β1-integrin regulates ovarian cancer invasion and metastasis. *Oncogene,* 30**,** 1566-1576.

MITRAGOTRI, S. 2005. Healing sound: the use of ultrasound in drug delivery and other therapeutic applications. *Nature Reviews Drug Discovery,* 4**,** 255-260.

MOGHIMI, S. M., HUNTER, A. C. & MURRAY, J. C. 2001. Long-circulating and target-specific nanoparticles: theory to practice. *Pharmacological reviews,* 53**,** 283-318.

MORELLO, V., CABODI, S., SIGISMUND, S., CAMACHO-LEAL, M., REPETTO, D., VOLANTE, M., PAPOTTI, M., TURCO, E. & DEFILIPPI, P. 2011. β1 integrin controls EGFR signaling and tumorigenic properties of lung cancer cells. *Oncogene,* 30**,** 4087-4096.

MUSUMECI, T., VENTURA, C. A., GIANNONE, I., RUOZI, B., MONTENEGRO, L., PIGNATELLO, R. & PUGLISI, G. 2006. PLA/PLGA nanoparticles for sustained release of docetaxel. *International journal of pharmaceutics,* 325**,** 172-179.

NAGANO, M., HOSHINO, D., KOSHIKAWA, N., AKIZAWA, T. & SEIKI, M. 2012. Turnover of focal adhesions and cancer cell migration. *International journal of cell biology,* 2012.

NAORA, H. & MONTELL, D. J. 2005. Ovarian cancer metastasis: integrating insights from disparate model organisms. *Nature Reviews Cancer,* 5**,** 355-366.

OTSUKA, H., NAGASAKI, Y. & KATAOKA, K. 2003. PEGylated nanoparticles for biological and pharmaceutical applications. *Advanced Drug Delivery Reviews,* 55**,** 403-419.

PAGET, S. 1889. The distribution of secondary growths in cancer of the breast. *The Lancet,* 133**,** 571-573.

PANYAM, J., DALI, M. M., SAHOO, S. K., MA, W., CHAKRAVARTHI, S. S., AMIDON, G. L., LEVY, R. J. & LABHASETWAR, V. 2003. Polymer degradation and in vitro release of a model protein from poly (d, l-lactide-< i> co</i>-glycolide) nano-and microparticles. *Journal of Controlled Release,* 92**,** 173-187.

PARMAR, M., LEDERMANN, J., COLOMBO, N., DU BOIS, A., DELALOYE, J., KRISTENSEN, G., WHEELER, S., SWART, A., QIAN, W. & TORRI, V. 2003. Paclitaxel plus platinum-based chemotherapy versus conventional platinum-based chemotherapy in women with relapsed ovarian cancer: the ICON4/AGO-OVAR-2.2 trial. *Lancet,* 361**,** 2099-2106.

PASAPERA, A. M., SCHNEIDER, I. C., RERICHA, E., SCHLAEPFER, D. D. & WATERMAN, C. M. 2010. Myosin II activity regulates vinculin recruitment to focal adhesions through FAK-mediated paxillin phosphorylation. *The Journal of cell biology,* 188**,** 877-890.

PATEL, J. 1996. Liposomal doxorubicin: Doxil®. *Journal of Oncology Pharmacy Practice,* 2**,** 201-210.

PEER, D., KARP, J. M., HONG, S., FAROKHZAD, O. C., MARGALIT, R. & LANGER, R. 2007. Nanocarriers as an emerging platform for cancer therapy. *Nature nanotechnology,* 2**,** 751-760.

PERSIKOV, A. V., OSADA, R. & SINGH, M. 2009. Predicting DNA recognition by Cys2His2 zinc finger proteins. *Bioinformatics,* 25**,** 22-29.

PETROS, R. A. & DESIMONE, J. M. 2010. Strategies in the design of nanoparticles for therapeutic applications. *Nature Reviews Drug Discovery,* 9**,** 615-627.

PFISTERER, J., PLANTE, M., VERGOTE, I., DU BOIS, A., HIRTE, H., LACAVE, A. J., WAGNER, U., STÄHLE, A., STUART, G. & KIMMIG, R. 2006. Gemcitabine plus carboplatin compared with carboplatin in patients with platinum-sensitive recurrent ovarian cancer: an intergroup trial of the AGO-OVAR, the NCIC CTG, and the EORTC GCG. *Journal of Clinical Oncology,* 24**,** 4699-4707.

PRADEEP, S., KIM, S. W., WU, S. Y., NISHIMURA, M., CHALUVALLY-RAGHAVAN, P., MIYAKE, T., PECOT, C. V., KIM, S.-J., CHOI, H. J. & BISCHOFF, F. Z. 2014. Hematogenous Metastasis of Ovarian Cancer: Rethinking Mode of Spread. *Cancer cell,* 26**,** 77-91.

PUJADE-LAURAINE, E., WAGNER, U., AAVALL-LUNDQVIST, E., GEBSKI, V., HEYWOOD, M., VASEY, P. A., VOLGGER, B., VERGOTE, I., PIGNATA, S. & FERRERO, A. 2010. Pegylated liposomal doxorubicin and carboplatin compared with paclitaxel and carboplatin for patients with platinum-sensitive ovarian cancer in late relapse. *Journal of clinical oncology,* 28**,** 3323-3329.

RIGOUTSOS, I. 2010. Short RNAs: how big is this iceberg? *Current Biology,* 20**,** R110-R113.

ROMERO, I. & BAST JR, R. C. 2012. Minireview: human ovarian cancer: biology, current management, and paths to personalizing therapy. *Endocrinology,* 153**,** 1593-1602.

SAKAMOTO, J. H., VAN DE VEN, A. L., GODIN, B., BLANCO, E., SERDA, R. E., GRATTONI, A., ZIEMYS, A., BOUAMRANI, A., HU, T. & RANGANATHAN, S. I. 2010. Enabling individualized therapy through nanotechnology. *Pharmacological Research,* 62**,** 57-89.

SANA, J., FALTEJSKOVA, P., SVOBODA, M. & SLABY, O. 2012. Novel classes of non-coding RNAs and cancer. *J Transl Med,* 10**,** 103.

SCAGGIANTE, B., DAPAS, B., FARRA, R., GRASSI, M., POZZATO, G., GIANSANTE, C., FIOTTI, N., TAMAI, E., TONON, F. & GRASSI, G. 2013. Aptamers as Targeting Delivery Devices or Anti-cancer Drugs for Fighting Tumors. *Current drug metabolism*.

SCHACKERT, G. & FIDLER, I. J. 1988. Site-specific metastasis of mouse melanomas and a fibrosarcoma in the brain or meninges of syngeneic animals. *Cancer research,* 48**,** 3478-3484.

SCHEFFEL, U., WAGNER, H. N., RHODES, B. A. & NATARAJA.TK 1972. Albumin Microspheres for Study of Reticuloendothelial System. *Journal of Nuclear Medicine,* 13**,** 498-&.

SCHILLER, H. B., HERMANN, M.-R., POLLEUX, J., VIGNAUD, T., ZANIVAN, S., FRIEDEL, C. C., SUN, Z., RADUCANU, A., GOTTSCHALK, K.-E. & THÉRY, M. 2013. β1-and αv-class integrins cooperate to regulate myosin II during rigidity sensing of fibronectin-based microenvironments. *Nature cell biology,* 15**,** 625-636.

SCHNELL, M. A., HARDY, C., HAWLEY, M., PROPERT, K. J. & WILSON, J. M. 2002. Effect of blood collection technique in mice on clinical pathology parameters. *Human gene therapy,* 13**,** 155-161.

SCHROEDER, A., HONEN, R., TURJEMAN, K., GABIZON, A., KOST, J. & BARENHOLZ, Y. 2009. Ultrasound triggered release of cisplatin from liposomes in murine tumors. *Journal of Controlled Release,* 137**,** 63-68.

SCOTT, A. M., WOLCHOK, J. D. & OLD, L. J. 2012. Antibody therapy of cancer. *Nature Reviews Cancer,* 12**,** 278-287.

SERRA, R. W., FANG, M., PARK, S. M., HUTCHINSON, L. & GREEN, M. R. 2014. A KRAS-directed transcriptional silencing pathway that mediates the CpG island methylator phenotype. *Elife,* 3.

SESSA, C. & DEL CONTE, G. 2010. Targeted therapies: Tailored treatment for ovarian cancer: are we there yet? *Nature Reviews Clinical Oncology,* 7**,** 80-82.

SHEN, H., RODRIGUEZ-AGUAYO, C., XU, R., GONZALEZ-VILLASANA, V., MAI, J., HUANG, Y., ZHANG, G., GUO, X., BAI, L. & QIN, G. 2013a. Enhancing chemotherapy response with sustained EphA2 silencing using multistage vector delivery. *Clinical Cancer Research*.

SHEN, H., RODRIGUEZ-AGUAYO, C., XU, R., GONZALEZ-VILLASANA, V., MAI, J., HUANG, Y., ZHANG, G., GUO, X., BAI, L. & QIN, G. 2013b. Enhancing chemotherapy response with sustained EphA2 silencing using multistage vector delivery. *Clinical Cancer Research,* 19**,** 1806-1815.

SHENOY, D., LITTLE, S., LANGER, R. & AMIJI, M. 2005. Poly (ethylene oxide)-modified poly (β-amino ester) nanoparticles as a pH-sensitive system for tumor-targeted delivery of hydrophobic drugs: part 2. In vivo distribution and tumor localization studies. *Pharmaceutical research,* 22**,** 2107-2114.

SHIBUE, T. & WEINBERG, R. A. 2009. Integrin β1-focal adhesion kinase signaling directs the proliferation of metastatic cancer cells disseminated in the lungs. *Proceedings of the National Academy of Sciences,* 106**,** 10290-10295.

SIEGEL, R., MA, J., ZOU, Z. & JEMAL, A. 2014. Cancer statistics, 2014. *CA: a cancer journal for clinicians*.

SILVERBERG, S. G. 2000. Histopathologic grading of ovarian carcinoma: a review and proposal. *International Journal of Gynecologic Pathology,* 19**,** 7-15.

SIMPSON, C. D., ANYIWE, K. & SCHIMMER, A. D. 2008. Anoikis resistance and tumor metastasis. *Cancer letters,* 272**,** 177-185.

SOOD, A. K., ARMAIZ-PENA, G. N., HALDER, J., NICK, A. M., STONE, R. L., HU, W., CARROLL, A. R., SPANNUTH, W. A., DEAVERS, M. T. & ALLEN, J. K. 2010. Adrenergic modulation of focal adhesion kinase protects human ovarian cancer cells from anoikis. *The Journal of clinical investigation,* 120**,** 1515.

SOOD, A. K., SEFTOR, E. A., FLETCHER, M. S., GARDNER, L. M., HEIDGER, P. M., BULLER, R. E., SEFTOR, R. E. & HENDRIX, M. J. 2001. Molecular determinants of ovarian cancer plasticity. *The American journal of pathology,* 158**,** 1279-1288.

SOSLOW, R. A. 2008. Histologic subtypes of ovarian carcinoma: an overview. *International Journal of Gynecologic Pathology,* 27**,** 161-174.

SPANNUTH, W. A., NICK, A. M., JENNINGS, N. B., ARMAIZ-PENA, G. N., MANGALA, L. S., DANES, C. G., LIN, Y. G., MERRITT, W. M., THAKER, P. H. & KAMAT, A. A. 2009. Functional significance of VEGFR-2 on ovarian cancer cells. *International journal of cancer,* 124**,** 1045-1053.

STEMKE-HALE, K., GONZALEZ-ANGULO, A. M., LLUCH, A., NEVE, R. M., KUO, W.-L., DAVIES, M., CAREY, M., HU, Z., GUAN, Y. & SAHIN, A. 2008. An integrative genomic and proteomic analysis of PIK3CA, PTEN, and AKT mutations in breast cancer. *Cancer research,* 68**,** 6084-6091.

SULTANA, S., KHAN, M. R., KUMAR, M., KUMAR, S. & ALI, M. 2013. Nanoparticles-mediated drug delivery approaches for cancer targeting: a review. *Journal of drug targeting,* 21**,** 107-125.

SUYAMA, K., SHAPIRO, I., GUTTMAN, M. & HAZAN, R. B. 2002. A signaling pathway leading to metastasis is controlled by N-cadherin and the FGF receptor. *Cancer cell,* 2**,** 301-314.

TABERNERO, J., SHAPIRO, G. I., LORUSSO, P. M., CERVANTES, A., SCHWARTZ, G. K., WEISS, G. J., PAZ-ARES, L., CHO, D. C., INFANTE, J. R. & ALSINA, M. 2013. First-in-humans trial of an RNA interference therapeutic targeting VEGF and KSP in cancer patients with liver involvement. *Cancer discovery,* 3**,** 406-417.

TADEPALLY, H. D., BURGER, G. & AUBRY, M. 2008. Evolution of C2H2-zinc finger genes and subfamilies in mammals: species-specific duplication and loss of clusters, genes and effector domains. *BMC evolutionary biology,* 8**,** 176.

TALMADGE, J. E. & FIDLER, I. J. 2010. AACR centennial series: the biology of cancer metastasis: historical perspective. *Cancer research,* 70**,** 5649-5669.

TANAKA, T., MANGALA, L. S., VIVAS-MEJIA, P. E., NIEVES-ALICEA, R., MANN, A. P., MORA, E., HAN, H.-D., SHAHZAD, M. M., LIU, X. & BHAVANE, R. 2010. Sustained small interfering RNA delivery by mesoporous silicon particles. *Cancer research,* 70**,** 3687-3696.

TARI, A. M., LOPEZ-BERESTEIN, G. & DEISSEROTH, A. B. 1995. Liposomal antisense methyl phosphonate oligonucleotides and methods for their preparation and use. Google Patents.

THAKER, P. H., DEAVERS, M., CELESTINO, J., THORNTON, A., FLETCHER, M. S., LANDEN, C. N., KINCH, M. S., KIENER, P. A. & SOOD, A. K. 2004. EphA2 expression is associated with aggressive features in ovarian carcinoma. *Clinical Cancer Research,* 10**,** 5145-5150.

TIBES, R., QIU, Y., LU, Y., HENNESSY, B., ANDREEFF, M., MILLS, G. B. & KORNBLAU, S. M. 2006. Reverse phase protein array: validation of a novel proteomic technology and utility for analysis of primary leukemia specimens and hematopoietic stem cells. *Molecular cancer therapeutics,* 5**,** 2512-2521.

TORCHILIN, V. P. 2001. Structure and design of polymeric surfactant-based drug delivery systems. *Journal of controlled release: official journal of the Controlled Release Society,* 73**,** 137.

TORCHILIN, V. P. 2005. Recent advances with liposomes as pharmaceutical carriers. *Nature Reviews Drug Discovery,* 4**,** 145-160.

TORCHILIN, V. P. & TRUBETSKOY, V. S. 1995. Which polymers can make nanoparticulate drug carriers long-circulating? *Advanced Drug Delivery Reviews,* 16**,** 141-155.

TORMO, M., TARI, A. M., MCDONNELL, T. J., CABANILLAS, F., GARCIA-CONDE, J. & LOPEZ-BERESTEIN, G. 1998. Apoptotic induction in transformed follicular lymphoma cells by Bcl-2 downregulation. *Leukemia & lymphoma,* 30**,** 367-380.

TUERK, C. & GOLD, L. 1990. Systematic evolution of ligands by exponential enrichment: RNA ligands to bacteriophage T4 DNA polymerase. *Science,* 249**,** 505-510.

VACHON, P. H. 2011. Integrin signaling, cell survival, and anoikis: distinctions, differences, and differentiation. *Journal of signal transduction,* 2011.

VALASTYAN, S. & WEINBERG, R. A. 2011. Tumor metastasis: molecular insights and evolving paradigms. *Cell,* 147**,** 275-292.

VAUGHAN, S., COWARD, J. I., BAST, R. C., BERCHUCK, A., BEREK, J. S., BRENTON, J. D., COUKOS, G., CRUM, C. C., DRAPKIN, R. & ETEMADMOGHADAM, D. 2011. Rethinking ovarian cancer: recommendations for improving outcomes. *Nature Reviews Cancer,* 11**,** 719-725.

WARENIUS, H., GALFRE, G., BLEEHEN, N. & MILSTEIN, C. 1981. Attempted targeting of a monoclonal antibody in a human tumour xenograft system. *European Journal of Cancer and Clinical Oncology,* 17**,** 1009-1015.

WEIS, S. M. & CHERESH, D. A. 2011. Tumor angiogenesis: molecular pathways and therapeutic targets. *Nature medicine,* 17**,** 1359-1370.

WILSON, R., PLUMMER, R., ADAM, J., EATOCK, M., BODDY, A., GRIFFIN, M., MILLER, R., MATSUMURA, Y., SHIMIZU, T. & CALVERT, H. 2008. Phase I and pharmacokinetic study of NC-6004, a new platinum entity of cisplatin-conjugated polymer forming micelles. *J Clin Oncol,* 26**,** 2573.

WONG, A. D., DEWIT, M. A. & GILLIES, E. R. 2012. Amplified release through the stimulus triggered degradation of self-immolative oligomers, dendrimers, and linear polymers. *Advanced Drug Delivery Reviews,* 64**,** 1031-1045.

WONG, J., BRUGGER, A., KHARE, A., CHAUBAL, M., PAPADOPOULOS, P., RABINOW, B., KIPP, J. & NING, J. 2008. Suspensions for intravenous (IV) injection: a review of development, preclinical and clinical aspects. *Advanced drug delivery reviews,* 60**,** 939-954.

WU, S. Y., LOPEZ-BERESTEIN, G., CALIN, G. A. & SOOD, A. K. 2014. RNAi therapies: drugging the undruggable. *Science translational medicine,* 6**,** 240ps7-240ps7.

YANG, S.-J., LIN, F.-H., TSAI, K.-C., WEI, M.-F., TSAI, H.-M., WONG, J.-M. & SHIEH, M.-J. 2010. Folic acid-conjugated chitosan nanoparticles enhanced protoporphyrin IX accumulation in colorectal cancer cells. *Bioconjugate chemistry,* 21**,** 679-689.

YAO, H., VEINE, D. M., FAY, K. S., STASZEWSKI, E. D., ZENG, Z.-Z. & LIVANT, D. L. 2011. The PHSCN dendrimer as a more potent inhibitor of human breast cancer cell invasion, extravasation, and lung colony formation. *Breast cancer research and treatment,* 125**,** 363-375.

YOKOE, J.-I., SAKURAGI, S., YAMAMOTO, K., TERAGAKI, T., OGAWARA, K.-I., HIGAKI, K., KATAYAMA, N., KAI, T., SATO, M. & KIMURA, T. 2008. Albumin-conjugated PEG liposome enhances tumor distribution of liposomal doxorubicin in rats. *International journal of pharmaceutics,* 353**,** 28-34.

YOO, H. S. & PARK, T. G. 2004. Folate receptor targeted biodegradable polymeric doxorubicin micelles. *Journal of Controlled Release,* 96**,** 273-283.

YOUNG, S. A., GRAF, R. & STUPACK, D. G. 2013. Neuroblastoma Integrins.

YUAN, F., DELLIAN, M., FUKUMURA, D., LEUNIG, M., BERK, D. A., TORCHILIN, V. P. & JAIN, R. K. 1995. Vascular permeability in a human tumor xenograft: molecular size dependence and cutoff size. *Cancer research,* 55**,** 3752-3756.

ZAHR, A. S., DAVIS, C. A. & PISHKO, M. V. 2006. Macrophage uptake of core-shell nanoparticles surface modified with poly (ethylene glycol). *Langmuir,* 22**,** 8178-8185.

ZHANG, Z., VUORI, K., REED, J. C. & RUOSLAHTI, E. 1995. The alpha 5 beta 1 integrin supports survival of cells on fibronectin and up-regulates Bcl-2 expression. *Proceedings of the National Academy of Sciences,* 92**,** 6161-6165.

ZHANG, Z., VUORI, K., WANG, H.-G., REED, J. C. & RUOSLAHTI, E. 1996. Integrin activation by R-ras. *Cell,* 85**,** 61-69.

ZHU, S., HONG, M., ZHANG, L., TANG, G., JIANG, Y. & PEI, Y. 2010. PEGylated PAMAM dendrimer-doxorubicin conjugates: in vitro evaluation and in vivo tumor accumulation. *Pharmaceutical research,* 27**,** 161-174.

Vita

Burcu Aslan was born in Trabzon, Turkey, on March 1,1985. After graduating from Haci Omer Tarman Anatolian High School, Ankara, in 2003, she attended Hacettepe University and received her Bachelors degree in biology in 2007. She built her interest in nanotechnology during undergrad and enrolled the master's program in The Department of Nanotechnology and Nanomedicine in Hacettepe University in 2007. She joined in Dr. Gabriel Lopez-Berestein laboratory as a research intern in December 2009, upon receiving her master's degree. She was then accepted into the University of Texas, Graduate School of Biomedical Sciences in January 2011 and continued her studies under supervision of Dr. Lopez-Berestein. During her research years, she developed a novel delivery system for sustained siRNA release and she identified the role of a novel transcription factor, zinc finger 304 (ZNF304), and investigated ZNF304 as a novel target for therapy in ovarian cancer.